Radiochemical and luminescence-based binding and functional assays for human histamine receptors using genetically engineered cells

Dissertation

zur Erlangung des Doktorgrades der Naturwissenschaften (Dr. rer. nat.)
der Naturwissenschaftlichen Fakultät IV - Chemie und Pharmazie -
der Universität Regensburg

vorgelegt von
Johannes Mosandl
aus Würzburg
2009

Die vorliegende Arbeit entstand in der Zeit von Januar 2006 bis Juli 2009 unter der Leitung von Herrn Prof. Dr. A. Buschauer und Herrn Prof. Dr. G. Bernhardt am Institut für Pharmazie der Naturwissenschaftlichen Fakultät IV – Chemie und Pharmazie – der Universität Regensburg.

Das Promotionsgesuch wurde eingereicht im Juli 2009.

Tag der mündlichen Prüfung: 07. August 2009

Prüfungsausschuss:	Prof. Dr. A. Mannschreck	(Vorsitzender)
	Prof. Dr. A. Buschauer	(Erstgutachter)
	Prof. Dr. G. Bernhardt	(Zweitgutachter)
	Prof. Dr. A. Göpferich	(Drittprüfer)

Danksagungen

An dieser Stelle möchte ich mich bedanken bei:

Herrn Prof. Dr. A. Buschauer für die Gelegenheit, an diesem interessanten Projekt arbeiten zu dürfen, für seine wissenschaftlichen Anregungen und seine konstruktive Kritik bei der Durchsicht der Arbeit,

Herrn Prof. Dr. G. Bernhardt für seine fachliche Anleitung, seine Anregungen bei experimentellen Problemen und seine konstruktive Kritik bei der Durchsicht der Arbeit,

Herrn Prof. Dr. S. Elz und seinen Mitarbeitern / -innen für die Bereitstellung verschiedener Histamin Rezeptor Liganden,

Herrn Prof. Dr. J. Heilmann und seinen Mitarbeitern / -innen für die Bereitstellung des Combi Cell Harvesters 11025,

Herrn Prof. Dr. R. Seifert (Institut für Pharmakologie, Medizinische Hochschule Hannover) für die Bereitstellung der Vektoren pcDNA3.0-Neo-FLAG-hH_2R-His_6 und pcDNA3.1(+)-Neo-hH_4R, der HL-60 HD Zellen, diverser Histamin Rezeptor Liganden und die Gelegenheit, Versuche am Lehrstuhl für Pharmakologie und Toxikologie der Universität Regensburg durchzuführen,

Herrn Prof. Dr. O. Wolfbeis und seinen Mitarbeitern / -innen für die Bereitstellung von Fluoreszenzfarbstoffen,

Herrn Prof. Dr. B. Conklin (University of California) für die Bereitstellung des pcDNA1-qi5-HA Vektors,

Herrn Prof. Dr. S. Thayer (University of Minnesota) für die Bereitstellung des pMTAEQ Vektors,

Den Mitarbeitern / -innen des Instituts für Medizinische Mikrobiologie und Hygiene, Universität Regensburg, für die Bereitstellung der Vektoren pcDNA3.1(+)-Hygro und pcDNA3.1(+)-Zeo sowie der HEK293 T Zellen,

Den Mitarbeitern / -innen der Firma Origenis, v. a. Herrn Dr. A. Treml und Frau C. Gilch, für die Bereitstellung verschiedener H_1 Rezeptorliganden und die Vorbereitung der Mikrotiterplatten,

Herrn Dr. R. Ziemek für seine Hilfe beim Erlernen der Zellkultur und beim theoretischen Einarbeiten in das Thema,

Frau N. Pop für ihre gute Zusammenarbeit beim Erlernen der Arbeitstechniken und ihre Hilfe am konfokalen Mikroskop,

Herrn Dr. D. Gross für seine Unterstützung bei der konfokalen Mikroskopie, der Agarose-gelelektrophorese, der RT-PCR und für die Bereitstellung der HEK293-FLAG-hH_2R-His_6 Zellen,

Herrn Dr. E. Schneider für seine wertvollen fachlichen Informationen vielfältiger Art, seine Hilfe bei den Radioligandbindungsstudien zur Bestimmung der Selektivität diverser H_1 Rezeptorliganden und die Bereitstellung der Primer für den Nachweis des β-Actins und der $H_{1/2}$ Rezeptoren,

Frau Dr. E. Hofinger für ihre Hilfe bei den molekularbiologischen Arbeiten, der SDS-PAGE und den Western Blots,

Frau G. Wilberg für ihre Unterstützung bei der SDS-PAGE und den Western Blots am Lehrstuhl für Pharmakologie und Toxikologie,

Frau D. Erdmann für die Bereitstellung der H_2 Rezeptorliganden **6**-**8**

Frau Dr. A. Kraus und Herrn T. Birnkammer für die Bereitstellung des H_2 Rezeptorliganden **9**,

Herrn Dr. P. Igel für die Bereitstellung des Radioliganden [^{3}H]UR-PI294,

Frau E. Schreiber für ihre Unterstützung bei der Betreuung der Zellkulturen sowie für ihre Hilfe bei der Durchführung der Fura-2 Assays und der Bindungsversuche am Durchflusszytometer,

Herrn D. Schnell für die Bereitstellung der Primer und Konstrukte für den Nachweis der $H_{3/4}$ Rezeptoren und der HEK293-FLAG-hH_4R-His_6 Zellen,

Herrn Dr. M. Memminger für seine hilfreichen Ratschläge bei der Durchführung des Luciferase Assays und die freundliche Atmosphäre beim Zusammenschreiben,

Frau M. Wechler, Frau S. Heinrich, Frau K. Reindl und Herrn P. Richthammer für die Unterstützung bei technischen und organisatorischen Problemen,

Herrn M. Kühnle, Frau S. Bollwein und Frau B. Wenzl für ihre Hilfe bei der Betreuung der Zellkulturen,

meinen Wahlpflicht- und Forschungspraktikanten / -innen für ihre engagierte Mitarbeit im Labor,

allen Mitgliedern des Lehrstuhls für ihre Hilfsbereitschaft und das gute Arbeitsklima,

dem Graduiertenkolleg 760 der Deutschen Forschungsgemeinschaft für die finanzielle Unterstützung und wissenschaftliche Förderung,

meinen Freunden Daniela, Janina, Nathalie, Tobias und Helmut, dass ich eine sehr schöne Zeit in Regensburg erleben durfte

und insbesondere meinen Eltern, auf die ich mich immer verlassen konnte.

Poster Presentations

Joint meeting of the GRK 677 (Bonn) and the GRK 760, Nuremberg, October 08th - 10th, 2007:
Mosandl J., Bernhardt G., Seifert R., Elz S., Buschauer A.
"A fluorescence-based calcium assay for the human histamine H_2 receptor (hH_2R)"

Annual meeting of the GDCh, Fachgruppe Medizinische Chemie, "Frontiers in Medicinal Chemistry", Regensburg, March 02nd – 05th, 2008:
Mosandl J., Bernhardt G., Seifert R., Elz S., Buschauer A.
"Characterisation of human histamine H_2 receptor ligands by a fluorescence-based calcium assay in the 384-well-format"

4th Summer School Medicinal Chemistry, Regensburg, September 29th – October 1st, 2008:
Mosandl J., Erdmann D., Bernhardt G., Seifert R., Elz S., Wolfbeis O., Buschauer A.
"A flow cytometric binding assay for the human histamine H_2 receptor (hH_2R)"

Annual meeting of the GDCh, Fachgruppe Medizinische Chemie, "Frontiers in Medicinal Chemistry", Heidelberg, March 15th – 18th, 2009:
Mosandl J., Gross D., Bernhardt G., Seifert R., Elz S., Buschauer A.
"Radiochemical binding assays for the characterisation of ligands of the human histamine H_2 receptor (hH_2R)"

CONTENTS

Abbreviations

AC	adenylyl cyclase
AM-ester	acetoxymethylester
AMP	adenosine monophosphate
APS	ammonium peroxodisulfate
ATCC	American Type Culture Collection
BSA	bovine serum albumin
B_{max}	maximal specific binding of a ligand
bp	base pair(s)
$[Ca^{2+}]_i$	intracellular calcium concentration
cAMP	cyclic 3',5'-adenosine monophosphate
cDNA	complementary DNA
CHO cells	chinese hamster ovary cells
CIP	calf intestinal phosphorylase
CTCM	cubic ternary complex model
CNS	central nervous system
CRE	cAMP response element
CREB	cAMP response element binding protein
d	day(s)
DAB	3,3'-diaminobenzidine
DAG	diacylglycerol
DMEM	Dulbecco's modified eagle medium
DMSO	dimethylsulfoxide
DNA	deoxyribonucleic acid
dNTP mix	mixture of deoxynucleoside triphosphates
dpm	decays per minute
DSMZ	Deutsche Sammlung von Mikroorganismen und Zellkulturen
DTT	dithiothreitole
EC_{50}	agonist concentration which induces 50 % of the maximum effect
E.coli	*Escherichia coli*
ECL	extracellular loop
EDRF	endothelium-derived relaxing factor
EDTA	ethylenediaminetetraacetic acid
EGTA	ethyleneglycol-O,O'-bis(2-aminoethyl)-N,N,N',N'-tetraacetic acid
EMEM	Eagle's minimum essential medium
ER	endoplasmic reticulum
ETCM	extended ternary complex model
FACS	fluorescence activated cell sorter
FBS	fetal bovine serum
Fl-1, Fl-2, Fl-3, Fl-4	fluorescence channels of the flow cytometer

FLAG	octapeptide epitope for the labelling of proteins (mostly DYKDDDDK)
FLIPR	fluorescence imaging plate reader
FSC	forward scatter light
FSK	forskolin
G418	geneticin
GDP	guanosine diphosphate
GEF	guanine nucleotide exchange factor
GF / C	a glass fibre filter grade (1.2 µm)
GPCR	G-protein coupled receptor
$G_{s\alpha S}$	short splice variant of the $G\alpha_s$-protein
GTP	guanosine triphosphate
h	hour(s) or human (in context with receptor subtypes)
H_1R, H_2R, H_3R, H_4R	histamine receptor subtypes
HA	hemagglutinin
HEPES	N-(2-Hydroxyethyl)piperazine-N'-(2-ethanesulfonic acid)
HEK293 cells	human embryonic kidney cells
His_6	hexahistidine tag for the labelling and purification of proteins
HL-60 HD cells	human promyelocytic leukemia cells (Heidelberg, Germany)
HRP	horse radish peroxidase
HSA	human serum albumin
IC_{50}	antagonist concentration which suppresses 50 % of an agonist induced effect (functional assay) or ligand concentration which inhibits the specific binding of a labelled ligand by 50 % (binding assay)
ICL	intracellular loop
IP_3	inositol-1,4,5-trisphosphate
K_b	dissociation constant (functional assay)
K_d	dissociation constant (saturation binding assay)
K_i	dissociation constant (competition binding assay)
LB	lysogeny broth (for *E.coli* culture)
MAPK	mitogen-activated protein kinase
MCS	multiple cloning site
min	minute(s)
mRNA	messenger RNA
mtAEQ	mitochondrially targeted apoaequorin
n.d.	not determined
OD	optical density
PAGE	polyacrylamide gel electrophoresis
PBS	phosphate buffered saline
PCR	polymerase chain reaction
pEC_{50}	negative decade logarithm of EC_{50}
PEI	polyethyleneimine

P_i	inorganic phosphate
PP_i	pyrophosphate
PIP_2	phosphatidylinositol-4,5-bisphosphate
PIPES	piperazine-1,4-bis(2-ethanesulfonic acid)
PKA, PKC	protein kinase A or C, respectively
pK_i	negative decade logarithm of K_i
PLCβ	phospholipase Cβ
PTX	pertussis toxin
qi5-HA, qs5-HA	chimeric $G\alpha_q$ proteins which incorporate a HA epitope
RGS	regulators of G-protein signalling
RLU	relative luminescence units
RNA	ribonucleic acid
rpm	revolutions per minute
RT	reverse transcription
RT-PCR	reverse transcription followed by polymerase chain reaction
s	second(s)
SDS	sodium dodecyl sulfate
SEM	standard error of the mean
Sf9	*Spodoptera frugiperda* (an insect cell line)
SOC	salt optimized + carbon broth (for transformation of *E. coli*)
SRE	serum response element
SSC	sideward scatter light
TAE	tris-acetate-EDTA-buffer
TBE	tris-borate-EDTA-buffer
TCM	ternary complex model
TEMED	N,N,N',N'-tetramethylethane-1,2-diamine
TM	transmembrane domaine
Tris	tris(hydroxymethyl)aminomethane
Y_1R, Y_2R, Y_4R	neuropeptide Y receptor subtypes

Chapter 1

General introduction

1.1 G-protein coupled receptors (GPCRs)

1.1.1 GPCRs as drug targets

Seven-transmembrane domain G-protein coupled receptors (GPCRs) constitute the largest and most diverse superfamily of cell surface receptors in the mammalian genome (Luttrell, 2008) and represent around 15 % of the druggable genome (Hopkins and Groom, 2002). With alternative splicing, it is estimated that 1000-2000 discrete receptor proteins may be expressed (Luttrell, 2008). GPCRs detect a diversity of extracellular stimuli ranging from neurotransmitters and peptide hormones to odorants and photons of light and therefore influence a lot of important physiological functions (Luttrell, 2008). Consequently, GPCRs are involved in a plethora of diseases, e.g. cardiovascular, gastrointestinal and CNS disorders or asthma and cancer (Fang et al., 2003). As around 30 % of the currently marketed drugs address GPCRs, those receptors represent one of the most important classes for pharmacotherapy (Jacoby et al., 2006). Until now, at least 46 GPCRs have been successfully targeted by drugs, but there still remain 323 GPCRs that could become future drug targets. In addition, 150 of those 323 GPCRs are orphan receptors, i.e., their endogenous ligands are unknown so far (Lagerström and Schiöth, 2008).
Thus, the (patho)physiological importance of those receptors opens a wide field for future developments with regard to basic research (de-orphanization) or to target already de-orphanized receptors by innovative ligands.

1.1.2 Structure and classification

The current state of the research suggests a seven-transmembrane domain architecture for all GPCRs: the seven membrane spanning α-helices are linked by three alternating intracellular and extracellular loops. The transmembrane domains share the highest degree of sequence conservation, whereas the intracellular and extracellular domains exhibit extensive variability with regard to size and complexity. The extracellular and transmembrane regions are involved in ligand binding while the intracellular domains are important for signal transduction and for feedback modulation of receptor function (Luttrell, 2008). In Fig.1.1, a schematic representation of a GPCR (human histamine H_2 receptor) in complex with one of its ligands (arpromidine) is shown.

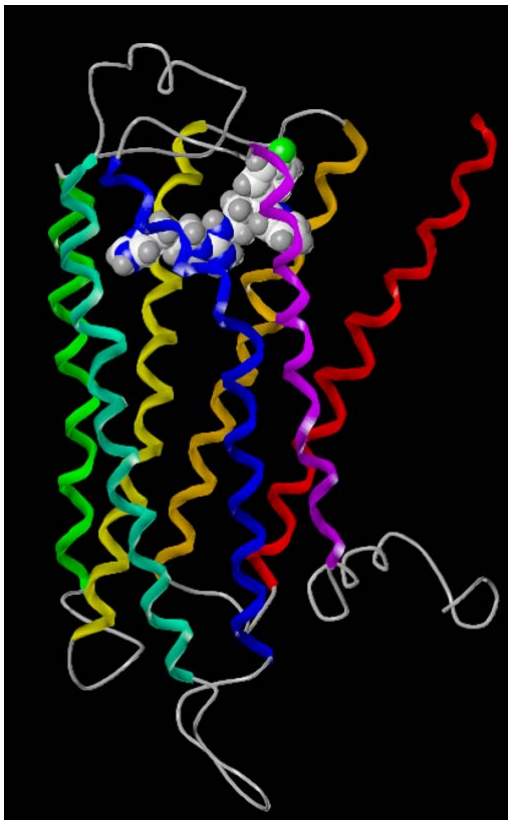

Fig. 1.1: *Model of the human histamine H_2 receptor in complex with the agonist arpromidine, based on the crystal structure of the β_2-adrenergic receptor (Cherezov et al., 2007). Transmembrane domains (TM) are illustrated in spectral colors: TM1: red, TM2: orange, TM3: yellow, TM4: green, TM5: greenblue, TM6: blue, TM7: purple. The homology model was created with SYBYL 7.3 (Tripos, St. Louis, USA) on a SGI Octane workstation. For further details see GHORAI (Ghorai et al., 2008).*

Important insights into the architecture of GPCRs were gained by determination of crystal structures. PALCZEWSKI and co-workers solved the crystal structure of bovine rhodopsin (Palczewski et al., 2000). More recently, the crystal structures of the human β_2-adrenergic receptor (Cherezov et al., 2007; Rasmussen et al., 2007; Rosenbaum et al., 2007) and the turkey β_1-adrenergic receptor (Warne et al., 2008) were elucidated. Interestingly, the crystal structures of those receptors disclosed unexpected differences relative to bovine rhodopsin: the salt bridge between $Arg^{3.50}$ and $Glu^{6.30}$ ("ionic lock"), which stabilizes the inactive state in bovine rhodopsin, is lacking in both adrenergic receptor subtypes (Warne et al., 2008). Very recently, the crystal structure of the adenosine A_{2A} receptor was solved (Jaakola et al., 2008). In the latter, there is also a lack of the ionic lock (Hanson and Stevens, 2009). Furthermore, the extracellular region of rhodopsin occludes the ligand binding pocket, whereas in the β-adrenergic and the adenosine A_{2A} receptors, the extracellular domains are highly constrained and held away from the ligand binding pocket opening. Those differences compromise the rhodopsin crystal structure as ideal representative for other GPCR family members (Hanson and Stevens, 2009). The recently elucidated crystal structures will contribute to an improved target-based drug design. Deeper insights into the structure of GPCRs can be gained from the reviews of HANSON (Hanson and Stevens, 2009) and TOPIOL (Topiol and Sabio, 2009).

GPCRs can be grouped by analysis of chromosomal positions and sequence fingerprints into five families according to the GRAFS classification system: Glutamate (G), Rhodopsin (R), Adhesion (A), Frizzled / Taste2 (F) and Secretin (S) (Fredriksson et al., 2003; Luttrell, 2008). The receptor families differ in several structural features, e.g. the length of the N-terminus, the presence or absence of a palmitoylation site in the C-terminal tail et cetera (Kristiansen, 2004; Lagerström and Schiöth, 2008). For more detailed information on the classification of GPCRs, the reviews of KRISTIANSEN (Kristiansen, 2004) and LAGERSTRÖM (Lagerström and Schiöth, 2008) are recommended.

The activation of GPCRs depends on their structural elements. At least the rhodopsin-like receptors are believed to be activated by a toggle switch of the transmembrane domain VI. Especially, the extracellular segment of this domain is supposed to tilt into the main ligand-binding pocket, while the intracellular segment tilts away from the receptor and thereby opens the receptor for binding to the G-protein (see also section 1.1.3.1). The three main micro-switches, which contribute to receptor activation, are mediated by the amino acids $Arg^{3.50}$, $Trp^{6.50}$ and $Tyr^{7.53}$ (Nygaard et al., 2009). Further interesting details with regard to GPCR activation were summarized in the review of NYGAARD (Nygaard et al., 2009).

1.1.3 Signal transduction

1.1.3.1 G-protein mediated signal transduction

The binding of an agonist to the transmembrane or extracellular domains of a GPCR leads to conformational changes in the receptor protein that are transmitted to the intracellular domains. A G-protein, which consists of a Gα-subunit and a Gβγ-heterodimer, is activated on the inner membrane surface of the cell by interaction with the activated receptor: GDP, which is bound to the Gα-subunit in the inactive state, is released and immediately replaced by GTP. Thus, the activated GPCR acts as a guanine nucleotide exchange factor (GEF) for the G-protein. This exchange leads to the dissociation of the Gα-subunit from the Gβγ-heterodimer and the receptor. Consequently, various effector proteins are activated by those two G-protein components. Due to the intrinsic GTPase activity of the Gα-subunit, GTP is converted to GDP and P_i accompanied with the termination of the Gα-induced signal transduction and reassociation of the subunits (Cabrera-Vera et al., 2003; Luttrell, 2008). The hydrolysis of GTP is accelerated by regulators of G-protein signalling (RGS, (Cabrera-Vera et al., 2003)). The G-protein-cycle is schematically shown in Fig. 1.2.

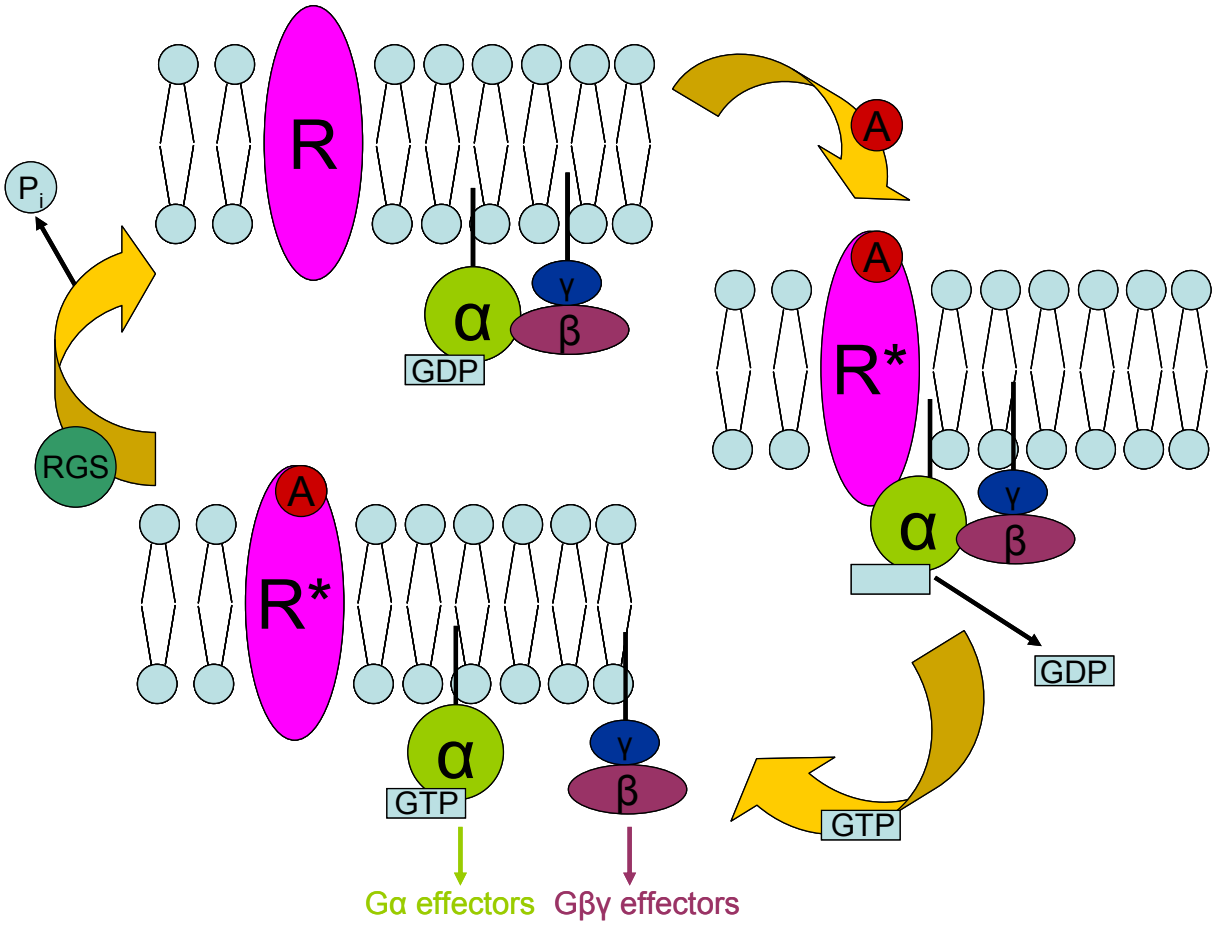

Fig. 1.2: *Activation of a heterotrimeric G-protein by interaction with an agonist-occupied GPCR. The activated receptor is represented by R*, whereas the inactive type is named R. Further details are described in the text (adapted from (Cabrera-Vera et al., 2003)).*

Both the Gα-subunit and the Gβγ-heterodimer are held in the cytoplasmic membrane and consequently in proximity to membrane proteins like GPCRs by lipid anchorage of the α- and the γ-subunit (Casey, 1994). A critical point for the interaction of the G-protein with the GPCR are the five C-terminal amino acids of the Gα-subunit as they interfere with the activated receptor (Bourne, 1997). Structural and functional similarities led to the classification of G-proteins according to their Gα-subunits into four main families: $G\alpha_S$, $G\alpha_i$, $G\alpha_q$ and $G\alpha_{12}$ (Cabrera-Vera et al., 2003).

Members of the $G\alpha_S$ family act by stimulation of adenylyl cyclase (AC). Consequently, the intracellular cAMP level is elevated, leading to the activation of proteinkinase A (PKA), a serine / threonine kinase phosphorylating numerous substrate proteins, resulting in a broad variety of cellular responses. For instance, the phosphorylation of the cAMP response element binding protein (CREB) influences transcription driven by the cAMP response element (CRE) (Hill et al., 2001).

The activation of proteins which belong to the $G\alpha_i$ family results in a decrease in AC activity and therefore accounts for a reduction of the intracellular cAMP level. Thus, the inverse effects observed for the stimulation of $G\alpha_S$-subunits are induced (Hill et al., 2001).

Members of the $G\alpha_q$ family stimulate phospholipase Cβ (PLCβ) which cleaves phosphatidyl-inositol-4,5-bisphosphate (PIP_2) to diacylglycerol (DAG) and inositol-1,4,5-trisphosphate (IP_3). IP_3 binds to IP_3 receptors located in the membrane of the endoplasmic reticulum and evokes the release of calcium ions into the cytoplasm. Calcium and DAG can stimulate proteinkinase C (PKC) which in turn activates various intracellular proteins by phosphorylation (Thomsen et al., 2005). Members of the $G\alpha_{12}$ family indirectly stimulate Rho A by interaction with RhoGEFs leading to further responses (Thomsen et al., 2005).
In addition to the Gα-subunits, the Gβγ-heterodimers also evoke diverse cellular effects, e.g. activation of PLCβ, regulation of ion channels (Cabrera-Vera et al., 2003) or stimulation of the mitogen-activated-protein-kinase (MAPK) pathway by interaction with the small G-protein Ras (Hill et al., 2001).
For more detailed information with regard to G-protein structure and signalling, the articles published by CABRERA-VERA (Cabrera-Vera et al., 2003) and SMRCKA (Smrcka, 2008) are recommended.

1.1.3.2 Alternative pathways of signal transduction

Besides the G-protein mediated signal transduction, alternative mechanisms of GPCR-triggered cellular effects are discussed. One interesting point is the role of GPCRs as signalling scaffolds: for example, the β_2-adrenergic receptor can be phosphorylated on tyrosine residues by the insulin receptor and subsequently directly associate with adapter proteins that control Ras activity (Karoor et al., 1997; Luttrell, 2008). In addition, the interaction of an agonist-occupied receptor with β-Arrestin in the scope of receptor desensitization could represent an alternative ternary complex (in contrast to the classical triad of agonist, receptor and G-protein) leading to an activation of the MAPK pathway (Luttrell, 2008; Miller and Lefkowitz, 2001; Perry and Lefkowitz, 2002). The alternative pathways of GPCR signaling are summarized in the review of LUTTRELL (Luttrell, 2008).

1.1.4 Models of receptor activation and ligand classification

The first attempts to describe the interaction of a ligand with its receptor were based on the law of mass action: CLARK assumed that the occupation of a receptor by a ligand evokes an effect (Clark, 1933; 1937). However, the discovery of G-proteins (Sternweis et al., 1981) revealed this theoretical approach as imperfect (Kenakin, 1989) and led to the development of the ternary complex model (TCM, (De Lean et al., 1980)). In the scope of the TCM, the occupation of the receptor by an agonist enables its interaction with the G-protein. The TCM contains four receptor species: the unoccupied receptor (R), the agonist-bound receptor

(AR), the receptor bound to the G-protein (RG) and the agonist-bound receptor with the G-protein (ARG) forming the ternary complex (Fig. 1.3).

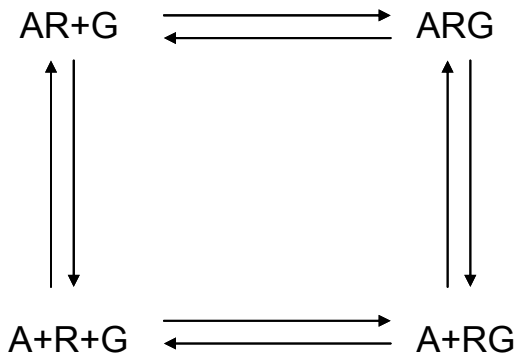

Fig. 1.3: *Illustration of the ternary complex model (TCM).* **A***: agonist,* **R***: receptor,* **G***: G-protein.*

As agonist-occupancy is regarded as a prerequisite for receptor activation, this model cannot explain constitutive activity of receptors, i.e., the active state of receptors in the absence of an agonist. In order to take this phenomenon into account, the extended ternary complex model (ETCM) was developed leading to six possible receptor species (Samama et al., 1993). This model considers the two-state model (Leff, 1995): a receptor can adopt an active or inactive conformation independent of the presence or absence of an agonist.

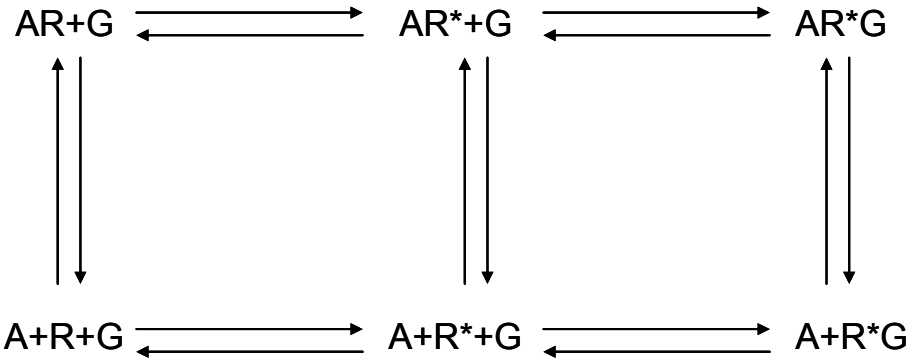

Fig. 1.4: *Scheme of the extended ternary complex model (ETCM).* **R***: inactive receptor conformation,* **R***: active receptor conformation,* **A***: agonist,* **G***: G-protein.*

The addition of a ligand shifts the equilibrium of the receptor states towards the preferred conformation. Agonists stabilize the active conformation of the receptor, whereas inverse agonists shift the equilibrium to the inactive state. Accordingly, partial agonists or partial inverse agonists shift the equilibrium to the particular conformation to a minor extent than full (inverse) agonists, respectively. Neutral antagonists do not differentiate between the two receptor states and do not change the basal activity of the receptor (Leff, 1995). Beyond this approach, the cubic ternary complex model (CTCM) considers the possible interaction of the inactive receptor with the G-protein. Thus, this model comprises eight receptor states (Fig. 1.5, (Kenakin et al., 2000)).

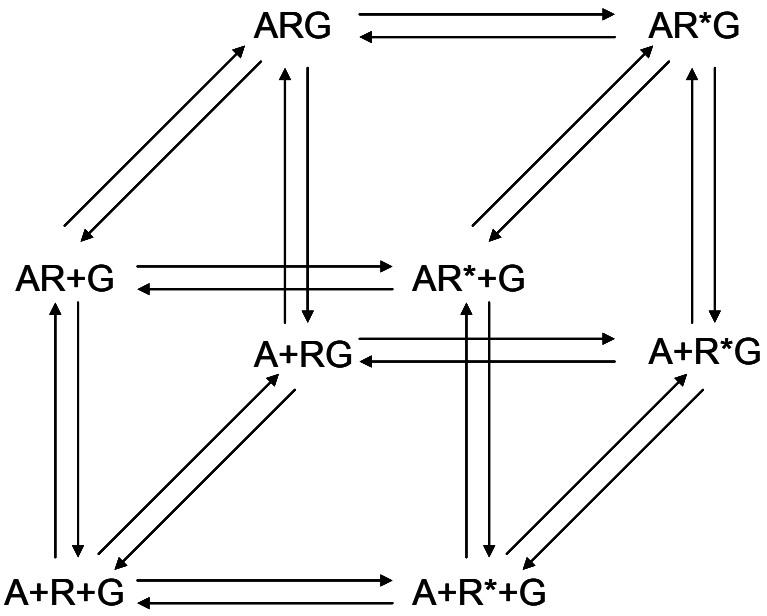

Fig. 1.5: *The cubic ternary complex model (CTCM). For explanation of R, R*, G and A see legend to Fig. 1.4.*

However, due to its complexity, the CTCM has just descriptive importance and is not appropriate for data analysis (Kenakin et al., 2000).

The advent of allosteric ligands for GPCRs further complicated the establishment of an appropriate model of receptor activation. Allosteric ligands bind to sites that are different from the orthosteric site where the endogenous agonist binds (Bridges and Lindsley, 2008). Thus, a 16-point quaternary complex model is required for the description of interactions between the G-protein, the receptor, the orthosteric and the allosteric ligand (Christopoulos and Kenakin, 2002). Furthermore, the two-state model of the receptor activation is also a simplification disregarding the possible existence of multiple active state conformations (Kew et al., 1996; Perez and Karnik, 2005).

Taken together, one must consider that all presented theoretical approaches remain models; none is capable to reflect the complete real situation. However, the ETCM can be regarded as an appropriate compromise of practicability and theory.

1.2 Histamine and its receptors

1.2.1 The biogenic amine histamine

Histamine is formed in the body by decarboxylation of the amino acid L-histidine by the enzyme L-histidine-decarboxylase (Schayer, 1956). Histamine can be inactivated by two pathways: in the scope of the major metabolic pathway, the N^{τ}-nitrogen of the imidazole ring is methylated by histamine *N*-methyltransferase. The side chain is subsequently metabolized by diamine oxidase and xanthine oxidase. In addition, histamine can be inactivated without methylation: the amine is stepwise oxidized to the respective carboxylic acid by diamine or xanthine oxidase, respectively, and finally conjugated to ribose (Fig. 1.6, (Beaven, 1982)).

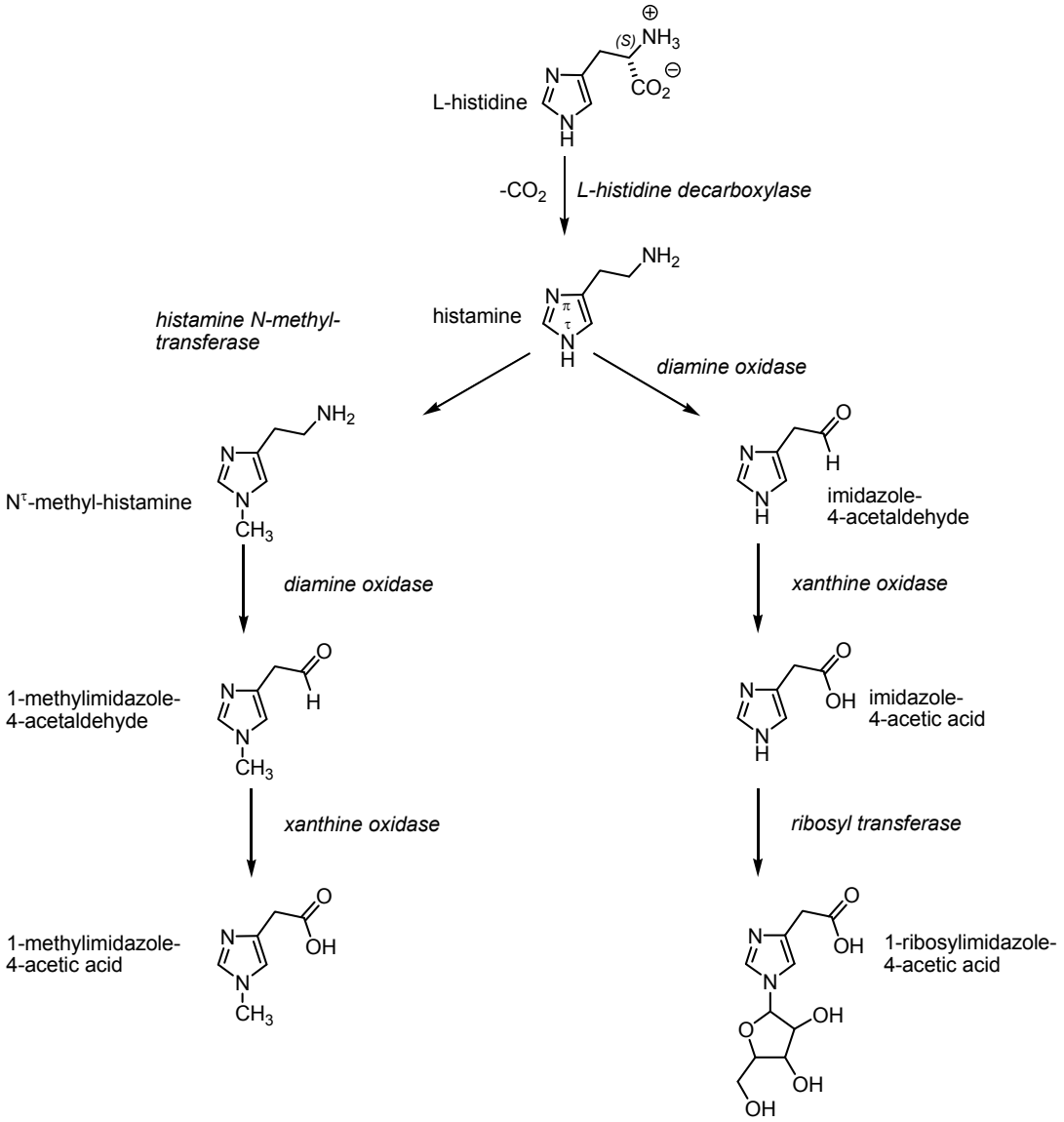

Fig. 1.6: *Biosynthesis and metabolism of histamine.*

Histamine exerts its biological effects through four receptor subtypes, designated H_1, H_2, H_3 and H_4 receptors (H_1R, H_2R, H_3R, H_4R), respectively (de Esch et al., 2005). All those receptors belong to the class A (rhodopsin-like family) of GPCRs (Fredriksson et al., 2003).

1.2.2 The histamine H_1 receptor

The hH_1R was first cloned in 1993 (De Backer et al., 1993). The corresponding receptor protein consists of 487 amino acids and preferentially couples to $G_{q/11}$-proteins upon agonist-stimulation (Hill, 1990). The signal is mainly transduced as explained in section 1.1.3.1 resulting in an increase in the intracellular calcium level which can be monitored by fluorescent calcium-chelating dyes like fura-2 (see also chapter 3). In addition, the activation of the hH_1R can also lead to an increase in the intracellular cAMP level (Esbenshade et al., 2003). Human histamine H_1 receptors are involved in a number of physiological events in the body. Most importantly, typical symptoms of allergic and inflammatory reactions are mediated by the activation of the H_1R: in airway smooth muscle cells, a contraction is observed due to the stimulation with histamine (Kotlikoff et al., 1987). Mainly the stimulation of the H_1R on endothelial cells leads to the release of EDRF (endothelium-derived relaxing factor) which provokes vasodilatation (Benedito et al., 1991). In addition, the activation of the H_1R leads to a contraction of endothelial cells which accounts for an increase of the vascular permeability (Majno et al., 1969).

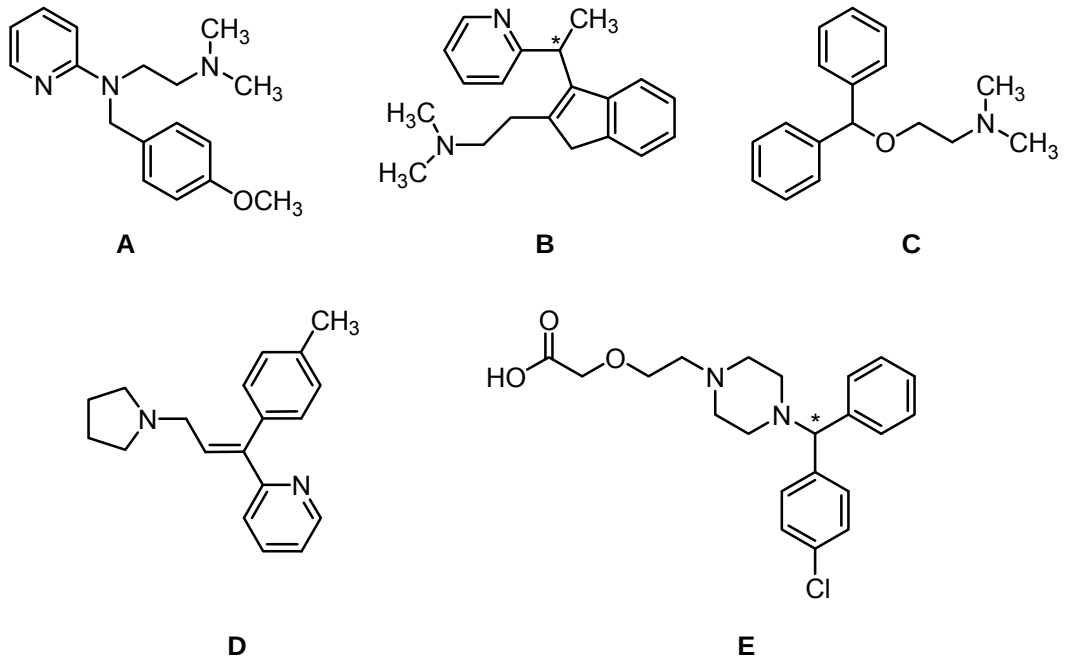

Fig. 1.7: *Examples of H_1R antagonists:* **A***: mepyramine,* **B***: dimethindene,* **C***: diphenhydramine,* **D***: triprolidine,* **E***: cetirizine. Structures* **A**-**D** *represent first generation H_1R antagonists, whereas compound* **E** *is a member of the second generation.*

Accordingly, H_1R antagonists were developed for the treatment of allergic diseases (Parsons and Ganellin, 2006). The first generation of H_1R antagonists like mepyramine showed undesired effects on attention. Due to their high lipophilicity, those drugs can cross the blood brain barrier and consequently block human histamine H_1 receptors in the CNS, which are involved in wakefulness and arousal. In order to damp this side effect, more hydrophilic compounds like cetirizine were developed (Hill et al., 1997). Examples for H_1R antagonists are shown in Fig. 1.7. H_1R-agonists are useful as pharmacological tools rather than as drugs. Betahistine is the only therapeutically used H_1R agonist: it represents a weakly potent centrally acting drug and is used for the therapy of Menière's Disease (Barak, 2008). Selective H_1R agonists were obtained by introduction of moieties in position 2 of the imidazole moiety of histamine: whilst 2-methyl-histamine showed just poor potency on the H_1R (Durant et al., 1975), 2-phenylhistamine and halogen-containing derivatives as 2-(3-trifluormethylphenyl)histamine are featured with potencies comparable or even superior to histamine (Leschke et al., 1995; Zingel et al., 1990). Further approaches resulted in the more potent (supra)histaprodifens (Elz et al., 2000; Menghin et al., 2003). The elongation of the spacer in position 2 of the imidazole moiety from propyl to butyl led to histabudifen, a compound that addresses the H_1R but is interestingly devoid of agonistic activity (Govoni et al., 2003). Especially the agonists of the suprahistaprodifen series represent valuable pharmacological tools.

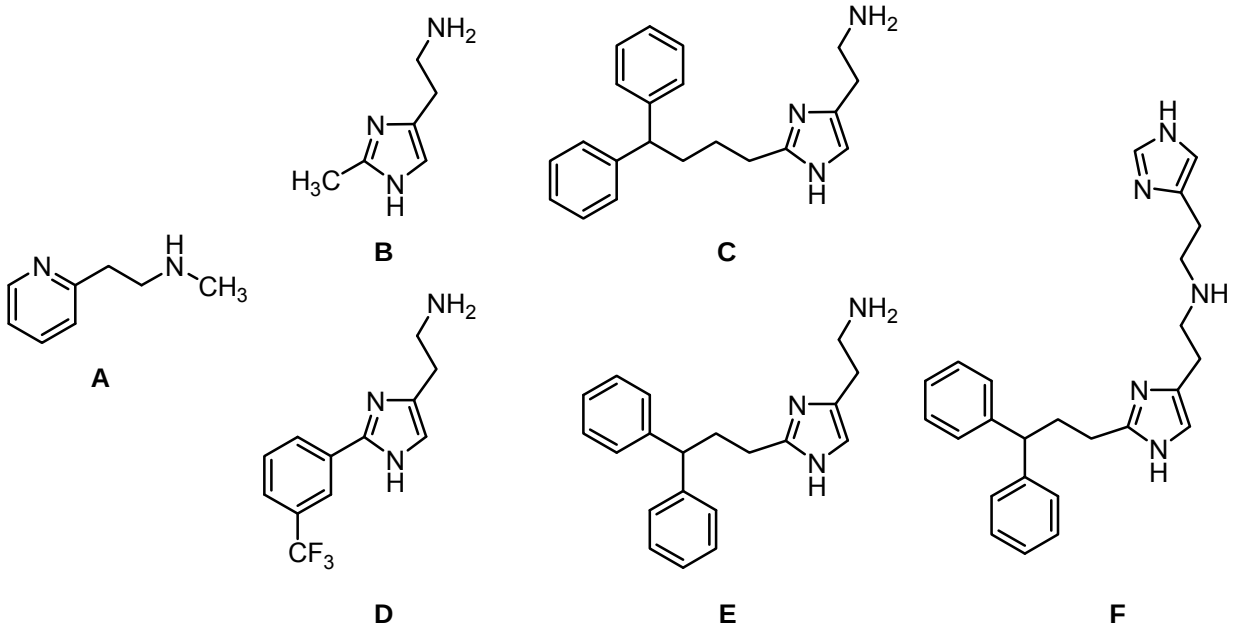

Fig. 1.8: *Chemical structure of the H_1R antagonist histabudifen (***C***) and several H_1R agonists:* **A***: betahistine,* **B***: 2-methylhistamine,* **D***: 2-(3-trifluoromethylphenyl)histamine,* **E***: histaprodifen,* **F***: suprahistaprodifen.*

1.2.3 The histamine H_2 receptor

The hH_2R was first cloned in 1991 by GANTZ and coworkers (Gantz et al., 1991). The respective GPCR consists of 359 amino acids and couples to G_s-proteins leading to an increase of the intracellular cAMP level (Gantz et al., 1991). Furthermore, the stimulation of hH_2R by agonists can lead to increases in the intracellular calcium level, possibly by coupling to G_q-proteins (Esbenshade et al., 2003). However, the mobilization of calcium due to receptor activation is not a common feature of the H_2R: in CHO cells expressing the hH_2R, no agonist-mediated increase of the intracellular calcium level was observed (Leurs et al., 1994). The different observations of LEURS (Leurs et al., 1994) and ESBENSHADE (Esbenshade et al., 2003) with regard to calcium transients mediated by hH_2R activation underline the dependence of signal transduction pathways on the used cellular system (Leurs et al., 1995) and, possibly, on other factors like transfection method, cell culture conditions et cetera. Therefore, with respect to assay development, in order to obtain robust calcium transients upon receptor activation, the stimulation of the hH_2R should be redirected to the PLCβ signal transduction pathway (consider also chapters 2,4 and 5). Histamine H_2 receptors are located in the gastric mucosa and mediate the histamine induced increase in gastric acid secretion (Soll and Berglindh, 1987). Accordingly, H_2R antagonists represent important drugs for the treatment of gastric ulcers (Black et al., 1972; Parsons and Ganellin, 2006). Examples of H_2R antagonists are shown in Fig. 1.9.

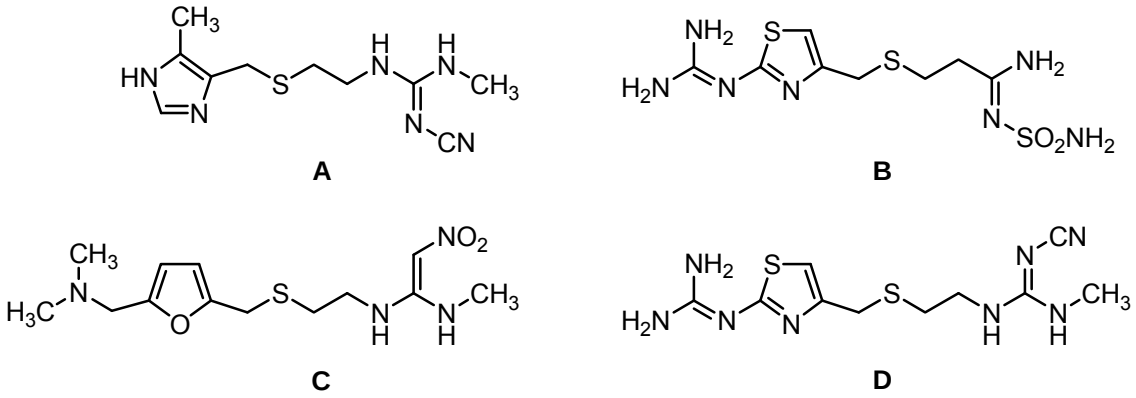

Fig. 1.9: *Examples of H_2R antagonists:* **A***: cimetidine,* **B***: famotidine,* **C***: ranitidine,* **D***: tiotidine.*

The H_2R is also found in the heart: its stimulation by histamine leads to positive chronotropic and inotropic effects (Levi and Alloatti, 1988). Consequently, H_2R agonists are of potential therapeutic interest for the treatment of congestive heart failure (Baumann et al., 1984). Especially agonists that incorporate a guanidine moiety like arpromidine and derivatives show a strongly increased potency as positive inotropic vasodilators compared to histamine

(Buschauer, 1989; Felix et al., 1995). However, those guanidine-type agonists have pharmacokinetic drawbacks like insufficient oral bioavailability. Recently, N^G-acylated imidazolylpropylguanidines were described as H_2R agonists with improved pharmacokinetic properties due to reduced basicity of the guanidine moiety. Prototypical acylguanidine-type H_2R agonists were found to be orally available and brain-penetrating (Ghorai et al., 2008).

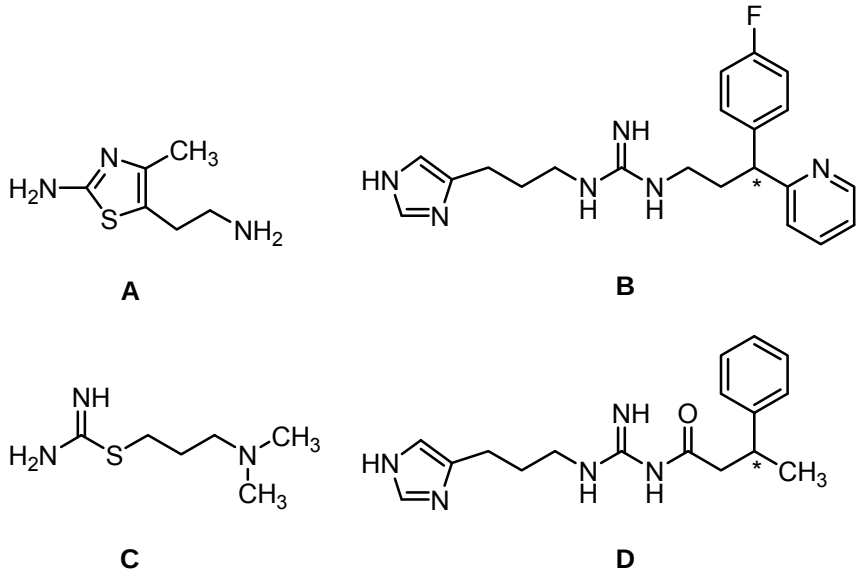

Fig. 1.10: *Chemical structures of H_2R agonists:* **A***: amthamine,* **B***: arpromidine,* **C***: dimaprit,* **D***: UR-AK24, a N^G-acylated imidazolylpropylguanidine (further details are described in the text).*

The replacement of the imidazole moiety by a 2-amino-4-methylthiazol-5-yl ring known from the H_2R agonist amthamine (Eriks et al., 1992) led to an improved selectivity for the H_2R over other histamine receptor subtypes (Kraus et al., 2009). The linkage of two of those modified pharmacophoric entities resulting in bivalent ligands (twin compounds) increased the potency on the H_2R (considerably for the chemical structure of such a compound see section 5.2.1.1; (Kraus, 2007)). As histamine H_2 receptors are also present in the CNS, deeper insights into their function could be gained by investigations with H_2R selective brain-penetrating agonists. Histamine H_2 receptors were proven to be involved in potentiation of excitation and in regulation of neuronal activity (Haas et al., 1988; Haas and Wolf, 1977).

1.2.4 The histamine H_3 receptor

The hH_3R was cloned in 1999 by LOVENBERG (Lovenberg et al., 1999). Interestingly, the cloned receptor shows only sequence homology to the hH_1R and hH_2R of about 20 %, which is comparable to other aminergic GPCRs (Lovenberg et al., 1999). In contrast to the hH_1R and hH_2R, the gene encoding the hH_3R is organized in two introns and three exons (Wiedemann et al., 2002) or even three introns and four exons (Cogé et al., 2001b). With

alternative splicing, at least 20 isoforms of the receptor protein can emerge (Bongers et al., 2007; Leurs et al., 2005). The best characterised hH_3R isoform incorporates 445 amino acids (Lovenberg et al., 1999). Compared to the hH_1R and hH_2R, histamine shows remarkably increased affinity (EC_{50} in the nanomolar range) to this isoform of the hH_3R (Lim et al., 2005). The other hH_3R isoforms consist of 200 to 453 amino acids (Bongers et al., 2007; Leurs et al., 2005). Receptor activation leads to the recruitment of $G_{i/o}$-proteins. The activated $G\alpha_{i/o}$-subunit decreases AC activity. Therefore, the cAMP level is reduced and the subsequent effects described in section 1.1.3.1 are mediated. In addition, diverse effects on the intracellular calcium level are reported. Activation of the H_3R can lead to a decrease of the Ca^{2+} influx through voltage-operated calcium channels (Bongers et al., 2007). In contrast, calcium mobilization from intracellular stores upon H_3R stimulation is reported, too (Bongers et al., 2007). Furthermore, other signal transduction pathways are discussed for the H_3R: inhibition of the Na^+ / H^+-exchanger is assumed as well as the stimulation of the phosphatidyl-inositol-3-kinase- and MAPK-pathways or the activation of the phospholipase A_2 (Bongers et al., 2007).

The H_3R acts as autoreceptor (Arrang et al., 1983) and is also thought to function as a heteroreceptor (Esbenshade et al., 2008). It is mainly located in the CNS (Lovenberg et al., 1999) and shows hallmarks of constitutive activity (Morisset et al., 2000). In its function as an autoreceptor, the H_3R regulates the synthesis (Arrang et al., 1987b) and release of histamine in the CNS (Arrang et al., 1983). Furthermore, the levels of neurotransmitters such as dopamine, serotonin, noradrenaline, acetylcholine and γ-amino butyric acid in the brain are modulated by activation of the H_3R (Esbenshade et al., 2008; Sander et al., 2008). Accordingly, many targets for pharmacotherapy are discussed: H_3R antagonists (inverse agonists) could become drugs against obesity (Tokita et al., 2006), schizophrenia (Browman et al., 2004; Prell et al., 1995), attention-deficit hyperactivity disorder (Horner et al., 2007), narcolepsy (Ligneau et al., 1998), Alzheimers disease (Giovannini et al., 1999) or nasal congestion (Varty et al., 2004). As H_3R inverse agonists effectively increase the release of histamine, those compounds might be of special therapeutic interest (Morisset et al., 2000). However, inverse agonists may cause receptor up-regulation, which could be unfavourable in drug therapy (Leurs et al., 2005; Milligan and Bond, 1997). Comprehensive reviews with regard to H_3R antagonists were recently published by ESBENSHADE (Esbenshade et al., 2008) and SANDER (Sander et al., 2008). H_3R agonists may play a role in the treatment of insomnia (Lin, 2000), pain (Cannon et al., 2003), inflammation (Cannon et al., 2007) or migraine (Millán-Guerrero et al., 2003). A classical H_3R antagonist (inverse agonist) is thioperamide (Arrang et al., 1987a). However, after discovery of the hH_4R this compound turned out to lack selectivity as it shows a similar affinity to both the hH_3R and the hH_4R (Lim et al., 2005). In order to increase the selectivity for the hH_3R over the hH_4R, "non-imidazoles"

such as JNJ-5207852 were developed (Barbier et al., 2004). The latter compound is a brain-penetrating (Barbier et al., 2004) H_3R antagonist supposed to have reduced affinity to cytochrome P450 enzymes (Sander et al., 2008). Classical H_3R agonists are (R)-α-methylhistamine (Arrang et al., 1987a) and N^{α}-methylhistamine (Babe and Serafín, 1996). Both agonists show selectivity for the hH_3R relative to the hH_4R (Lim et al., 2005) with higher hH_3R selectivity residing in (R)-α-methylhistamine (Gbahou et al., 2006).

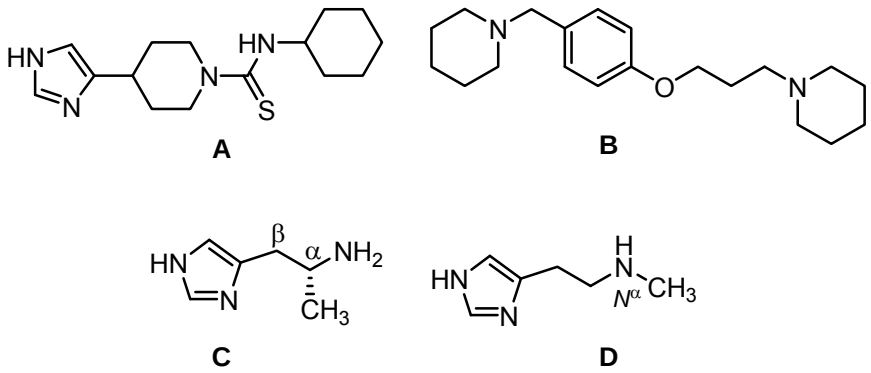

Fig. 1.11: *Chemical structures of H_3R antagonists (inverse agonists):* **A***: thioperamide,* **B***: JNJ-5207852, and H_3R agonists:* **C***: (R)-α-methylhistamine,* **D***: N^{α}-methylhistamine.*

1.2.5 The histamine H_4 receptor

The hH_4R was first cloned and functionally expressed in 2000 (Oda et al., 2000). The existence of the receptor was confirmed by several other workgroups (Liu et al., 2001; Morse et al., 2001; Nakamura et al., 2000; Nguyen et al., 2001; Zhu et al., 2001), however, those sequences slightly varied from the first reported one (de Esch et al., 2005). Showing a homology of 37 – 43 % (58 % in transmembrane regions), the hH_4R is most closely related to the hH_3R (Hough, 2001). The affinity of histamine to the hH_3R and the hH_4R is in the same range (Lim et al., 2005). The hH_4R protein consists of 390 amino acids. Like the hH_3R, the hH_4R shows a relatively high constitutive activity (Morse et al., 2001). The hH_4R gene is organized in two introns and three exons (Cogé et al., 2001a). This enables alternative splicing. Accordingly, the existence of two splice variants ($hH_4R_{(302)}$ and $hH_4R_{(67)}$, respectively) was recently reported (van Rijn et al., 2008). Those splice variants were mainly localized intracellularly, inactive with regard to ligand binding and had a dominant negative effect on the surface expression of the full-length $hH_4R_{(390)}$ (van Rijn et al., 2008). Activation of the H_4R leads to $G_{i/o}$-mediated signal transduction: $G\alpha_{i/o}$-subunits inhibit AC activity which in turn decreases the cAMP level, the PKA activity and the CRE-driven transcription. The activation of Gβγ-subunits increases gene transcription by stimulation of the MAPK-pathway.

Furthermore, intracellular calcium transients emerge due to receptor activation, most probably mediated by the Gβγ-subunits (Lim et al., 2006).

The H_4R is discussed to play an important role in the immune system. It is localized on several immune cell types like basophils and mast cells (Hofstra et al., 2003), eosinophils (O'Reilly et al., 2002), dendritic cells (Damaj et al., 2007) and T-cells (Gantner et al., 2002). In eosinophils, H_4R activation induces calcium mobilization, actin polymerization, upregulation of adhesion proteins, shape change and chemotaxis (Buckland et al., 2003; Ling et al., 2004). Chemotaxis and calcium mobilization are also reported for mast cells (Hofstra et al., 2003). However, calcium transients due to receptor activation are not a feature of recombinant expression systems (de Esch et al., 2005; Morse et al., 2001; Oda et al., 2000). Therefore, the coexpression of adapter proteins redirecting the stimulation of the H_4R to robust calcium signals represents a reasonable approach to the development of a functional assay (see also chapter 2 and appendix). Due to the described effects mediated by H_4R activation on immune cells, the blockade of this receptor by antagonists is considered a promising approach to the treatment of diseases like asthma, pruritus, rheumatoid arthritis or inflammatory bowel disease (Lim et al., 2006). In addition, a role of the H_4R in colorectal and breast cancer is currently discussed (Cianchi et al., 2005; Maslinska et al., 2006). The first highly selective H_4R antagonist was JNJ-7777120 (Jablonowski et al., 2003). Current drug research in the hH_4R field is focused on antagonists, mainly due to the prospect of new pharmacotherapies for the treatment of inflammatory diseases. The potential therapeutic value of H_4R agonists is still unclear. However, selective agonists definitely represent valuable tools for the pharmacological investigation of the hH_4R and its splice variants. An agonist with slight selectivity for the hH_4R is OUP-16 (Hashimoto et al., 2003). Interestingly, 5-methylhistamine (also referred to as 4-methylhistamine), which was reported as a selective hH_2R agonist in the 1970s, turned out to be considerably more potent as a hH_4R agonist (Lim et al., 2005). In contrast to the aforementioned agonists, UR-PI376, a compound developed in our workgroup, is an hH_4R selective agonist devoid of agonistic activity at other histamine receptor subtypes (Igel, 2008).

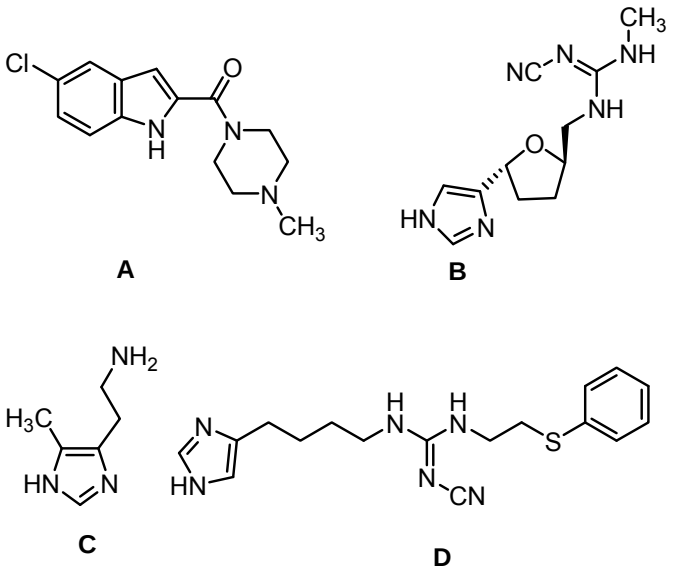

Fig. 1.12: *Chemical structures of H_4R ligands:* **A***: the H_4R antagonist JNJ-7777120; the H_4R agonists OUP-16 (***B***), 5-methylhistamine (***C***) and UR-PI376 (***D***).*

1.3 References

Arrang, J.-M., Garbarg, M., Schwartz, J.-C., 1983. Auto-inhibition of brain histamine release mediated by a novel class (H_3) of histamine receptor. *Nature* **302**, 832-837.

Arrang, J.M., Garbarg, M., Lancelo, J.C., Lecomte, J.M., Pollard, H., Robba, M., Schunack, W., Schwartz, J.C., 1987a. Highly potent and selective ligands for histamine H_3-receptors. *Nature* **327**, 117-123.

Arrang, J.M., Garbarg, M., Schwartz, J.C., 1987b. Autoinhibition of histamine synthesis mediated by presynaptic H_3-receptors. *Neuroscience* **23**, 149-157.

Babe, K.S., Serafín, W.E., 1996. Histamine, bradicinine and its antagonists. In: *Pharmacological bases of therapeutics*, Goodman, A., Gilman (Eds.). México, DF: Interamerican McGraw-Hill, pp. 621-641.

Barak, N., 2008. Betahistine: what's new on the agenda? *Expert Opin. Investig. Drugs* **17**, 795-804.

Barbier, A.J., Berridge, C., Dugovic, C., Laposky, A.D., Wilson, S.J., Boggs, J., Aluisio, L., Lord, B., Mazur, C., Pudiak, C.M., et al., 2004. Acute wake-promoting actions of JNJ-5207852, a novel, diamine-based H_3 antagonist. *Br. J. Pharmacol.* **143**, 649-661.

Baumann, G., Permanetter, B., Wirtzfeld, A., 1984. Possible value of H_2-receptor agonists for treatment of catecholamine-insensitive congestive heart failure. *Pharmacol. Ther.* **24**, 165-177.

Beaven, M.A., 1982. Factors Regulating Availability of Histamine at Tissue Receptors. In: *Pharmacology of Histamine Receptors*, Ganellin, C.R., Parsons, M.E. (Eds.). Wright PSG, Bristol, London, Boston, pp. 102-145.

Benedito, S., Prieto, D., Nielsen, P., Nyborg, N., 1991. Histamine induces endothelium-dependent relaxation of bovine retinal arteries. *Invest. Ophthalmol. Vis. Sci.* **32**, 32-38.

Black, J.W., Duncan, W.A.M., Durant, C.J., Ganellin, C.R., Parsons, E.M., 1972. Definition and Antagonism of Histamine H_2-receptors. *Nature* **236**, 385-390.

Bongers, G., Bakker, R.A., Leurs, R., 2007. Molecular aspects of the histamine H3 receptor. *Biochem. Pharmacol.* **73**, 1195-1204.

Bourne, H.R., 1997. How receptors talk to trimeric G proteins. *Curr. Opin. Cell Biol.* **9**, 134-142.

Bridges, T.M., Lindsley, C.W., 2008. G-Protein-Coupled Receptors: From Classical Modes of Modulation to Allosteric Mechanisms. *ACS Chem. Biol.* **3**, 530-541.

Browman, K.E., Komater, V.A., Curzon, P., Rueter, L.E., Hancock, A.A., Decker, M.W., Fox, G.B., 2004. Enhancement of prepulse inhibition of startle in mice by the H_3 receptor antagonists thioperamide and ciproxifan. *Behav. Brain Res.* **153**, 69-76.

Buckland, K.F., Williams, T.J., Conroy, D.M., 2003. Histamine induces cytoskeletal changes in human eosinophils via the H_4 receptor. *Br. J. Pharmacol.* **140**, 1117-1127.

Buschauer, A., 1989. Synthesis and in vitro pharmacology of arpromidine and related phenyl(pyridylalkyl)guanidines, a potential new class of positive inotropic drugs. *J. Med. Chem.* **32**, 1963-1970.

Cabrera-Vera, T.M., Vanhauwe, J., Thomas, T.O., Medkova, M., Preininger, A., Mazzoni, M.R., Hamm, H.E., 2003. Insights into G Protein Structure, Function, and Regulation. *Endocr. Rev.* **24**, 765-781.

Cannon, K.E., Leurs, R., Hough, L.B., 2007. Activation of peripheral and spinal histamine H_3 receptors inhibits formalin-induced inflammation and nociception, respectively. *Pharmacol. Biochem. Behav.* **88**, 122-129.

Cannon, K.E., Nalwalk, J.W., Stadel, R., Ge, P., Lawson, D., Silos-Santiago, I., Hough, L.B., 2003. Activation of spinal histamine H_3 receptors inhibits mechanical nociception. *Eur. J. Pharmacol.* **470**, 139-147.

Casey, P.J., 1994. Lipid modifications of G proteins. *Curr. Opin. Cell Biol.* **6**, 219-225.

Cherezov, V., Rosenbaum, D.M., Hanson, M.A., Rasmussen, S.G.F., Thian, F.S., Kobilka, T.S., Choi, H.-J., Kuhn, P., Weis, W.I., Kobilka, B.K., et al., 2007. High-Resolution Crystal Structure of an Engineered Human 2-Adrenergic G Protein Coupled Receptor. *Science* **318**, 1258-1265.

Christopoulos, A., Kenakin, T., 2002. G Protein-Coupled Receptor Allosterism and Complexing. *Pharmacol. Rev.* **54**, 323-374.

Cianchi, F., Cortesini, C., Schiavone, N., Perna, F., Magnelli, L., Fanti, E., Bani, D., Messerini, L., Fabbroni, V., Perigli, G., et al., 2005. The Role of Cyclooxygenase-2 in Mediating the Effects of Histamine on Cell Proliferation and Vascular Endothelial Growth Factor Production in Colorectal Cancer. *Clin. Cancer. Res.* **11**, 6807-6815.

Clark, A.J., 1933. *The mode of action of drugs on cells.* Edward Arnold, London

Clark, A.J., 1937. General Pharmacology. In: *Heffner's Handbuch der Experimentellen Pharmakologie. Ergänzungswerk, Band 4*. Springer-Verlag, Berlin Heidelberg New York.

Cogé, F., Guénin, S.-P., Rique, H., Boutin, J.A., Galizzi, J.-P., 2001a. Structure and Expression of the Human Histamine H_4-Receptor Gene. *Biochem. Biophys. Res. Commun.* **284**, 301-309.

Cogé, F., Guénin, S.P., Audinot, V., Renouard-Try, A., Beauverger, P., Macia, C., Ouvry, C., Nagel, N., Rique, H., Boutin, J.A., et al., 2001b. Genomic organization and characterization of splice variants of the human histamine H_3 receptor. *Biochem. J.* **355**, 279-288.

Damaj, B.B., Becerra, C.B., Esber, H.J., Wen, Y., Maghazachi, A.A., 2007. Functional Expression of H_4 Histamine Receptor in Human Natural Killer Cells, Monocytes, and Dendritic Cells. *J. Immunol.* **179**, 7907-7915.

De Backer, M.D., Gommeren, W., Moereels, H., Nobels, G., Vangompel, P., Leysen, J.E., Luyten, W.H.M.L., 1993. Genomic Cloning, Heterologous Expression and Pharmacological Characterization of a Human Histamine H_1 Receptor. *Biochem. Biophys. Res. Commun.* **197**, 1601-1608.

de Esch, I.J.P., Thurmond, R.L., Jongejan, A., Leurs, R., 2005. The histamine H_4 receptor as a new therapeutic target for inflammation. *Trends Pharmacol. Sci.* **26**, 462-469.

De Lean, A., Stadel, J., Lefkowitz, R., 1980. A ternary complex model explains the agonist-specific binding properties of the adenylate cyclase-coupled beta-adrenergic receptor. *J. Biol. Chem.* **255**, 7108-7117.

Durant, G.J., Ganellin, C.R., Parsons, M.E., 1975. Chemical differentiation of histamine H_1- and H_2-receptor agonists. *J. Med. Chem.* **18**, 905-909.

Elz, S., Kramer, K., Pertz, H.H., Detert, H., ter Laak, A.M., Kuhne, R., Schunack, W., 2000. Histaprodifens: Synthesis, Pharmacological in Vitro Evaluation, and Molecular Modeling of a New Class of Highly Active and Selective Histamine H_1-Receptor Agonists. *J. Med. Chem.* **43**, 1071-1084.

Eriks, J.C., Van der Goot, H., Sterk, G.J., Timmerman, H., 1992. Histamine H_2-receptor agonists. Synthesis, in vitro pharmacology, and qualitative structure-activity relationships of substituted 4- and 5-(2-aminoethyl)thiazoles. *J. Med. Chem.* **35**, 3239-3246.

Esbenshade, T.A., Browman, K.E., Bitner, R.S., Strakhova, M., Cowart, M.D., Brioni, J.D., 2008. The histamine H_3 receptor: an attractive target for the treatment of cognitive disorders. *Br. J. Pharmacol.* **154**, 1166-1181.

Esbenshade, T.A., Kang, C.H., Krueger, K.M., Miller, T.R., Witte, D.G., Roch, J.M., Masters, J.N., Hancock, A.A., 2003. Differential Activation of Dual Signaling Responses by Human H_1 and H_2 Histamine Receptors. *J. Recept. Signal Transduct.* **23**, 17 - 31.

Fang, Y., Lahiri, J., Picard, L., 2003. G protein-coupled receptor microarrays for drug discovery. *Drug Discov. Today* **8**, 755-761.

Felix, S.B., Buschauer, A., Baumann, G., 1995. Haemodynamic profile of new H_2-receptor agonists in congestive heart failure. *Eur. J. Clin. Invest.* **25, Suppl. 1**, 42-46.

Fredriksson, R., Lagerström, M.C., Lundin, L.-G., Schiöth, H.B., 2003. The G-Protein-Coupled Receptors in the Human Genome Form Five Main Families. Phylogenetic Analysis, Paralogon Groups, and Fingerprints. *Mol. Pharmacol.* **63**, 1256-1272.

Gantner, F., Sakai, K., Tusche, M.W., Cruikshank, W.W., Center, D.M., Bacon, K.B., 2002. Histamine H_4 and H_2 Receptors Control Histamine-Induced Interleukin-16 Release from Human $CD8^+$ T Cells. *J. Pharmacol. Exp. Ther.* **303**, 300-307.

Gantz, I., Munzert, G., Tashiro, T., Schäffer, M., Wang, L., DelValle, J., Yamada, T., 1991. Molecular cloning of the human histamine H_2 receptor. *Biochem. Biophys. Res. Commun.* **178**, 1386-1392.

Gbahou, F., Vincent, L., Humbert-Claude, M., Tardivel-Lacombe, J., Chabret, C., Arrang, J.-M., 2006. Compared pharmacology of human histamine H_3 and H_4 receptors: structure–activity relationships of histamine derivatives. *Br. J. Pharmacol.* **147**, 744-754.

Ghorai, P., Kraus, A., Keller, M., Götte, C., Igel, P., Schneider, E., Schnell, D., Bernhardt, G., Dove, S., Zabel, M., et al., 2008. Acylguanidines as Bioisosteres of Guanidines: N^G-Acylated Imidazolylpropylguanidines, a New Class of Histamine H_2 Receptor Agonists. *J. Med. Chem.* **51**, 7193-7204.

Giovannini, M.G., Bartolini, L., Bacciottini, L., Greco, L., Blandina, P., 1999. Effects of histamine H_3 receptor agonists and antagonists on cognitive performance and scopolamine-induced amnesia. *Behav. Brain Res.* **104**, 147-155.

Govoni, M., Bakker, R.A., van de Wetering, I., Smit, M.J., Menge, W.M.B.P., Timmerman, H., Elz, S., Schunack, W., Leurs, R., 2003. Synthesis and Pharmacological Identification of Neutral Histamine H_1-Receptor Antagonists. *J. Med. Chem.* **46**, 5812-5824.

Haas, H.L., Greene, R.W., Heimrich, B., Xie, X., 1988. LTP in slices from human hippocampus. In: *Synaptic Plasticity in the Hippocampus*, Haas, H.L., Buzsaki, G. (Eds.). Berlin: Springer, pp. 77-80.

Haas, H.L., Wolf, P., 1977. Central actions of histamine: Microelectrophoretic studies. *Brain Res.* **122**, 269-279.

Hanson, M.A., Stevens, R.C., 2009. Discovery of New GPCR Biology: One Receptor Structure at a Time. *Structure* **17**, 8-14.

Hashimoto, T., Harusawa, S., Araki, L., Zuiderveld, O.P., Smit, M.J., Imazu, T., Takashima, S., Yamamoto, Y., Sakamoto, Y., Kurihara, T., et al., 2003. A Selective Human H_4-Receptor Agonist: (-)-2-Cyano-1-methyl-3-{(2R,5R)-5- [1H-imidazol-4(5)-yl]tetrahydrofuran-2-yl}methylguanidine. *J. Med. Chem.* **46**, 3162-3165.

Hill, S., 1990. Distribution, properties, and functional characteristics of three classes of histamine receptor. *Pharmacol. Rev.* **42**, 45-83.

Hill, S.J., Baker, J.G., Rees, S., 2001. Reporter-gene systems for the study of G-protein-coupled receptors. *Curr. Opin. Pharmacol.* **1**, 526-532.

Hill, S.J., Ganellin, C.R., Timmerman, H., Schwartz, J.C., Shankley, N.P., Young, J.M., Schunack, W., Levi, R., Haas, H.L., 1997. International Union of Pharmacology. XIII. Classification of Histamine Receptors. *Pharmacol. Rev.* **49**, 253-278.

Hofstra, C.L., Desai, P.J., Thurmond, R.L., Fung-Leung, W.-P., 2003. Histamine H_4 Receptor Mediates Chemotaxis and Calcium Mobilization of Mast Cells. *J. Pharmacol. Exp. Ther.* **305**, 1212-1221.

Hopkins, A.L., Groom, C.R., 2002. The druggable genome. *Nat. Rev. Drug Discov.* **1**, 727-730.

Horner, W.E., Johnson, D.E., Schmidt, A.W., Rollema, H., 2007. Methylphenidate and atomoxetine increase histamine release in rat prefrontal cortex. *Eur. J. Pharmacol.* **558**, 96-97.

Hough, L.B., 2001. Genomics Meets Histamine Receptors: New Subtypes, New Receptors. *Mol. Pharmacol.* **59**, 415-419.

Igel, P., 2008. Synthesis and structure-activity relationships of N^G-acylated arylalkylguanidines and related compounds as histamine receptor ligands: Searching for selective H_4R agonists. In: *Doctoral Thesis, University of Regensburg*. http://www.opus-bayern.de/uni-regensburg/volltexte/2009/1107/.

Jaakola, V.-P., Griffith, M.T., Hanson, M.A., Cherezov, V., Chien, E.Y.T., Lane, J.R., IJzerman, A.P., Stevens, R.C., 2008. The 2.6 Angstrom Crystal Structure of a Human A_{2A} Adenosine Receptor Bound to an Antagonist. *Science* **322**, 1211-1217.

Jablonowski, J.A., Grice, C.A., Chai, W., Dvorak, C.A., Venable, J.D., Kwok, A.K., Ly, K.S., Wei, J., Baker, S.M., Desai, P.J., et al., 2003. The First Potent and Selective Non-Imidazole Human Histamine H_4 Receptor Antagonists. *J. Med. Chem.* **46**, 3957-3960.

Jacoby, E., Bouhelal, R., Gerspacher, M., Seuwen, K., 2006. The 7 TM G-Protein-Coupled Receptor Target Family. *ChemMedChem* **1**, 760-782.

Karoor, V., Malbon, C.C., David S. Goldstein, G.E., Richard, M., 1997. G-Protein-Linked Receptors as Substrates for Tyrosine Kinases: Cross-Talk in Signaling. *Adv. Pharmacol.* **42**, 425-428.

Kenakin, T., Morgan, P., Lutz, M., Weiss, J., 2000. The evolution of drug-receptor models: The cubic ternary complex model for G protein-coupled receptors. In: *Handbook of Experimental Pharmacology.* Vol. 148, Kenakin, T., Angus, J.A. (Eds.). Springer-Verlag, Berlin Heidelberg New York, pp. 147-165.

Kenakin, T.P., 1989. Challenges for receptor theory as a tool for drug and drug receptor classification. *Trends Pharmacol. Sci.* **10**, 18-22.

Kew, J.N.C., Trube, G., Kemp, J.A., 1996. A novel mechanism of activity-dependent NMDA receptor antagonism describes the effect of ifenprodil in rat cultured cortical neurones. *J. Physiol. (Lond).* **497.3**, 761-772.

Kotlikoff, M.I., Murray, R.K., Reynolds, E.E., 1987. Histamine-induced calcium release and phorbol antagonism in cultured airway smooth muscle cells. *Am. J. Physiol.* **253**, 561-566.

Kraus, A., 2007. Highly potent, Selective Acylguanidine-Type Histamine H_2 Receptor Agonists: Synthesis and Structure-Activity Relationships. In: *Doctoral Thesis, University of Regensburg*. http://www.opus-bayern.de/uni-regensburg/volltexte/2008/904/.

Kraus, A., Ghorai, P., Birnkammer, T., Schnell, D., Elz, S., Seifert, R., Dove, S., Bernhardt, G., Buschauer, A., 2009. N^G-Acylated Aminothiazolylpropylguanidines as Potent and Selective Histamine H_2 Receptor Agonists. *ChemMedChem* **4**, 232-240.

Kristiansen, K., 2004. Molecular mechanisms of ligand binding, signaling, and regulation within the superfamily of G-protein-coupled receptors: molecular modeling and mutagenesis approaches to receptor structure and function. *Pharmacol. Ther.* **103**, 21-80.

Lagerström, M.C., Schiöth, H.B., 2008. Structural diversity of G protein-coupled receptors and significance for drug discovery. *Nat. Rev. Drug Discov.* **7**, 339-357.

Leff, P., 1995. The two-state model of receptor activation. *Trends Pharmacol. Sci.* **16**, 89-97.

Leschke, C., Elz, S., Garbarg, M., Schunack, W., 1995. Synthesis and Histamine H_1 Receptor Agonist Activity of a Series of 2-Phenylhistamines, 2-Heteroarylhistamines, and Analogs. *J. Med. Chem.* **38**, 1287-1294.

Leurs, R., Bakker, R.A., Timmerman, H., de Esch, I.J.P., 2005. The histamine H_3 receptor: from gene cloning to H_3 receptor drugs. *Nat. Rev. Drug Discov.* **4**, 107-120.

Leurs, R., Smit, M.J., Timmerman, H., 1995. Molecular pharmacological aspects of histamine receptors. *Pharmacol. Ther.* **66**, 413-463.

Leurs, R., Smit, M.J., Wiro, M.B.P., Timmerman, H., 1994. Pharmacological characterization of the human histamine H_2 receptor stably expressed in Chinese hamster ovary cells. *Br. J. Pharmacol.* **112**, 847-854.

Levi, R., Alloatti, G., 1988. Histamine modulates calcium current in guinea pig ventricular myocytes. *J. Pharmacol. Exp. Ther.* **246**, 377-383.

Ligneau, X., Lin, J.-S., Vanni-Mercier, G., Jouvet, M., Muir, J.L., Ganellin, C.R., Stark, H., Elz, S., Schunack, W., Schwartz, J.-C., 1998. Neurochemical and Behavioral Effects of Ciproxifan, A Potent Histamine H_3-Receptor Antagonist. *J. Pharmacol. Exp. Ther.* **287**, 658-666.

Lim, H.D., Smits, R.A., Leurs, R., De Esch, I.J.P., 2006. The Emerging Role of the Histamine H_4 Receptor in Anti-inflammatory Therapy. *Curr. Top. Med. Chem.* **6**, 1365-1373.

Lim, H.D., van Rijn, R.M., Ling, P., Bakker, R.A., Thurmond, R.L., Leurs, R., 2005. Evaluation of Histamine H_1-, H_2-, and H_3-Receptor Ligands at the Human Histamine H_4 Receptor: Identification of 4-Methylhistamine as the First Potent and Selective H_4 Receptor Agonist. *J. Pharmacol. Exp. Ther.* **314**, 1310-1321.

Lin, J.S., 2000. Brain structures and mechanisms involved in the control of cortical activation and wakefulness, with emphasis on the posterior hypothalamus and histaminergic neurons. *Sleep Med. Rev.* **4**, 471-503.

Ling, P., Ngo, K., Nguyen, S., Thurmond, R.L., Edwards, J.P., Karlsson, L., Fung-Leung, W.-P., 2004. Histamine H_4 receptor mediates eosinophil chemotaxis with cell shape change and adhesion molecule upregulation. *Br. J. Pharmacol.* **142**, 161-171.

Liu, C., Ma, X.-J., Jiang, X., Wilson, S.J., Hofstra, C.L., Blevitt, J., Pyati, J., Li, X., Chai, W., Carruthers, N., et al., 2001. Cloning and Pharmacological Characterization of a Fourth Histamine Receptor (H_4) Expressed in Bone Marrow. *Mol. Pharmacol.* **59**, 420-426.

Lovenberg, T.W., Roland, B.L., Wilson, S.J., Jiang, X., Pyati, J., Huvar, A., Jackson, M.R., Erlander, M.G., 1999. Cloning and Functional Expression of the Human Histamine H_3 Receptor. *Mol. Pharmacol.* **55**, 1101-1107.

Luttrell, L.M., 2008. Reviews in Molecular Biology and Biotechnology: Transmembrane Signaling by G Protein-Coupled Receptors. *Mol. Biotechnol.* **39**, 239-264.

Majno, G., Shea, S.M., Leventhal, M., 1969. Endothelial contraction induced by histamine-type mediators: An Electron Microscopic Study. *J. Cell Biol.* **42**, 647-672.

Maslinska, D., Laure-Kamionowska, M., Maslinski, K., Deregowski, K., Szewczyk, G., Maslinski, S., 2006. Histamine H_4 receptors on mammary epithelial cells of the human breast with different types of carcinoma. *Inflammation Res.* **55**, S77-S78.

Menghin, S., Pertz, H.H., Kramer, K., Seifert, R., Schunack, W., Elz, S., 2003. N^{α}-Imidazolylalkyl and Pyridylalkyl Derivatives of Histaprodifen: Synthesis and in Vitro Evaluation of Highly Potent Histamine H_1-Receptor Agonists. *J. Med. Chem.* **46**, 5458-5470.

Millán-Guerrero, R.O., Pineda-Lucatero, A.G., Hernández-Benjamín, T., Tene, C.E., Pacheco, M.F., 2003. N^{α}-Methylhistamine Safety and Efficacy in Migraine Prophylaxis: Phase I and Phase II Studies. *Headache* **43**, 389-394.

Miller, W.E., Lefkowitz, R.J., 2001. Expanding roles for β-arrestins as scaffolds and adapters in GPCR signaling and trafficking. *Curr. Opin. Cell Biol.* **13**, 139-145.

Milligan, G., Bond, R.A., 1997. Inverse agonism and the regulation of receptor number. *Trends Pharmacol. Sci.* **18**, 468-474.

Morisset, S., Rouleau, A., Ligneau, X., Gbahou, F., Tardivel-Lacombe, J., Stark, H., Schunack, W., Ganellin, C.R., Arrang, J.-M., 2000. High constitutive activity of native H_3 receptors regulates histamine neurons in brain. *Nature* **408**, 860-864.

Morse, K.L., Behan, J., Laz, T.M., West, R.E., Jr., Greenfeder, S.A., Anthes, J.C., Umland, S., Wan, Y., Hipkin, R.W., Gonsiorek, W., et al., 2001. Cloning and Characterization of a Novel Human Histamine Receptor. *J. Pharmacol. Exp. Ther.* **296**, 1058-1066.

Nakamura, T., Itadani, H., Hidaka, Y., Ohta, M., Tanaka, K., 2000. Molecular Cloning and Characterization of a New Human Histamine Receptor, HH4R. *Biochem. Biophys. Res. Commun.* **279**, 615-620.

Nguyen, T., Shapiro, D.A., George, S.R., Setola, V., Lee, D.K., Cheng, R., Rauser, L., Lee, S.P., Lynch, K.R., Roth, B.L., et al., 2001. Discovery of a Novel Member of the Histamine Receptor Family. *Mol. Pharmacol.* **59**, 427-433.

Nygaard, R., Frimurer, T.M., Holst, B., Rosenkilde, M.M., Schwartz, T.W., 2009. Ligand binding and micro-switches in 7TM receptor structures. *Trends Pharmacol. Sci.* **30**, 249-259.

O'Reilly, M., Alpert, R., Jenkinson, S., Gladue, R.P., Foo, S., Trim, S., Peter, B., Trevethick, M., Fidock, M., 2002. Identification of a histamine H_4 receptor on human eosinophils-role in eosinophil chemotaxis. *J. Recept. Signal Transduct.* **22**, 431 - 448.

Oda, T., Morikawa, N., Saito, Y., Masuho, Y., Matsumoto, S.-i., 2000. Molecular Cloning and Characterization of a Novel Type of Histamine Receptor Preferentially Expressed in Leukocytes. *J. Biol. Chem.* **275**, 36781-36786.

Palczewski, K., Kumasaka, T., Hori, T., Behnke, C.A., Motoshima, H., Fox, B.A., Trong, I.L., Teller, D.C., Okada, T., Stenkamp, R.E., et al., 2000. Crystal Structure of Rhodopsin: A G Protein-Coupled Receptor. *Science* **289**, 739-745.

Parsons, M.E., Ganellin, C.R., 2006. Histamine and its receptors. *Br. J. Pharmacol.* **147(S1)**, S127-S135.

Perez, D.M., Karnik, S.S., 2005. Multiple Signaling States of G-Protein-Coupled Receptors. *Pharmacol. Rev.* **57**, 147-161.

Perry, S.J., Lefkowitz, R.J., 2002. Arresting developments in heptahelical receptor signaling and regulation. *Trends Cell Biol.* **12**, 130-138.

Prell, G.D., Green, J.P., Kaufmann, C.A., Khandelwal, J.K., Morrishow, A.M., Kirch, D.G., Linnoila, M., Wyatt, R.J., 1995. Histamine metabolites in cerebrospinal fluid of patients with chronic schizophrenia: their relationships to levels of other aminergic transmitters and ratings of symptoms. *Schizophr. Res.* **14**, 93-104.

Rasmussen, S.G.F., Choi, H.-J., Rosenbaum, D.M., Kobilka, T.S., Thian, F.S., Edwards, P.C., Burghammer, M., Ratnala, V.R.P., Sanishvili, R., Fischetti, R.F., et al., 2007. Crystal structure of the human β_2 adrenergic G-protein-coupled receptor. *Nature* **450**, 383-387.

Rosenbaum, D.M., Cherezov, V., Hanson, M.A., Rasmussen, S.G.F., Thian, F.S., Kobilka, T.S., Choi, H.-J., Yao, X.-J., Weis, W.I., Stevens, R.C., et al., 2007. GPCR Engineering Yields High-Resolution Structural Insights into β_2-Adrenergic Receptor Function. *Science* **318**, 1266-1273.

Samama, P., Cotecchia, S., Costa, T., Lefkowitz, R., 1993. A mutation-induced activated state of the beta 2-adrenergic receptor. Extending the ternary complex model. *J. Biol. Chem.* **268**, 4625-4636.

Sander, K., Kottke, T., Stark, H., 2008. Histamine H_3 Receptor Antagonists Go to Clinics. *Biol. Pharm. Bull.* **31**, 2163-2181.

Schayer, R.W., 1956. The origin and fate of histamine in the body. In: *Ciba Foundation Symposium on Histamine*, Wolstenholme, G.E.W., O'Connor, C.M. (Eds.). London: J. and A. Churchill Ltd., pp. 183-188.

Smrcka, A.V., 2008. G protein βγ subunits: Central mediators of G protein-coupled receptor signaling. *Cell. Mol. Life Sci.* **65**, 2191-2214.

Soll, A.H., Berglindh, T., 1987. Physiology of isolated gastric glands and parietal cells: receptors and effectors regulating function In: *Physiology of the gastrointestinal tract*, Johnson, L.R. (Ed.). New York: Raven Press, pp. 883-909.

Sternweis, P., Northup, J., Smigel, M., Gilman, A., 1981. The regulatory component of adenylate cyclase. Purification and properties. *J. Biol. Chem.* **256**, 11517-11526.

Thomsen, W., Frazer, J., Unett, D., 2005. Functional assays for screening GPCR targets. *Curr. Opin. Biotechnol.* **16**, 655-665.

Tokita, S., Takahashi, K., Kotani, H., 2006. Recent Advances in Molecular Pharmacology of the Histamine Systems: Physiology and Pharmacology of Histamine H_3 Receptor: Roles in Feeding Regulation and Therapeutic Potential for Metabolic Disorders. *J. Pharmacol. Sci.* **101**, 12-18.

Topiol, S., Sabio, M., 2009. X-ray structure breakthroughs in the GPCR transmembrane region. *Biochem. Pharmacol.* **78**, 11-20.

van Rijn, R.M., van Marle, A., Chazot, P.L., Langemeijer, E., Qin, Y., Shenton, F.C., Lim, H.D., Zuiderveld, O.P., Sansuk, K., Dy, M., et al., 2008. Cloning and characterization of dominant negative splice variants of the human histamine H_4 receptor. *Biochem. J.* **414**, 121-131.

Varty, L.M., Gustafson, E., Laverty, M., Hey, J.A., 2004. Activation of histamine H_3 receptors in human nasal mucosa inhibits sympathetic vasoconstriction. *Eur. J. Pharmacol.* **484**, 83-89.

Warne, T., Serrano-Vega, M.J., Baker, J.G., Moukhametzianov, R., Edwards, P.C., Henderson, R., Leslie, A.G.W., Tate, C.G., Schertler, G.F.X., 2008. Structure of a β_1-adrenergic G-protein-coupled receptor. *Nature* **454**, 486-491.

Wiedemann, P., Bönisch, H., Oerters, F., Brüss, M., 2002. Structure of the human histamine H_3 receptor gene (HRH3) and identification of naturally occurring variations. *J. Neural Transm.* **109**, 443-453.

Zhu, Y., Michalovich, D., Wu, H.-L., Tan, K.B., Dytko, G.M., Mannan, I.J., Boyce, R., Alston, J., Tierney, L.A., Li, X., et al., 2001. Cloning, Expression, and Pharmacological Characterization of a Novel Human Histamine Receptor. *Mol. Pharmacol.* **59**, 434-441.

Zingel, V., Elz, S., Schunack, W., 1990. Histamine analogues. 33rd communication: 2-phenylhistamines with high histamine H_1-agonistic activity. *Eur. J. Med. Chem.* **25**, 673-680.

Chapter 2

Scope and objectives

Within the research programme of the Graduiertenkolleg (Research Training Group) Medicinal Chemistry (GRK 760) at the University of Regensburg, special effort is made on the design, synthesis and pharmacological investigation of selective agonists and antagonists of histamine receptors. As a sub-project of this complex multidisciplinary project, this work is aiming at the development of binding and functional assays for the human histamine H_1, H_2 and H_4 receptor, respectively. Such methods are required for the screening of compound libraries and the detailed pharmacological characterisation of substances with respect to affinity, potency and quality of action (agonism or antagonism), and receptor subtype selectivity.

In order to economize the characterisation of ligand effects on hH_1R-expressing cells, spectrofluorimetric measurements of agonist-mediated intracellular calcium mobilization using the fluorescent calcium chelator fura-2 ought to be adapted to the microtitre format. For assay validation, the agonist histamine and a series of reference antagonists will be investigated and compared with data reported in the literature. Since the applicability of the procedure for the investigation of compound libraries ought to be considered, different series of such libraries provided by Origenis GmbH (Martinsried, Germany) should be investigated for their effects on the hH_1R with optimized assay parameters. Radioligand binding studies using the four human histamine receptor subtypes represents a straight forward approach in order to elaborate receptor-selectivity of hits identified in the screening programme.

HEK293 cells will be investigated for their suitability to express human histamine receptor subtypes using mRNA analysis and Western Blot experiments.

As histamine H_2 receptors are coupling to G_s, cells will be genetically engineered by the cDNA encoding the hH_2R and the chimeric G-protein qs5-HA in order to redirect the activation of the receptor to an increase in the intracellular calcium level. Calcium transients ought to be determined by fura-2 assay in a spectrofluorimetric or a microtitre format, respectively. Furthermore, cotransfection of the mitochondrially targeted apoaequorin should enable the performance of bioluminescence-based calcium measurements in the microtitre format.

In order to explore the scope of applications of fluorescent selective histamine receptor ligands in cellular studies, fluorescence-labelled H_2R ligands will be investigated for receptor binding on transfected cells using confocal microscopy and flow cytometry. For validation, the affinities of known H_2R ligands will be determined in flow cytometric competition binding experiments using the fluorescent tracers. Additionally, for comparison of the pharmacological results from flow cytometric measurements with data determined by conventional methods, it is planned to establish a radioligand binding assay.

Although the assay procedures developed for the hH_2R should in principle be transferable to the hH_4R, cAMP measurements are planned in addition to the determination of calcium transients.

Chapter 3

Adaptation of the fura-2 assay to the microtitre format for the screening of ligands of the human histamine H_1 receptor

3.1 Introduction

Measurements of intracellular calcium transients are a popular method for the determination of ligand activity at GPCRs. Favoured readout systems are the FLIPR-assay which uses the non-ratiometric, calcium chelating dye fluo-4 or the aequorin-assay (Siehler, 2008; Takahashi et al., 1999). Both assays are applicable to the microtitre format (Siehler, 2008). In our workgroup, a spectrofluorimetric assay in cuvettes for the human histamine H_1 receptor (hH_1R) was developed using the ratiometric fluorescent dye fura-2 (Kracht, 2001). Fura-2 as a ratiometric Ca^{2+}-indicator shows a shift of the excitation maximum upon Ca^{2+} binding (Fig. 3.1). By measuring fluorescence emission intensities upon excitation at two different wavelengths, pairs of data are generated, of which a ratio can be calculated. Fura-2 is excited alternately at 340 and 380 nm and in both cases the fluorescence emission at 510 nm is determined. Ratiometric dyes have several advantages over non-ratiometric indicators e.g. that the signal is nearly independent of intracellular dye concentration and almost not influenced by dye leakage. Moreover, the measurement is not affected by fluctuations in illumination intensity.

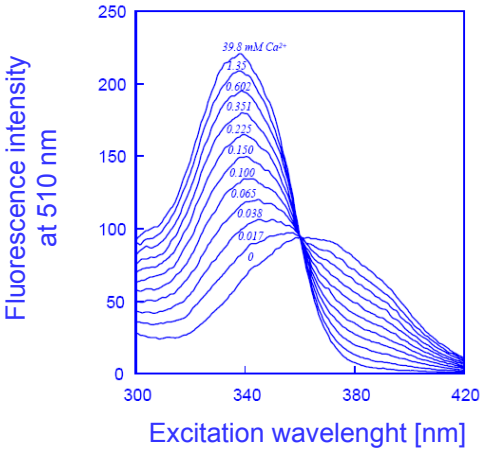

Fig. 3.1: *Spectral properties of the calcium-chelating dye fura-2. Increasing amounts of Ca^{2+} lead to an increased fluorescence intensity at 510 nm upon excitation with 340 nm, whereas the respective emission upon excitation with 380 nm is decreased (Gessele, 1998).*

This study aimed at the exploitation of the ratiometic detection in microplates with respect to a higher throughput compared to measurements in cuvettes to save costs and time. When equipped with an injector, fluorescent plate readers such as the GENios Pro™ (Tecan, Salzburg, Austria) enable automatic measurements of calcium transients in either the 96-well or the 384-well format, respectively.

As a GENios Pro™ plate reader was available, human U-373 MG glioblastoma cells, constitutively expressing the hH_1R (Arias-Montaño et al., 1994) were investigated for calcium responses upon histamine challenge before the effects of hH_1R-antagonists on the agonist mediated calcium signals were determined. Measurements were performed in the 96-well

and the 384-well format. The chemical structures of the investigated ligands can be found in the general introduction (chapter 1).

As Origenis GmbH (Martinsried, Germany) is interested in substances for undisclosed pharmaceutical targets, different series of compound families provided by this company were investigated for their effects on the hH_1R. In the scope of this cooperation, substances were both investigated in the 96-well and the 384-well format for their hH_1R activity. The results from those investigations were considered for the optimization of specific biopharmacological parameters of different compound series in order to achieve the desired behaviour. Radioligand binding experiments were performed for all human histamine receptor subtypes in order to elaborate receptor-selectivity of selected potent compounds which were previously identified within the screening programme.

3.2 Materials and methods

3.2.1 Cell culture

The human U-373 MG (HTB-17) glioblastoma cells were obtained from the American Type Culture Collection (ATCC, Rockville, USA). Cells were cultured in Eagle´s minimum essential medium (EMEM, Sigma, Deisenhofen, Germany) containing L-glutamine, 2.2 g / L $NaHCO_3$, 110 mg / L sodium pyruvate and 5 % fetal bovine serum (FBS, Biochrom, Berlin, Germany). Cells were maintained in a water saturated atmosphere (95 % air / 5 % carbon dioxide) at 37 °C in 75-cm² culture flasks (Nunc, Wiesbaden, Germany) and serially passaged following trypsinization using 0.05 % trypsin / 0.02 % EDTA. Passaging was performed once a week by 1:10 dilution after trypsin / EDTA treatment for approx. 5 min. The trypsin / EDTA stock solution (PAA, Pasching, Austria) was 1:10 diluted with phosphate buffered saline (PBS: KCl 2.7 mM; KH_2PO_4 1.5 mM; NaCl 137 mM; Na_2HPO_4 5.6 mM; NaH_2PO_4 1.1 mM in Millipore water, pH 7.4; all chemicals were from Merck, Darmstadt, Germany) and sterile-filtered prior to use.

Cell banking and quality control were performed according to the "seed stock concept" (Hay, 1988). Every 3 months, cells were routinely monitored for Mycoplasma contamination by PCR, using the VenorGEM™ kit (Minerva Biolab, Berlin, Germany). Only Mycoplasma free cultures were used.

For cryopreservation, cells were frozen by slow cooling (approx. 1 °C / min) in 9 parts of EMEM supplemented with 5 % FBS and 1 part of DMSO (p. a.) under sterile conditions: cells were stored in the refrigerator for at least 1 h, transferred into the -20 °C freezer for 4 h prior to the storage in the -80 °C freezer over night. Cells were stored under liquid nitrogen after the proof of the absence of mycoplasms. When required, cells were thawn from liquid nitrogen and reseeded at a relatively high concentration to optimize recovery. A cryo vial containing approx. $1 \cdot 10^6$ cells was immersed into a water bath at 37 °C and rapidly shaken. Cells were transferred to a 75-cm^2 flask. 20 mL of EMEM containing 5 % FBS were added dropwise within 1 min. The cells were transferred to the CO_2 incubator for 30 min. When the cells had adhered to the plastic surface, the DMSO-containing medium was removed and replaced by fresh cell culture medium.

3.2.2 Loading of U-373 MG cells with fura-2 / AM

For fura-2 assays, the confluent cells of a 75-cm^2 culture flask were trypsinized and passaged 1:5 into 175-cm^2 culture flasks under sterile conditions. The cells were cultured in a CO_2 incubator for 1 week at 37 °C.

The cell culture medium was removed from the 175-cm^2 culture flasks, cells were trypsinized and detached with EMEM containing 5 % of FBS for trypsine inactivation. Cells were centrifuged at 300 g (Minifuge 2, Heraeus Christ, Osterode, Germany, 5 min), washed and resuspended in loading buffer (NaCl 120 mM; KCl 5 mM; $MgCl_2$ 2 mM; $CaCl_2$ 1.5 mM; HEPES 25 mM; glucose 10 mM in Millipore water, pH 7.4; HEPES was from Serva, Heidelberg, Germany; all other chemicals were from Merck). Cells were counted and adjusted to a density of $1.3 \cdot 10^6$ cells / mL. 0.75 mL of cell suspension were added to 0.25 mL of loading suspension containing 20 mg of BSA (Serva, Heidelberg, Germany), 5 µL of 20 % Pluronic® F-127 / DMSO solution (Pluronic® F-127 was from Calbiochem-Novabiochem Corporation, La Joila, Canada, whereas DMSO was obtained from Merck) and 4 µL of fura-2 / AM (Invitrogen, Karlsruhe, Germany; 1 mM stock solution in anhydrous DMSO) in 1 mL of loading buffer. Final concentrations were: $1 \cdot 10^6$ cells / mL, 1 µM fura-2 / AM, 0.2 % DMSO and 0.025 % Pluronic® F-127. The cells were incubated at room temperature under light protection for 30 min, centrifuged and resuspended in the same volume of loading buffer. The cell suspension was incubated for another 30 min in order to ensure the complete intracellular cleavage of the AM-ester. Cells were washed and resuspended to a density of $1 \cdot 10^6$ cells / mL prior to the assay.

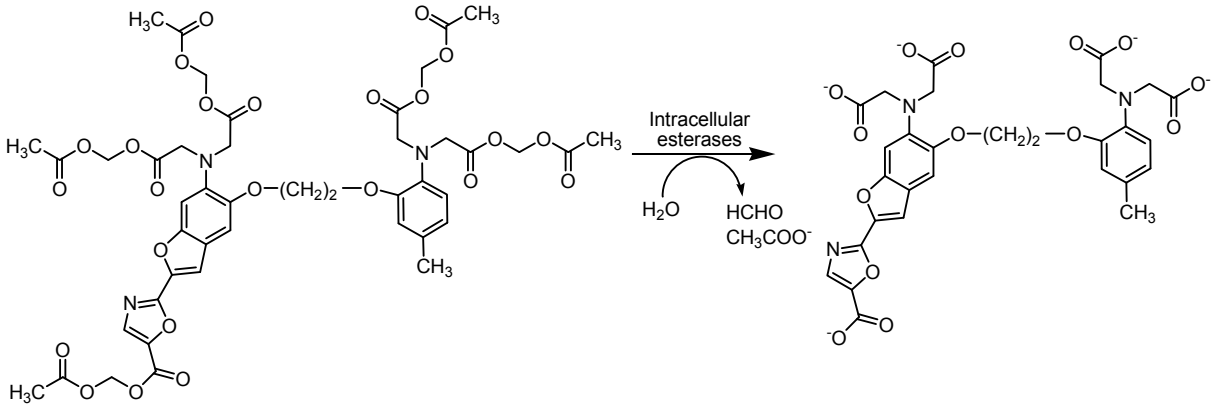

Fig. 3.2: *Cleavage of fura-2 / AM by intracellular esterases. The calcium chelating dye fura-2 is formed by hydrolysis of the ester.*

3.2.3 Investigations on the suitability of the plate reader

3.2.3.1 Ratiometric detection of Ca^{2+}-complexation by fura-2

10 µL of the fura-2 / AM stock solution (1 mM in anhydrous DMSO) were mixed with 4 µL of an esterase from porcine liver (Sigma, 4.6 U / µL of $(NH_4)_2SO_4$ (3 M)) and 86 µL of sodium phosphate buffer (10 mM; pH = 7.4). Incubation was performed at 37 °C for 1 h.
The reaction mixture was diluted with Millipore water to a final volume of 500 µL. 10 µL of this mixture were pipetted per cavity of a transparent 96-well plate (Greiner, Frickenhausen, Germany). 190 µL of calcium-buffers with concentrations ranging from 0 to 39 µM of free Ca^{2+} (Calcium Calibration Buffer Kit #2, Invitrogen) were added to the respective wells.
The plate was inserted into the GENios Pro™ plate reader.
Instrument settings were: measurement mode: endpoint; excitation wavelengths: 340 and 380 nm (alternating), slits: 10 nm (in each case); emission wavelength: 535 nm, slit: 25 nm; gain: 40; number of reads: 3; integration time: 40 µs; lag time: 0 µs; mirror selection: top (dichroic mirror 3); time between move and flash: 100 ms.

3.2.3.2 Effect of the injection-speed on the calcium signal

20 µL of PBS were pipetted into the cavities of a transparent 96-well plate (Greiner).
After 4 aquisition cycles (1 cycle equals to 0.66 s), 160 µL of the cell-suspension ($1 \cdot 10^6$ cells / mL) were added by injector A. After the 79^{th} cycle, 20 µL of a 10-fold concentrated feed solution of histamine (300 µM in PBS; histamine was from Sigma) relative to the final concentration were inserted by injector B in order to elicit a calcium response in the fura-2 loaded cells. The measurement was continued until cycle 200.
Instrument settings were maintained according to section 3.2.3.1 with subsequent modifications: measurement mode: well kinetic; gain: 46-80 (as required for the respective experiment); mirror selection: bottom; well kinetic interval (minimal) 660 ms; injector A delay: 2640 ms; injector B delay: 53040 ms; injector speed (injector A): 25-200 µL / s; injector speed (injector B): 200 µL / s; injection mode: standard.

3.2.4 Investigation of the effect of hH_1R ligands on the mobilisation of intracellular calcium in U-373 MG cells

3.2.4.1 Concentration-dependent increase in the intracellular calcium level by histamine

The cavities of a transparent 96-well plate were loaded with 40 µL of 5-fold concentrated feed solutions of histamine relative to the final concentration (in PBS). Before the 5th cycle, 160 µL of the gently stirred cell suspension ($1 \cdot 10^6$ cells / mL) were added by injector A. Calcium signals were recorded until the 200th cycle was reached. The instrument settings were similar to those specified in 3.2.3.2, but the injection-speed of the cell suspension was reduced to 25 µL / s and the injector B was not used. Furthermore, measurements were performed from top with the dichroic mirror 3.
Most of the instrument settings that were used for the investigation in the 96-well format were maintained in the 384-well format. Minor modifications were the reduction of the measurement time from 200 to 60 cycles and the raise of injection speed from 25 µL / s to 200 µL / s. Furthermore, the volume of agonist and of injected cell suspension was reduced by a factor of 2 compared to the 96-well format.

3.2.4.2 Investigation of H_1R antagonists

3.2.4.2.1 Optimisation of assay parameters

In contrast to the agonist mode (section 3.2.4.1), in the antagonist mode injection of the fura-2 / AM loaded cells did not provide reproducible results. Therefore, cells were preincubated with mepyramine in the microtitre plate before the injection of histamine.
To construct a competiton curve with mepyramine (Sigma), several alternative approaches were performed by using the dichroic mirror 3 from top in the 96-well or the 384-well format, respectively.

3.2.4.2.2 Investigation of standard antagonists in the optimized assay

(*R*)-dimethindene, racemic dimethindene, triprolidine and levocetirizine were obtained from the Origenis company whereas mepyramine was from Sigma.
10-fold concentrated feed solutions compared to the final assay concentration of the respective antagonist were prepared in PBS except levocetirizine: as this ligand is poorly soluble in PBS, the stock solution (10 mM) and the feed solution with the highest

concentration (100 µM) were prepared in 50 % DMSO / PBS (v/v). For the preparation of all lower concentrated feed solutions, PBS was used.

10 µL of 10-fold concentrated feed solutions compared to the final concentration of the respective antagonist in PBS and 80 µL of the fura-2 / AM loaded cell-suspension were pipetted in the cavities of a transparent 384-well plate (Greiner). The plate was allowed to stand under light protection for 15 min at room temperature without movement or mixing. Calcium signals were evoked by injection of histamine (300 µM in PBS; 10 µL) before cycle 5. Recordings were performed for 120 cycles.

3.2.5 Screening of potential H_1R ligands by the mobilisation of intracellular calcium in U-373 MG cells

Transparent 96-well plates (Nunc) were prepared with 10-fold concentrated feed solutions compared to the final concentration of the respective ligands (20 µL in each case, in DMSO / PBS 2.5 % (v/v)) by the Origenis Company. U-373 MG cells were loaded with fura-2 according to section 3.2.2. To enable shaking of the plate for 15 min (speed: 60 rpm, mode: orbital, settle time: 0 s) before starting the kinetic registration in the well kinetic mode, the absorbance of one representative well was measured in the endpoint mode (the software of the GENios Pro™ reader does not allow shaking without preceding injection). After this initial shaking step, the measurement mode was changed to well kinetics. The plate was shaked for another 30 s before the registration of each well kinetic for 160 cycles by injection of histamine (30 µM).

36 compounds were characterised in duplicate per plate. 18 maximum signals and each 3 wells containing mepyramine leading to final assay concentrations of 8 or 100 nM, respectively, were distributed on the plate.

Transparent 384-well plates (Nunc) were assayed according to 3.2.4.2.2. In one assay, one half of the plate was investigated, the second part of the plate was stored at -20 °C and analyzed another day. 160 compounds were investigated in duplicate per plate. 32 maximal signals and each 16 wells with mepyramine according to final concentrations of 8 or 100 nM, respectively, were distributed on the plate.

For the investigation of the concentration-dependent decrease in the intracellular calcium level, transparent 384-well plates were assayed as described in section 3.2.4.2.2 or with a reduced measurement time of 46 cycles, respectively. Ligands of interest were distributed on the plate as shown exemplarily in table 3.1. 32 maximal signals and 32 wells with mepyramine according to final assay concentrations of 0.1 to 100 nM were distributed on the plate.

Table 3.1: *Sector of a 384-well plate with compounds at various concentrations. Bold letters represent lines whereas bold numbers are columns of the plate. Italic numbers represent the final assay concentrations of mepyramine in [nM], Max are maximal signals and letters A-D represent investigated compounds according to various final assay concentrations in [µM] (1: 0.02; 2: 0.2; 3: 2 and 4: 20 µM).*

	1	**2**	**3**	**4**
A	Max	Max	A1	A2
B	Max	Max	A3	A4
C	*0.5*	*5*	B1	B2
D	*50*	*100*	B3	B4
E	Max	Max	C1	C2
F	Max	Max	C3	C4
G	*0.1*	*10*	D1	D2
H	*10*	*100*	D3	D4

3.2.6 Radioligand binding assays

Compounds **1**, **2**, **3**, **4** and **5** were further investigated by radioligand binding experiments. All binding studies were performed with membranes from Sf9 insect cells expressing the respective receptor subtype and appropriate radioactive tracers. As control, a high concentration of an antagonist for the receptor of interest was included in every assay (table 3.2 and Fig. 3.3).

Table 3.2: *Background information on the radioligand binding experiments.*

Receptor	hH_1R	hH_2R	hH_3R	hH_4R
Additional proteins	RGS4	$G_{s\alpha S}$	$G\alpha_{i2}$, $G\beta_1\gamma_2$, RGS4	$G\alpha_{i2}$, $G\beta_1\gamma_2$
Status of expression	coexpression	fusion protein (hH_2R-$G_{s\alpha S}$)	coexpression	coexpression
Membrane protein per sample [µg]	13	35	25	45
Radioactive tracer	[^{3}H]-mepyramine (5 nM)	[^{3}H]-tiotidine (10 nM)	[^{3}H]-N-α-methylhistamine (1 nM)	[^{3}H]-histamine (10 nM)
Antagonist (control)	diphenhydramine (10 µM)	famotidine (10 µM)	thioperamide (10 µM)	thioperamide (10 µM)

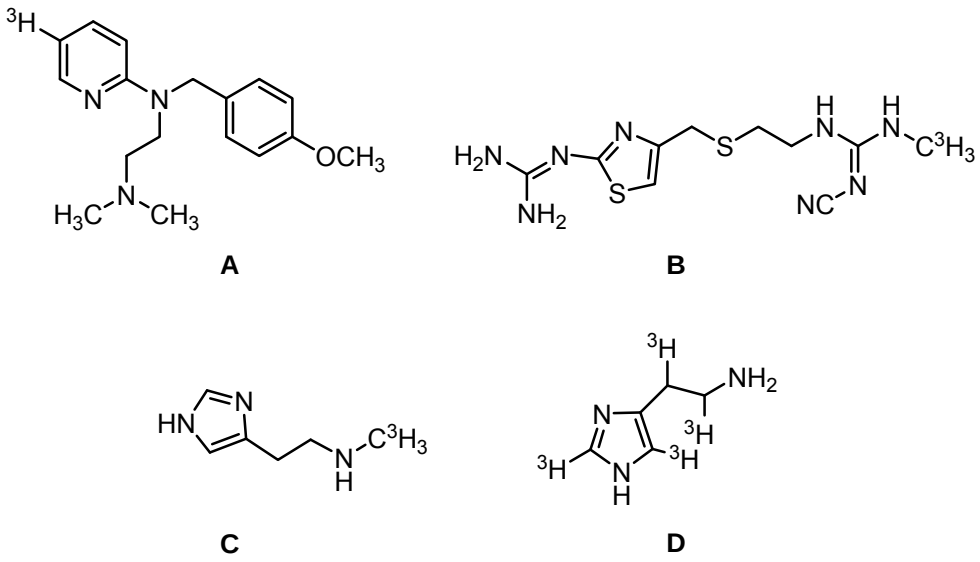

Fig. 3.3: *Chemical structures of the radioactive tracers used for the assays:* **A***: [^{3}H]-mepyramine,* **B***: [^{3}H]-tiotidine,* **C***: [^{3}H]-N-α-methylhistamine,* **D***: [^{3}H]-histamine.*

All radioactive tracers were from PerkinElmer Life Sciences (Boston, USA), famotidine was from Sigma, diphenhydramine and thioperamide were from Tocris Cookson (Ballwin, USA). The chemical structures of the antagonists used as positive controls can be found in the general introduction (chapter 1).

Membranes were thawed, centrifuged (15 min at 4°C and 15,000 g) and resuspended in binding buffer (12.5 mM $MgCl_2$, 1 mM EDTA, 75 mM Tris / HCl, pH 7.4; $MgCl_2$ and EDTA were from Merck whereas Tris / HCl was from Serva). For the preparation of the samples, 150 µL of binding buffer including 0.33 % BSA were mixed with 25 µL of the compounds (10-fold concentrated feed solutions compared to the final concentration in 10 % DMSO) and 25 µL of the radioactive tracer (10-fold concentrated feed solution compared to the final concentration). Samples were completed by addition of the membrane suspension (50 µL per sample).

Incubations were conducted for 60 min at room temperature under continuous shaking (250 rpm). Free radioactive tracer was separated by filtration through GF / C filters (Whatman, Kent, UK) that were pretreated with 0.3 % polyethylenimine (v/v) (undiluted polyethylenimine was from Sigma) 10 min prior to the suction by the M-48 Robotic Cell Harvester (Brandel, Gaithersburg, USA). Samples were washed three times with 2 mL of binding buffer (4 °C). Filterdiscs were transferred into 6 mL mini-vials (Sarstedt, Nümbrecht, Germany). Every vial was filled with 3 mL of Rotiszint® eco plus (Carl Roth, Karlsruhe, Germany) and closed. Samples were collected in racks and inversed 15 times in order to elute radioactivity from the filter discs into the fluid. Samples were stored under light protection in the LS 6500 Liquid Scintillation Counter (Beckman Coulter, Krefeld, Germany) for at least 30 min in order to diminish errors due to light irradiation. Samples were counted in the automatic mode (measurement time: 5 min for each sample).

3.2.7 Data analysis

Ratios were determined from raw data in Microsoft® Office Excel 2003. Increases of the intracellular calcium level were determined by subtraction of the ratio recorded before the injection of loaded cells (agonists) or histamine (antagonists) from the maximal ratio which was detected after the injection process. For the determination of agonistic potencies, ligand-induced increases in the intracellular calcium level were related to those calculated for 100 µM of the reference compound histamine (maximal signal in the agonist mode) in %. The blank value (PBS without histamine) was subtracted from all values and the resulting differences were again related on 100 µM of histamine in %.

In the case of the characterisation of antagonists, the calcium responses to histamine determined in the presence of the test compound were related to the maximal increases in %. Plots were created with the multiple scatter error bars option in SigmaPlot® 9.0. Curve fitting was performed according to the standard curves, four parameter logistic function.

3.3 Results and discussion

3.3.1 Investigations on the suitability of the plate reader

3.3.1.1 Ratiometric detection of Ca^{2+}-complexation by fura-2

Using the GENios Pro™ plate reader, a saturation of fura-2 by increasing concentrations of Ca^{2+} was detected indicating the adequacy of the optical setup of the instrument (Fig. 3.4).

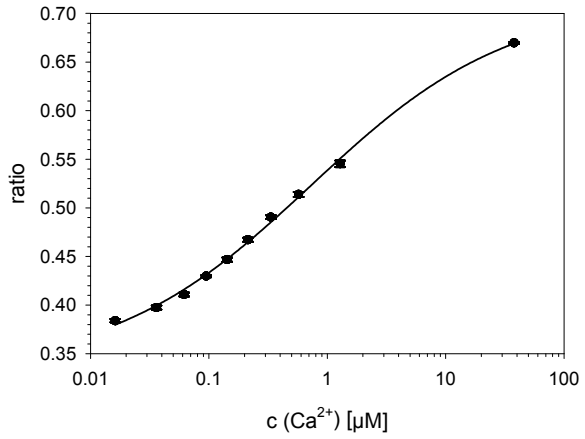

Fig. 3.4: *Saturation of fura-2 by increasing concentrations of Ca^{2+} (mean values ± SEM; n = 3). Calcium-signals were registered as the ratio of emission at 510 nm after excitation at 340 nm and 380 nm, respectively.*

3.3.1.2 Effect of the injection of the cells on the calcium signal

Interestingly, the injection of the loaded cells at a speed of 200 µL / s led to an increase of the ratio before the injection of the agonist (Fig. 3.5). The explanation for this observation is the damage of the cells due to shear stress by injection. This undesired effect is avoided by the reduction of the injection-speed to 25 µL / s (Fig. 3.5). Hence, this injection-speed was chosen for experiments in the 96-well format (3.3.2.1).

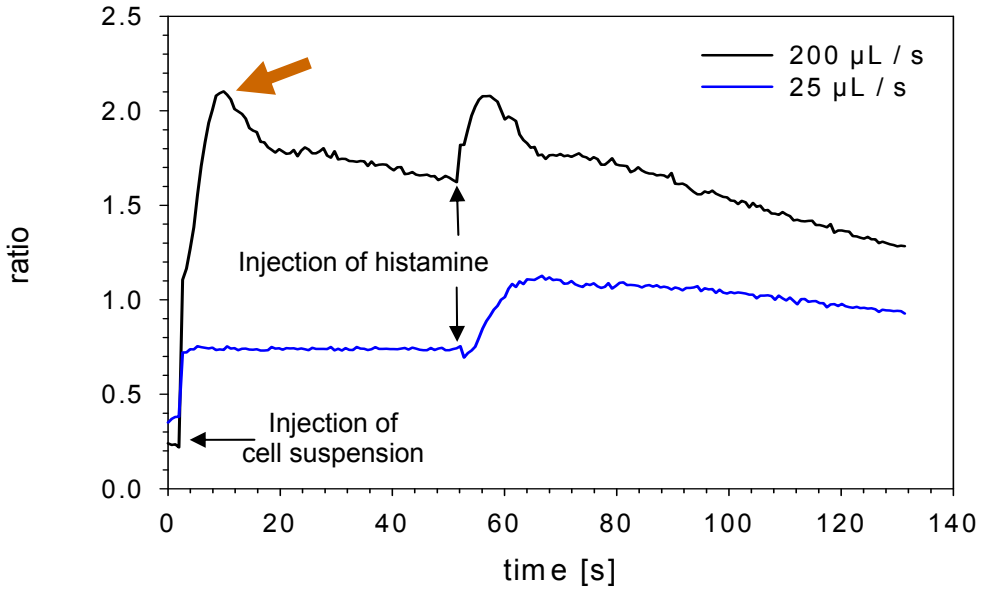

Fig. 3.5: *Effect of the injection-speed on the calcium signal. Injection of the fura-2 / AM loaded cells at a speed of 200 µL / s resulted in an undesired calcium transient (red arrow) that was avoided at an injection-speed of 25 µL / s.*

3.3.2 Investigation of the effect of hH_1R ligands on the mobilisation of intracellular calcium in U-373 MG cells

3.3.2.1 Concentration-dependent increase in the intracellular calcium level by histamine

Histamine increased the intracellular calcium level in a concentration-dependent manner when investigated in the 96-well and the 384-well format (Fig. 3.6).

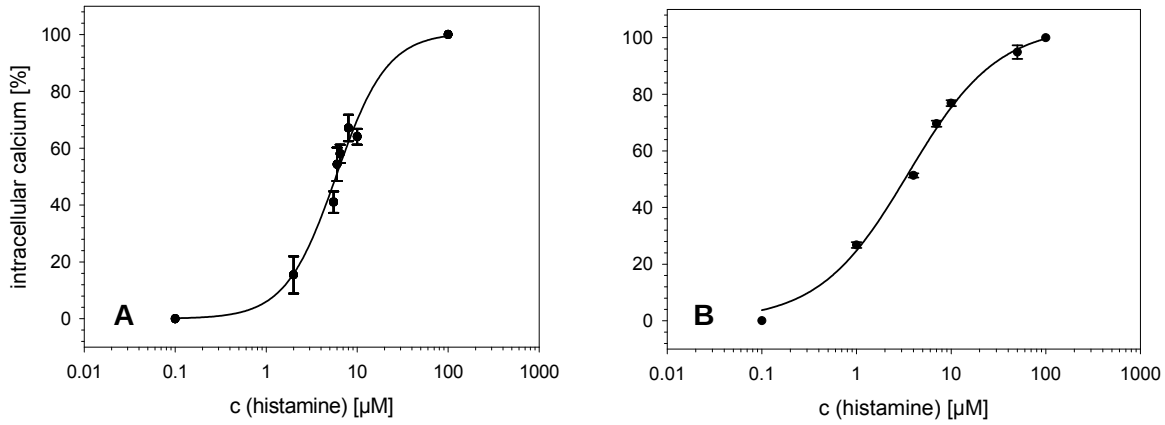

Fig. 3.6: *Concentration-dependent increase in the intracellular calcium level by histamine* **A***: in 96-well plates;* **B***: in the 384-well format (mean values ± SEM; n = 3).*

The EC_{50}-values of histamine calculated from data collected in the two microplate formats, 5.9 ± 0.6 µM (96-well plates) and 3.5 ± 0.4 µM (384-well plates), are in the same range and

in agreement with data which were previously determined in our workgroup at the LS 50 B spectrofluorimeter: 5.4 ± 0.6 µM (Kracht, 2001).

3.3.2.2 Investigation of H_1R antagonists

3.3.2.2.1 Optimisation of assay parameters

To avoid an additional injection process, the fura-2 / AM loaded cells were pre-incubated with mepyramine in the 96-well plate before histamine was injected. 160 µL of the fura-2 / AM loaded cell suspension ($1 \cdot 10^6$ cells / mL) and 20 µL of mepyramine (Sigma) (10-fold concentrated feed solutions compared to final assay concentration in PBS) were pipetted into the cavities of a 96-well plate. Before the 5th cycle, 10 µL of PBS were added by injector A at a speed of 200 µL / s in order to initialize shaking of the microplate in the well kinetic mode (note: the software of the GENios Pro™ reader does not enable shaking without preceding injection). Histamine (600 µM in PBS; 10 µL; speed injector B: 200 µL / s) was injected after cycle 79. To accelerate equilibration after addition of the antagonist to the fura-2 / AM loaded cells, the plates were shaken for 5 min per well kinetic (speed: 60 rpm, mode: orbital, settle time: 0 s) before the agonist was injected. This procedure revealed a concentration-dependent decrease in the intracellular calcium level by the antagonist (Fig. 3.7).

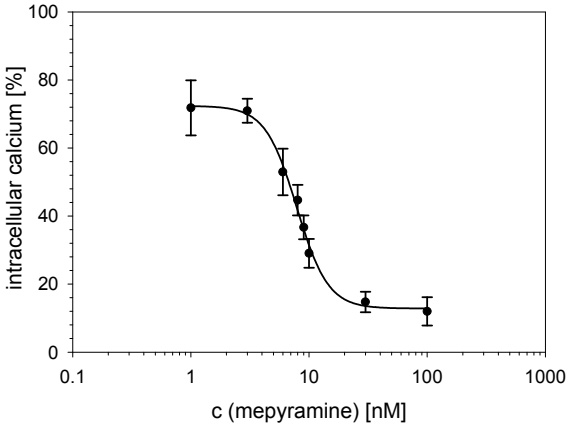

Fig. 3.7: *Concentration-dependent decrease in the calcium signal elicited with histamine (30 µM) by mepyramine (mean values ± SEM; n = 6)*

An IC_{50}-value of 7.9 ± 0.7 nM was determined. The respective K_b-value was calculated according to the Cheng-Prusoff equation (Cheng and Prusoff, 1973) amounting to 1.3 nM ± 0.1 nM: $K_b = IC_{50} \cdot EC_{50} / (EC_{50} + [A])$, where [A] represents the concentration of the agonist used in the assay (30 µM of histamine). The EC_{50} value of the agonist histamine was determined to be 5.9 ± 0.6 µM (cf. 3.3.2.1).

The K_b-value is in agreement with data (3.0 nM (Kracht, 2001)) that were previously determined at U-373 MG cells using the LS 50 B spectrofluorimeter.

Attempts to increase the throughput by reducing the time required for data acquisition were performed according to section 3.2.5, transparent 96-well plates. Under these conditions, a K_b-value of 1.3 ± 0.2 nM (IC_{50} = 8.0 ± 1.0 nM) was calculated for mepyramine (Fig. 3.8, A).

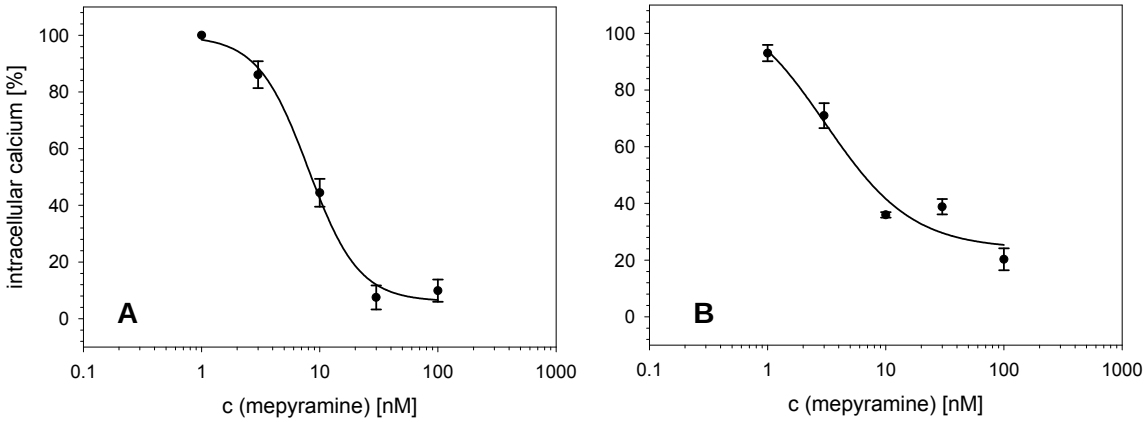

Fig. 3.8: *Concentration-dependent decrease in the histamine (30 µM)-induced calcium signal by mepyramine.* **A***: Assay performance according to section 3.2.5;* **B***: for specific assay conditions see text below. Indicated are mean values ± SEM; n = 3.*

Alternatively, the fura-2-loaded cells were preincubated in the 96-well-plate with mepyramine at various concentrations without shaking at room temperature for 15 min under light protection prior to the challenge with histamine (20 µL; 300 µM in PBS; Fig. 3.8, B). The respective K_b-value of mepyramine for this experiment without shaking was 0.5 ± 0.3 nM (IC_{50} = 3.1 ± 2.0 nM).

The procedure without shaking of the plate was also applied to 384-well plates. Here, mepyramine suppressed the histamine-induced calcium signal in a concentration-dependent manner, too (Fig. 3.9). The corresponding K_b-value of mepyramine was determined to be 0.7 ± 0.1 nM (IC_{50} = 6.4 ± 0.3 nM; EC_{50} of histamine in the 384-well format: 3.5 ± 0.4 µM; cf. section 3.3.2.1).

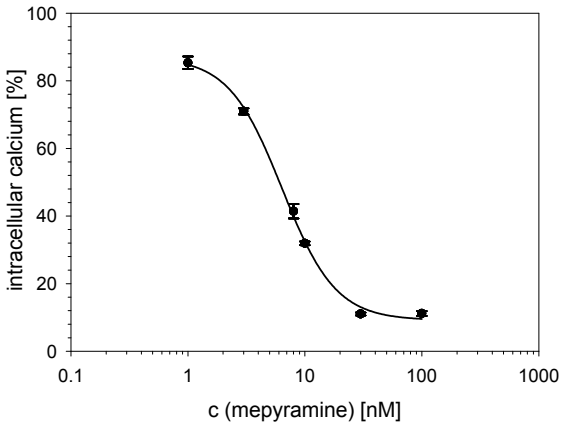

Fig. 3.9: *Suppression of the histamine (30 µM)-induced calcium signal by mepyramine in the 384-well format (mean values ± SEM; n = 3).*

The investigation of the reference H_1R antagonist mepyramine in the 384-well format enabled the correct determination of the K_b-value and gave the most precise results (compare SEM in Fig. 3.9). Therefore, this experimental setup was selected for further investigations because of practicability and reliability.

Final assay concentrations of DMSO up to 1 % (v/v) did not impair the appropriate calculation of the K_b-value of mepyramine (Fig. 3.10): 0.4 ± 0.2 nM (IC_{50} = 3.6 ± 2.1 nM).

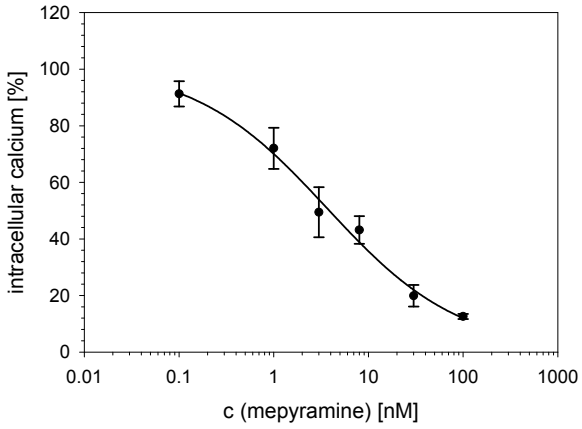

Fig. 3.10: *Competition curve of mepyramine in the presence of 1.0 % DMSO (v/v) (Mean values ± SEM; n = 3). Calcium signals were elicited with 30 µM of histamine.*

In order to determine the contribution of the injection process to the increase in the intracellular calcium level, the solvent of histamine (PBS) was added to the loaded cells by injection. The increase in the intracellular calcium level, probably due to cell rupture, was amounting to 3.25 % relative to the calcium transient evoked by histamine (30 µM) (Fig. 3.11). This result was considered as a correction value for the calculation of antagonistic activities.

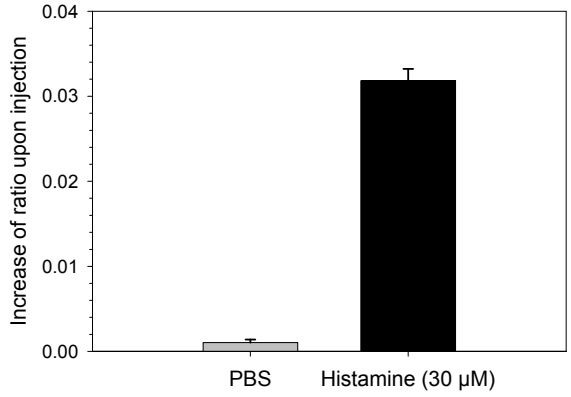

Fig. 3.11: *Comparison of the increase in the intracellular calcium level in fura-2 loaded U-373 MG cells upon injection of PBS or histamine, respectively. Indicated are mean values ± SEM, n = 6.*

In order to investigate the reliability of calcium signals with respect to the time period between the loading procedure with fura-2 / AM and the registration of the fluorescence (i.e. time period of post-incubation), the antagonistic activity of mepyramine was determined. The competition curve which was constructed from data calculated from 15 to 57 min after termination of the loading procedure (Fig. 3.12, A) revealed an antagonistic activity of

mepyramine (K_b-value: 0.3 ± 0.1 nM; IC_{50} = 2.6 ± 0.4 nM) in the same order of magnitude as the K_b-values calculated from samples assayed from 311 to 353 min after completion of the loading procedure (Fig. 3.12, B; K_b = 0.4 ± 0.1 nM; IC_{50} = 4.3 ± 0.8 nM).

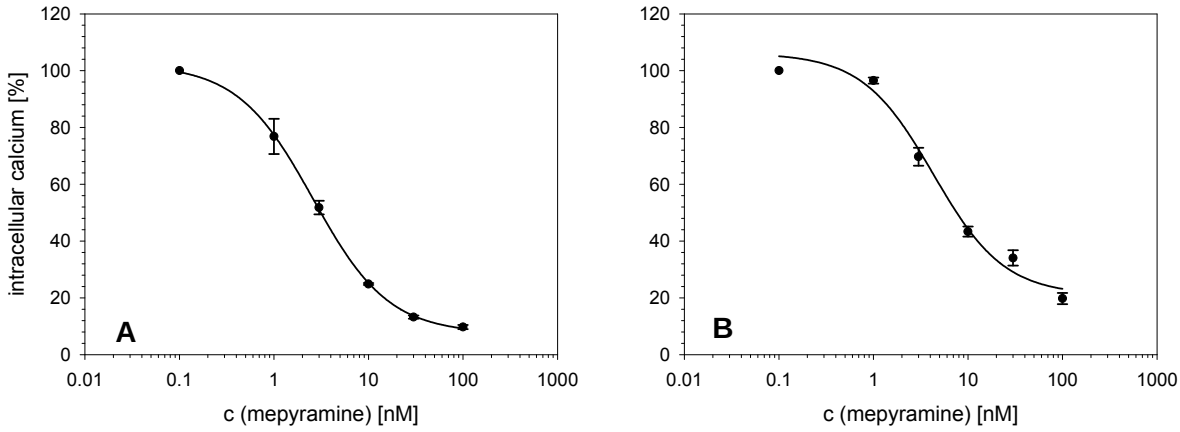

Fig. 3.12: *Investigation of the concentration-dependent decrease of the histamine-mediated calcium response by mepyramine at various time periods of post-incubation.* **A***: from 15 to 57 min;* **B***: from 311 to 353 min. Indicated are mean values ± SEM; n = 3.*

3.3.2.2.2 Investigation of standard antagonists in the optimized assay

Additional hH_1R-antagonists were investigated in the optimized assay using 384-well plates (Fig. 3.13).

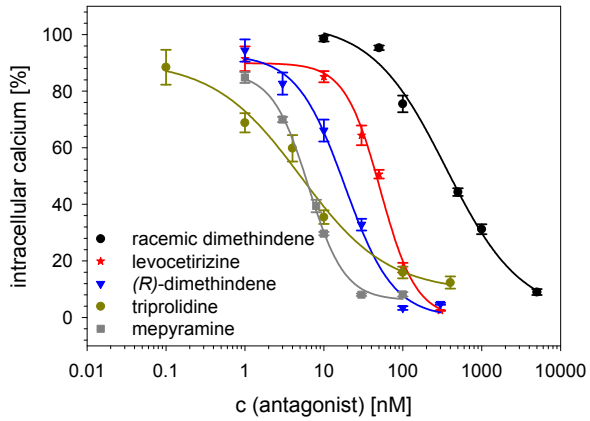

Fig. 3.13: *Concentration-dependent decrease in the histamine-induced calcium response (final assay concentration of histamine: 30 µM) by various hH_1R antagonists (mean values ± SEM; n = 3).*

For all ligands, the obtained pharmacological data are in agreement with data reported in literature (Table 3.3): The K_b-value calculated for (*R*)-(-)-dimethindene agrees to that determined by SEIFERT (Seifert et al., 2003). The K_b-value obtained for (*R,S*)-dimethindene is higher compared to that of the eutomer, but lower than reported for the pure distomer (Seifert et al., 2003). The K_i-value for (*R*)-(-)-cetirizine reported by GILLARD (Gillard et al., 2002) was confirmed by a comparable K_b-value with the calcium assay in the 384-well format. The K_b-values determined for triprolidine and mepyramine are in the same order of magnitude as those reported in literature (Kracht, 2001; Seifert et al., 2003).

Table 3.3: *Comparison of pharmacological data of reference H_1R antagonists determined in the fura-2 assay (384-well format) with results reported in literature.*

Ligand	GTPase assay[1] K_b [nM]	Radioligand binding assay[2] K_i [nM]	Fura-2 assay, cuvettes (U-373 MG cells)[3] K_b [nM]	Fura-2 assay, 384-well format (U-373 MG cells) K_b [nM]
(*S*)-(+)-dimethindene	113.2 ± 30.9	n.d.	n.d.	n.d.
(*R*)-(-)-dimethindende	2.7 ± 1.5	n.d.	n.d.	1.9 ± 0.2
(*R,S*)-dimethindene	n.d.	n.d.	n.d.	37.1 ± 5.8
(*R*)-(-)-cetirizine	n.d.	2.5-4.0	n.d.	5.5 ± 0.4
triprolidine	4.4 ± 1.6	n.d.	n.d.	0.5 ± 0.2
mepyramine	5.7 ± 0.9	n.d.	3.0	0.7 ± 0.1

[1]Seifert et al., 2003; [2]Gillard et al., 2002: K_i-value was calculated from the reported mean ± S.D. of the pK_i value; [3]Kracht, 2001

3.3.3 Screening of a library of potential H_1R ligands in the microplate fura-2 calcium assay on U-373 MG cells

The appropriate performance of the assays both in the 96-well and the 384-well format for the investigation of compounds in duplicate was confirmed by the suppression of the histamine-induced calcium signal with mepyramine: 8 nM of the antagonist suppressed the calcium transient by approx. 50 %, whereas in the presence of 100 nM of mepyramine, only a slight increase in the intracellular calcium level elicited by the injection process was observed (Fig. 3.14 A and B).

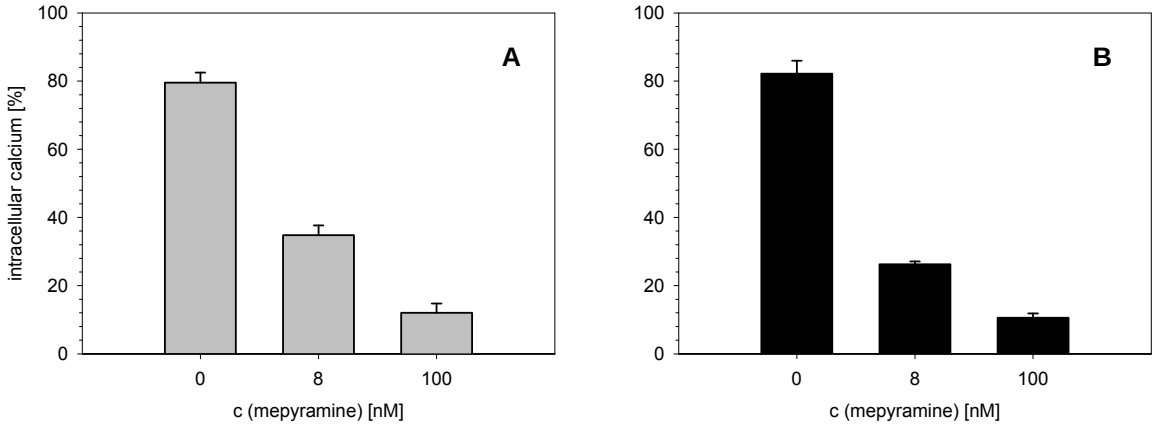

Fig. 3.14: *Suppression of the hH_1R-mediated calcium signal elicited with histamine (30 µM) in U-373 MG cells by increasing concentrations of mepyramine in* **A***: 96-well plates (n = 18 (no antagonist) or n = 3 (8 and 100 nM of mepyramine, respectively));* **B***: 384-well plates (n = 16 (no antagonist) or n = 8 (8 and 100 nM of mepyramine, respectively)). Indicated are mean values ± SEM in each case.*

The correct performance of the assays for the concentration-dependent decrease in the intracellular calcium level by putative hH_1R-antagonists was confirmed by investigation of mepyramine concentrations ranging from 0.1 to 100 nM. The results for a measurement time of 120 cycles per well were comparable to assays performed with a reduced measurement time per well of 46 cycles (Fig. 3.15).

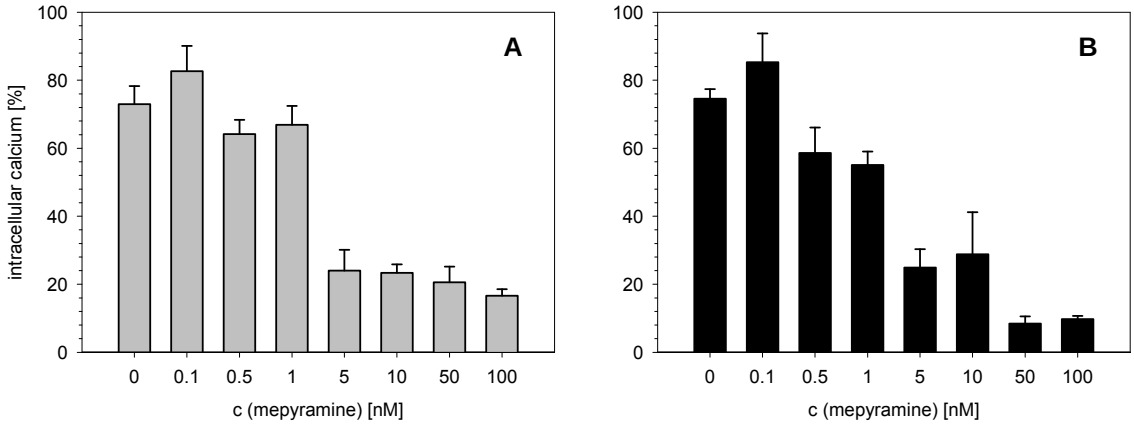

Fig. 3.15: *Comparison of the concentration-dependent decrease in the intracellular calcium level (evoked with 30 µM of histamine in U-373 MG cells) by mepyramine on an assay plate* **A***: measured with 120 cycles and* **B***: determined with 46 cycles per well kinetic. Indicated are mean values ± SEM; n = 16 (no antagonist); n = 2 (0.1-50 nM); n = 4 (100 nM) in each case.*

The recording of 120 cycles per well kinetic enabled the investigation of 192 samples in one assay per day. However, the monitoring of 46 cycles per well kinetic in the same time period drastically increased the throughput to 480 samples in one assay per day.

The screening of the compounds in the microtitre format for their antagonistic activity at the hH_1R contributed to the identification of several lead structures which were further optimized by chemical modification of the respective scaffold by the coworkers of the Origenis company. Five of those optimized compounds (structures not disclosed due to possible conflict with intellectual properties) were investigated by radioligand binding experiments (section 3.3.4) on hH_1R, hH_2R, hH_3R and hH_4R with respect to histamine receptor subtype selectivity.

3.3.4 Radioligand binding assays

None of the 5 selected compounds did significantly displace the respective radioactive tracer up to a concentration of 10 µM at the human histamine receptors hH_2R, hH_3R or hH_4R, respectively, indicating negligibly low affinity to histamine receptors other than hH_1R. The antagonist controls (10 µM of famotidine at the hH_2R or 10 µM of thioperamide at the hH_3R and the hH_4R, respectively) clearly decreased the binding of the respective radioligands (Fig.

3.16). Therefore, the performance of the assay was appropriate and the observed low affinity of the investigated compounds is valid.

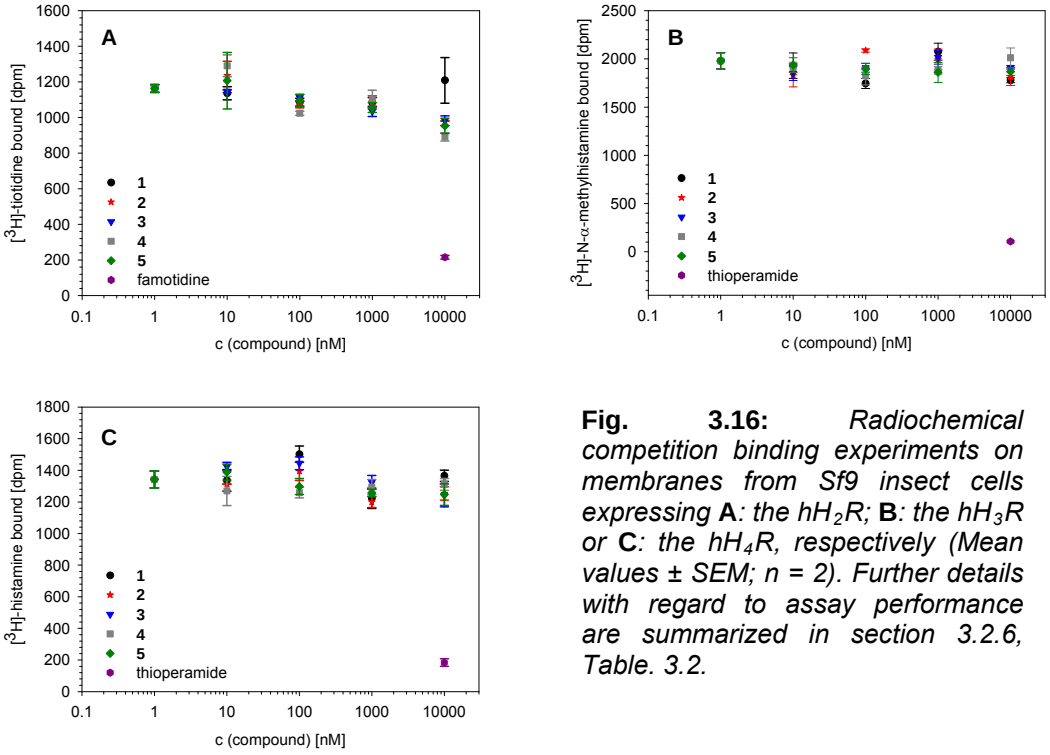

Fig. 3.16: *Radiochemical competition binding experiments on membranes from Sf9 insect cells expressing* **A***: the hH_2R;* **B***: the hH_3R or* **C***: the hH_4R, respectively (Mean values ± SEM; n = 2). Further details with regard to assay performance are summarized in section 3.2.6, Table. 3.2.*

In contrast, the investigated new chemical entities displaced [^{3}H]-mepyramine from the hH_1R. Compounds **1** and **3** at concentrations ≥ 1 µM inhibited the radioligand binding by around 30 and 50 %, respectively. Compounds **2** and **4** suppressed the binding of [^{3}H]-mepyramine by nearly 90 %, whereas compound **5** almost completely displaced the radioactive tracer at concentrations ≥ 1 µM. The latter compound showed the highest affinity of the 5 investigated ligands. The antagonist control (10 µM of diphenhydramine) displaced almost completely the binding of the radioactive tracer which demonstrates the appropriate performance of the binding assay (Fig. 3.17).

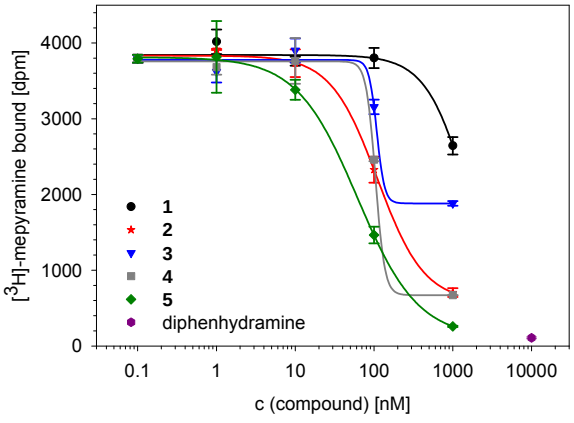

Fig. 3.17: *Competition of [^{3}H]-mepyramine (5 nM) by the investigated compounds (Mean values ± SEM; n = 2).*

3.4 Summary and conclusions

The adaptation of the fura-2 assay to the microtitre format was successful. The agonist histamine was appropriately characterised by a concentration-dependent increase in the intracellular calcium level in both the 96- and the 384-well format. For the pharmacological characterisation of hH_1R antagonists, measurements performed in the 384-well format led to more reliable data than those in the 96-well format. Optimization of the conditions, especially sequential reduction of the measurement time, enabled the characterisation of 480 samples in one assay per day in the 384-well format.

In order to prove the applicability of the developed assay for the screening of potential hH_1R antagonists, a compound library of more than thousand new substances (cooperation with Origenis GmbH) was investigated in the 384-well format. Among these substances compound **5** was identified as a highly affinic and selective hH_1R antagonist. Thus, this work successfully contributed to the identification of a potential drug candidate, confirming the prospect of the developed calcium assay in drug discovery.

3.5 References

Arias-Montaño, J.A., Berger, V., Young, J.M., 1994. Calcium-dependence of histamine- and carbachol-induced inositol phosphate formation in human U373 MG astrocytoma cells: comparison with HeLa cells and brain slices. *Br. J. Pharmacol.* **111**, 598-608.

Cheng, Y.-C., Prusoff, W.H., 1973. Relationship between the inhibition constant (K_i) and the concentration of inhibitor which causes 50 per cent inhibition (IC_{50}) of an enzymatic reaction. *Biochem. Pharmacol.* **22**, 3099-3108.

Gessele, K., 1998. Zelluläre Testsysteme zur pharmakologischen Charakterisierung neuer Neuropeptid Y-Rezeptorantagonisten. In: *Doctoral Thesis, University of Regensburg*.

Gillard, M., Van Der Perren, C., Moguilevsky, N., Massingham, R., Chatelain, P., 2002. Binding Characteristics of Cetirizine and Levocetirizine to Human H_1 Histamine Receptors: Contribution of Lys191 and Thr194. *Mol. Pharmacol.* **61**, 391-399.

Hay, R.J., 1988. The seed stock concept and quality control for cell lines. *Anal. Biochem.* **171**, 225-237.

Kracht, J., 2001. Bestimmung der Affinität und Aktivität subtypselektiver Histamin- und Neuropeptid Y-Rezeptorliganden an konventionellen und neuen pharmakologischen In-vitro-Modellen. In: *Doctoral Thesis, University of Regensburg*.

Seifert, R., Wenzel-Seifert, K., Bürckstümmer, T., Pertz, H.H., Schunack, W., Dove, S., Buschauer, A., Elz, S., 2003. Multiple Differences in Agonist and Antagonist Pharmacology between Human and Guinea Pig Histamine H_1-Receptor. *J. Pharmacol. Exp. Ther.* **305**, 1104-1115.

Siehler, S., 2008. Cell-based assays in GPCR drug discovery. *Biotechnol. J.* **3**, 722-727.

Takahashi, A., Camacho, P., Lechleiter, J.D., Herman, B., 1999. Measurement of Intracellular Calcium. *Physiol. Rev.* **79**, 1089-1125.

Chapter 4

Determination of ligand binding to the human histamine H_2 receptor by radiochemical and fluorescence-based methods

4.1 Introduction

4.1.1 Investigation of HEK293 cells for the expression of human histamine receptors

In contrast to hH_1R expressing U-373 MG cells (see chapter 3), cell types which endogenously express the hH_2R previously revealed as less appropriate for the establishment of cellular assays. For instance, MKN-45 cells which constitutively express the hH_2R (Arima et al., 1991) were investigated in our workgroup for specific binding of [^{3}H]-tiotidine (Kracht, 2001). Unfortunately, the radioligand showed only low binding on those cells accompanied with a relative high extent of unspecific binding (Kracht, 2001). In addition, neither a histamine-mediated increase in the intracellular cAMP level (Kracht, 2001) nor in intracellular Ca^{2+} (Schneider, 2005) was detectable. Other cells which express the hH_2R like HL-60 cells additionally express hH_1 receptors (Burde and Seifert, 1996). Coexpression of different receptor subtypes may lead to misinterpretation of binding or functional data when non-selective ligands such as histamine interact with both receptor subtypes simultaneously. Hence, their affinity to the receptor subtype of interest could be underestimated. Furthermore, interacting signalling cascades would be activated by a non-selective agonist such as histamine. This could become especially relevant in case of the coexpression of the hH_2R and the hH_3R or hH_4R, as the activation of the hH_2R leads to an increase in the intracellular cAMP level, whereas the stimulation of both other receptor subtypes provokes the opposite effect. Thus, the chosen cell line should only express the histamine receptor subtype of interest. Due to the lack of appropriate wild-type cells expressing either the hH_2R or the hH_4R (the hH_4R is preferentially expressed on immune cells which are laborious in view of handling, see for instance BUCKLAND (Buckland et al., 2003)), respectively, transfection experiments were considered most promising to establish cellular binding and functional assays.

In the present work experiments were focussed on HEK293 cells, as these are well characterised (Thomas and Smart, 2005), can be conveniently detached (trypsinization is not required) and are rapidly growing. Since little information on human histamine receptor subtypes expressed in HEK293 cells has been available, RT-PCR was performed to investigate histamine receptor expression at the mRNA level. Furthermore, the potential expression of the hH_2 receptor protein was analyzed in western blot experiments.

4.1.2 Stable co-expression of the human histamine H_2 receptor and the chimeric Gα–protein qs5-HA in HEK293 cells

The cDNAs encoding the proteins of interest have to be cloned in appropriate plasmids which enable the amplification of DNA in competent bacteria and the stable transfection of mammalian cells. The commercially available pcDNA3.1 vectors (Invitrogen, Karlsruhe, Germany) were used for those experiments. The vectors contain an ampicillin resistance for the propagation of DNA in bacteria and various genes according to resistances against G418, hygromycin B or Zeocin™, respectively (for a vector map see 4.2.2.2). As there is no evidence of cross-resistances between the latter antibiotics, co-transfection of mammalian cells using the respective DNA constructs and subsequent selection should enable the establishment of cells which stably express the proteins of interest.

4.1.3 Determination of ligand affinity in binding assays

The determination of ligand affinity with binding assays is an essential step in the scope of drug development and characterisation of substance libraries. Binding assays can be performed on membrane preparations, whole cells, solubilised receptor preparations or whole tissues (Hulme and Buckley, 1992). The classical approach for the determination of ligand affinity is the radioligand binding assay. An ideal radioligand for the performance of that kind of assay is a high affinity neutral antagonist (dissociant constant (K_d) in the range of 0.01 to 1 nM) which binds in a reversible competitive manner (Hulme and Birdsall, 1992). Neutral antagonists are favoured compared to agonists because undesired effects like agonist locking (Hulme and Birdsall, 1992), dependency of binding data on G-protein status (Lazareno, 2001) or misinterpretations due to receptor internalization are often observed when using radioactive agonists for binding studies. Tritiated radioactive tracers like [^{3}H]-tiotidine are very useful tools as the pharmacological properties of a receptor ligand are usually not apparently changed by introduction of tritium in the molecule. Due to a half-life of approx. 12 years, corrections for decay during the lifetime of the experiment are not required when using tritiated compounds. The high specific activity of tritium enables an economic use of respective radioligands (McFarthing, 1992). In conventional radiochemical assays, bound and free tracer have to be separated before measurement. In addition, radioactive substances are hazardous, require special handling of waste, and so are expensive (Keen, 1995; Schneider et al., 2006). The most convenient method for the separation of unbound from bound ligand is filtration due to its advantages compared to other separation techniques like centrifugation. Filtration provides high efficiency of the separation process, relative low complexity and time requirement, a low non-specific background due to minor radioligand

binding to cellular components which differ from the receptors of interest and good reproducibility (Wang et al., 1992).

For the purpose of validation, a radioligand binding assay was established for HEK293-hH_2R-qs5-HA cells using the Combi Cell Harvester 11025 (Skatron, Norderstedt, Germany) which was kindly provided from Prof. Heilmann (Institute of Pharmacy, Department of Pharmaceutical Biology, University of Regensburg). As washing steps during assay performance could lead to the detachment of HEK293-hH_2R-qs5-HA cells due to their relative weak adherence, assays were not performed in 24-well plates but with suspended cells. Samples were prepared in 96-well plates and after incubation, cells (bound radioactivity) were transferred row-wise onto a glass fibre filter (Fig. 4.1, A) by the shorter outlet tubes. Cold washing buffer (4 °C) was added through the longer inlet tubes with the smaller diameters (Fig. 4.1, B). Thus, separation of bound from free radioligand at the end of the incubation was performed by filtration.

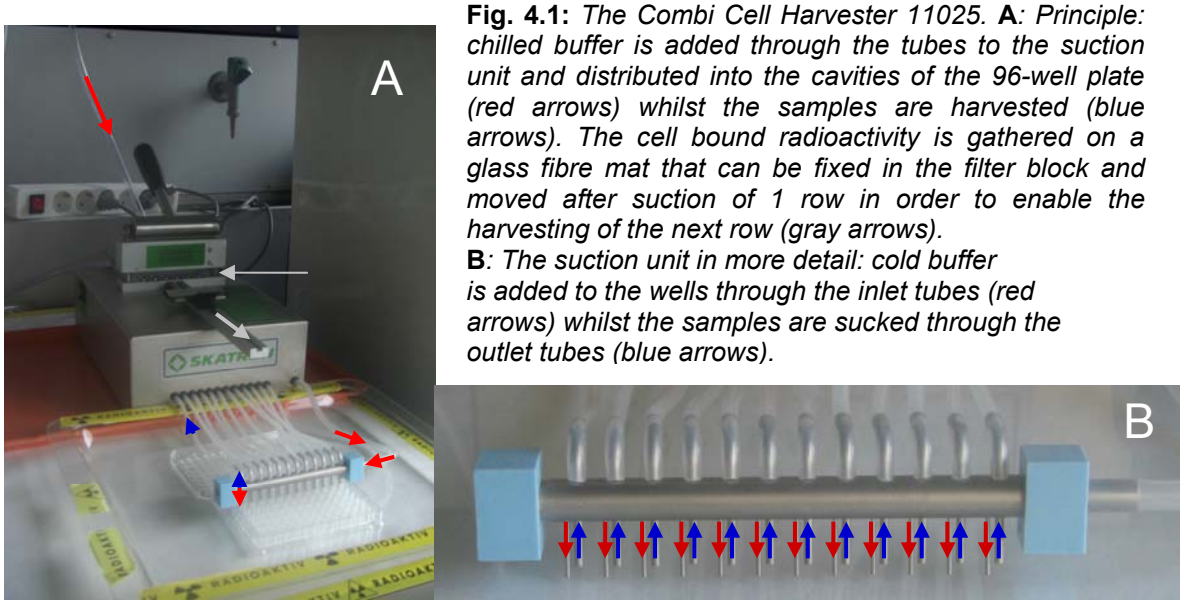

Fig. 4.1: *The Combi Cell Harvester 11025.* **A***: Principle: chilled buffer is added through the tubes to the suction unit and distributed into the cavities of the 96-well plate (red arrows) whilst the samples are harvested (blue arrows). The cell bound radioactivity is gathered on a glass fibre mat that can be fixed in the filter block and moved after suction of 1 row in order to enable the harvesting of the next row (gray arrows).*
B*: The suction unit in more detail: cold buffer is added to the wells through the inlet tubes (red arrows) whilst the samples are sucked through the outlet tubes (blue arrows).*

In order to reduce unspecific binding of the radioactive tracer ([^{3}H]-tiotidine) to the glass fibre mat (negatively charged at pH 7.4), the negative charges of the filter were compensated by pre-treatment with the polycation polyethylenimine (PEI).

After a washing step to remove excessive radioligand, the filter mat was moved to the next position. The filter discs are transferred to scintillation vials and analyzed by liquid scintillation counting.

The determination of ligand affinity with fluorescence-based methods is a promising alternative to radiochemical binding assays. Flow cytometric measurements with fluorescence-labelled ligands addressing the respective receptor are of special interest because binding data can be determined under equilibrium conditions without washing steps.

The receptor-expressing cells pass through laser beams in a thin sample stream which is hydrodynamically focused in the surrounding sheath fluid. As the laser beam is precisely directed towards the surfaces of the cells, it is mainly cell-associated fluorescence that is detected. Hence, the signal is hardly impaired by free fluorescent ligand in solution (Bohn, 1980; Schneider et al., 2006). Advances in sample delivery systems make flow cytometry also applicable to the requirements of high throughput screening (Edwards et al., 2004; Kuckuck et al., 2001; Ramirez et al., 2003; Young et al., 2009). In addition, flow cytometry provides the occasion to determine multiple parameters in only one sample (Schneider et al., 2006).

4.2 Materials and methods

4.2.1 Investigation of HEK293 cells for the expression of human histamine receptors

4.2.1.1 Expression analysis of human histamine receptors in HEK293 cells at the mRNA level

4.2.1.1.1 Cell culture

HEK293 cells (Deutsche Sammlung für Mikroorganismen und Zellkulturen (DSMZ), Braunschweig, Germany) were maintained in DMEM (Sigma, Deisenhofen, Germany) supplemented with 10 % FBS. Cells were passaged 1:10 twice a week without trypsinization. Cells were grown to approx. 90 % confluency in a 75-cm^2 culture flask prior to the isolation of total mRNA.

4.2.1.1.2 Isolation of total mRNA from HEK293 cells

The isolation of RNA was performed with the RNeasy Kit (Qiagen, Hilden, Germany) according to the manufacturer´s instruction "Isolation of RNA from animal cells, spin column method". In order to avoid overloading of the spin column, approx. $1 \cdot 10^6$ cells were processed per spin column. Isolated mRNA was stored at -80 °C until use.

4.2.1.1.3 Determination of mRNA concentration

Isolated mRNA was diluted 1:50 with RNAse-free water from the RNeasy Kit and analyzed by UV spectrometry at 260 nm: c (RNA) [µg / mL] = $50 \cdot 40 \cdot A_{260}$.

4.2.1.1.4 Synthesis of cDNA by reverse transcription (RT) and amplification by polymerase chain reaction (PCR)

RT was performed according to SCHNEIDER (Schneider, 2005): 1 µg of total mRNA and 1 µL of an oligo(dT_{12}) primer solution (100 µM; MWG, Ebersberg, Germany) were diluted to 10 µL with RNAse-free water. The mixture was heated at 70 °C for 5 min and cooled down to 4 °C with the Master Cycler (Eppendorf, Hamburg, Germany). 1 µL of M-MLV reverse transcriptase (Invitrogen, Karlsruhe, Germany), 2 µL of a dNTPmix (2 mM; MBI Fermentas,

St. Leon-Rot, Germany), 4 µL of 5x first strand buffer (Invitrogen) and 2 µL of DTT (Roche, Basel, Switzerland) were added. The sample was diluted to 20 µL with RNAse-free water. Snythesis of cDNA and amplification by PCR was performed with the Master Cycler: reverse transcription was accomplished at 37 °C for 1 h. Thereafter, the enzyme was inactivated at 95 °C for 2 min. Samples were stored at -20 °C.

PCR samples were prepared by mixing 2 µL of cDNA, 8 µL of Millipore water, 8 µL of Master Mix (Eppendorf) and 2 µL of the primer pair for the amplification of the respective human histamine receptor subtype (1 µL of the sense and the antisense primer in each case, 1 µM; MWG).

As a control for the successful isolation of the mRNA, a sample was prepared with a primer pair that enables the amplification of the sequence of β-actin: 1 µL of each primer was used (1 µM; MWG).

Two plasmids comprising hH_3R or hH_4R cDNA, respectively, were kindly provided by David Schnell (Institute of Pharmacy, Department of Pharmacology and Toxicology, Regensburg) and were used as controls for the suitability of the PCR conditions. Instead of 2 µL of cDNA solution, 2 µL of the respective plasmid (10 µg / mL) were used. In case of the hH_1R and the hH_2R, primer pairs were used, previously proven to give reproducible results under the chosen PCR conditions (Schneider, 2005). Primers, lengths of amplification products and positive controls are summarised in table 4.1.

Table 4.1: *PCR analysis of histamine receptor expression in HEK293 cells. Overview about used primers, product lengths and positive controls.*

gene	sense primer	antisense primer	product length [bp]	positive control
hH_1R	5'-GGT GCT GTA TGC CGT ACG GA-3'	5'-TGG ACA GAG CGG TAG CGA TCA-3'	229	-
hH_2R	5'-CCA TCA GGG AGC ACA AAG CC-3'	5'-TTC TGT CCC ACT CCA CAC CTG G-3'	370	-
hH_3R	5'-GAC GAT GAT GAC GCC ATG GAG CGC GCG CCG CC-3'	5'-GAT CCT CTA GAT TAG TGA TGG TGA TGA TGG TGC TTC CAG CAG TGC TC-3'	1382	pVL1392-SF-hH_3R
hH_4R	5'-GAC GAT GAT GAC GCC ATG CCA GAT ACT AAT AG-3'	5'-GAT CCT CTA GAT TAG TGA TGG TGA TGA TGG TGA GAA GAT ACT GAC CG-3'	1217	pGEM-3Z-SF-hH_4R
β-actin	5'-CGG GAT CCC CAA CTG GGA C-3'	5'-GGA ATT CTG GCG TGA GGG A-3'	304	-

PCR was performed under the following conditions (Schneider, 2005):

(1) initial denaturation:	95 °C,	120 s
(2) denaturation:	95 °C,	30 s
(3) annealing:	60 °C,	60 s
(4) extension:	72 °C,	30 s
(5) hold:	4 °C	

Steps (2)-(4) were repeated 34 times. Samples were subsequently stored at -20 °C.

4.2.1.1.5 Agarose gel electrophoresis

Analysis by agarose gel electrophoresis was performed according to SCHNEIDER (Schneider, 2005) with minor modifications: 5x TBE buffer was prepared by dissolving 445 mM of tris base (USB, Cleveland, USA), 445 mM of boric acid (Merck, Darmstadt, Germany) and 10 mM of Titriplex® III (Merck) in Millipore water. 1x TBE buffer was prepared by dilution of the respective stock solution (5x) with Millipore water. 0.75 g of agarose (pegGOLD Universal-Agarose; Peqlab, Erlangen Germany) were dissolved in 50 mL of 1x TBE buffer with heating and continuous stirring.
2 µL of an aqueous ethidium bromide solution (10 mg / mL; Janssen Chimica, Beerse, Belgium) were added. The solution was poured into the gel chamber of the PerfectBlue™ Mini S gel system (Peqlab). In order to create pockets for the application of the samples, 2 combs were adjusted into the solution. After solidification, the gel was covered with the 1x TBE buffer, and the combs were carefully removed. 10 µL of each PCR sample were mixed with 2 µL of 6x loading dye solution (MBI Fermentas). 5 µL of each mixture were added per pocket of the gel. 5 µL of the Mass Ruler DNA Ladder mix, ready to use (MBI Fermentas) were used for reference (grading: 80, 100, 200, 300, 400, 500, 600, 700, 800, 900, 1031, 1500, 2000, 2500, 3000, 4000, 5000, 6000, 8000 and 10000 bp).
The voltage was set to 90 V during a gel running time of approx. 90 min. The gels were analysed by transillumination at 254 nm (Gel Doc 2000; Bio-Rad Laboratories, Munich, Germany) using the Quantity One software (Bio-Rad Laboratories).

4.2.1.2 Western blot analysis of the hH_2R expression

4.2.1.2.1 Cell culture and membrane preparation

HEK293 and HEK293 T cells, which express the SV-40 large T-antigen (Wurm and Bernard, 1999), were cultured as described in 4.2.1.1.1. HL-60 HD cells (HD is an abbreviation for

Heidelberg, Germany) were obtained from the Department of Pharmacology and Toxicology, University of Regensburg, and maintained in RPMI 1640 medium (Sigma) including 10 % FBS. This cell type emerged from HL-60 cells which were obtained from the American Type Culture Collection. In contrast to the latter cell type, calcium transients upon H_2R stimulation can be more readily monitored in HL-60 HD cells. The reason for this observation is not elucidated yet. Furthermore, it is neither known, how HL-60 HD cells emerged from HL-60 cells, nor in what respect both cell types differ on the molecular level (Prof. Dr. Roland Seifert, Institute of Pharmacology, Medical School of Hannover, Germany, 2009, personal communication).

HEK293 and HEK293 T cells were seeded in sixteen 175-cm^2 culture flasks (Nunc) in each case and grown to confluency within 1 week (approx. $5 \cdot 10^6$ cells were seeded per flask). Membranes were essentially prepared according to MAYER (Mayer, 2002): briefly, washing steps with the homogenizing buffer prior to the detachment of the cells were omitted due to the weak adherence of both investigated cell types. Cells of four 175-cm^2 flasks were harvested in portions with homogenizing buffer at 4 °C. Cells were disrupted in a Potter-Elvejham-homogenizer (B. Braun Melsungen, Melsungen, Germany) by 10 strokes at 1500 rpm on ice (30 s break after 5 strokes) and subsequently centrifuged for 5 min at 650 g. The supernatant was centrifuged at 40000 g for 30 min. The resulting pellet was washed with homogenizing buffer and centrifuged again at 40000 g for 30 min. The pellet was re-suspended in 1000 µL of homogenizing buffer by a 1 mL syringe with a 0.4 x 20 mm needle. The amount of membrane protein was determined according to Bradford by 1:5 dilution of the Bio-Rad protein assay dye reagent concentrate (Bio-Rad Laboratories). Membranes were frozen in liquid nitrogen and stored at -80 °C.

In case of HL-60 HD cells, four 175-cm^2 culture flasks were grown to confluency within 4 days (approx. $5 \cdot 10^6$ cells were seeded per flask, the final volume in each flask was 50 mL). HL-60 HD cells, which grow in suspension, were collected in 50 mL tubes and centrifuged for 5 min at 300 g. The cell pellet was resuspended in homogenizing buffer and then handled as described for HEK293 and HEK293 T cells.

4.2.1.2.2 Investigation of membranes from mammalian cells in semi-dry western blots

For the preparation of a 2-fold concentrated electrophoresis buffer, 28.8 g of urea were dissolved under heating in approx. 20 mL of Millipore water. The solution was cooled to room temperature and 1.5 g of SDS, 1.8 g of dithiothreitole, 1.5 mL of Tris-base (1M, pH 8.0;), 6.0 mL of glycerol (50 % (v/v)) and 6.0 mg of bromophenol blue were added and dissolved. The solution was filled up with Millipore water at 27.0 mL. The buffer was aliquoted and stored at -20 °C (all chemicals used for the preparation of the buffer were from Merck).

As positive and negative controls, membranes from Sf9 cells, either expressing the hH_2R or the hH_1R and RGS4, respectively, were provided by the Department of Pharmacology and Toxicology, University of Regensburg. Every sample contained 15 µg of membrane protein. Discontinuous SDS-PAGE was performed according to HOFINGER (Hofinger, 2007). Samples were diluted with the electrophoresis buffer, heated for 3 min at 100 °C and pipetted in the gel pockets. Semi-dry western blots were essentially performed as described previously (Hofinger, 2007). The anti-FLAG primary antibody (4.5 mg protein / mL; M1, monoclonal antibody, Sigma) and the secondary antibody (biotinylated anti-mouse / rabbit IgG; Vector Laboratories, Burlingame, USA) were diluted 1:1000 with PBS including Tween 20 (0.05 % (v/v); Tween 20 was from Roth, Karlsruhe, Germany) prior to use. The membrane with the blotted proteins was incubated both with the primary and the secondary antibody for 2 h. Visualization, further handling of the membrane and data analysis were performed as described previously (Hofinger, 2007). Briefly, after washing, the membrane was incubated with a biotin / avidin / horseradish peroxidase (HRP) reaction kit (VECTASTAIN® ABC-kit Standard, Vector laboratories, Burlingame, USA), which was prepared 30 min before the use according to the manufacturer's instructions. Alternatively, a secondary antibody, which is linked to horseradish peroxidase (sheep anti-mouse IgG coupled to peroxidase; Amersham Biosciences, Freiburg, Germany; the antibody was provided by the Department of Pharmacology and Toxicology, University of Regensburg), was used for visualization in a dilution of 1:1000 with PBS including Tween 20 (0.05 % (v/v)). Readout was performed with the diaminobenzidine (DAB) staining solution according to the manufacturer's instruction (DAB Kit, Vector Laboratories). Brown bands appeared after 5-10 min. Excessive substrate was removed by washing with water and the dry membrane was scanned with a DAB / HRP filter on the Bio-Rad gel detection system (GS-710 Imaging Densitometer) using the Quantity One software (version 4.0.3, Bio-Rad Laboratories).

4.2.1.2.3 Investigation of membranes from mammalian cells in wet western blots

Separation gels containing 12 % of acrylamide (v/v) were prepared by mixing 2.2 mL of Millipore water, 2 mL of buffer A (18.17 g of Tris base and 4.0 mL of SDS 10 % (w/v) ad 100.0 mL of Millipore water, pH 8.8), 3.2 mL of acrylamide / bisacrylamide (30 % solution, acrylamide / bisacrylamide = 29 / 1; Sigma) and 0.53 mL of glycerol 50 % (v/v). Polymerization was initialized by addition of 3.35 µL of TEMED and 33.35 µL of APS 10 % (v/v) (TEMED and APS were from Serva, Heidelberg, Germany). The solution was poured into the gel chamber and isobutyl alcohol (Merck) was added in order to smooth the emerging separation gel. After 45 min, the alcohol was discarded and the stacking gel was prepared: 3.25 mL of Millipore water were mixed with 2.5 mL of buffer B (6.0 g of Tris base

and 4.0 mL of SDS 10 % (w/v) ad 100.0 mL of Millipore water, pH 6.8) and 1 mL of acrylamide / bisacrylamide. Polymerization was started with 3.35 µL of TEMED and 50 µL of APS 10 % (v/v). The mixture was poured on the separation gel. Gel pockets were prepared by addition of suited combs to the stacking gel. After another 45 min, the gel was stored at 4 °C or directly used for gel electrophoresis. The stacking gel contained 3 % of acrylamide (v/v).

Samples were prepared according to 4.2.1.2.2 and separated in a Mini Protean II Electrophoresis Cell (Bio-Rad Laboratories) for 150 min at room temperature (110 V). For reference, 5 µL of the Precision Plus Protein™ pre-stained standard, dual color (Bio-Rad Laboratories) were used (grading: 20, 25, 37, 50, 75, 100, 150, 250 kDa). The running buffer used for electrophoresis was prepared by 1:10 dilution of a 10-fold concentrated stock solution containing 30 g of Tris base, 144 g of glycine (Merck) and 10 g of SDS in 1000 mL of Millipore water, pH 8.3.

Separated proteins were blotted by the Mini Trans-Blot Electrophoretic Transfer Cell (Bio-Rad Laboratories): 4 layers of filter paper, 2 glass fibre mats and 1 nitrocellulose-membrane (0.45 µm) were equilibrated for 5 min in the blotting buffer containing 14 g of glycine, 3 g of Tris base, 800 mL of Millipore water and 200 mL of methanol. The gel and the membrane were enclosed by 2 layers of filter paper and 1 glass fibre mat on each side. Transfer of separated proteins to the membrane was realized for 120 min at 4 °C (0.15 A).

In order to suppress unspecific binding of the antibodies, the membrane was subsequently incubated in a 5 % (w/v) mixture of fat-free milk (Saliter, Obergünzburg, Germany) in TBS including 0.1 % of Tween 20 for 2 h. TBS buffer was prepared by 1:10 dilution of a 10x buffer containing 80 g of NaCl (Merck) and 24.23 g of Tris-base in 1000 mL Millipore water, pH 7.6. The membrane was washed twice for 5 min in TBS including 0.1 % of Tween 20 (v/v). Primary antibodies were diluted 1:1000 in fat-free milk, Tween 20 and TBS (composition according to the step for the suppression of unspecific binding). The membrane was incubated with the mixture containing the primary antibody at 4 °C without shaking for 3 h (section 4.3.1.2.2) or overnight (section 4.3.1.2.1), respectively.

The membrane was washed three times with Tween 20 / TBS 0.1 % (v/v) and incubated with the secondary antibody linked to horseradish peroxidase described in 4.2.1.2.2 (diluted in the same manner as described for the primary antibodies) for another hour at room temperature under continuous shaking. The membrane was again washed three times with Tween 20 / TBS 0.1 % (v/v) and analyzed by enhanced chemoluminescence according to the manufacturers instructions (Pierce, Rockford, USA).

In addition to the anti-FLAG primary antibody and the respective peroxidase-linked secondary antibody, a rabbit anti-hH_2R primary antibody (Biozol, Eching, Germany) and a

suited secondary antibody (donkey anti-rabbit IgG coupled to peroxidase, Amersham Biosciences, Freiburg, Germany) were used for the investigations.

4.2.2 Stable co-expression of the human histamine H_2 receptor and the chimeric Gα–protein qs5-HA in HEK293 cells

4.2.2.1 Cloning, propagation and characterisation of DNA

4.2.2.1.1 PCR and product purification

Samples for PCR were prepared in a final volume of 200 µL containing 10 µL of each primer (10 µM in each case; MWG, Ebersberg, Germany), 200 ng of template, 28 µL of $MgSO_4$ (25 mM; MBI Fermentas), 20 µL of Pfu-buffer (10x, MBI Fermentas), 20 µL of DMSO, 20 µL of dNTP mix (2 mM, MBI Fermentas), 2 µL of Pfu-Polymerase (2.5 U / µL; MBI Fermentas) and Millipore water as required.
PCR reactions were performed according to the following conditions:

(1) initial denaturation:	95 °C, 180 s
(2) denaturation:	95 °C, 60 s
(3) annealing:	65 °C, 120 s
(4) extension:	72 °C, 120 s
(5) final extension:	72 °C, 300 s
(6) hold:	4 °C

steps (2)-(4) were repeated 24 times

PCR products were stored at -20 °C or mixed with 40 µL of loading-dye solution (6x, MBI Fermentas) and separated by agarose gel electrophoresis at 90 V for approx. 1 h.
Agarose gels were prepared according to 4.2.1.1.5 with minor modifications: Instead of 0.5 g of agarose, 1.0 g of agarose leading to a final gel concentration of 2 % (w/v) was used. Furthermore, the TBE buffer described in 4.2.1.1.5 was replaced by a TAE buffer containing 4.84 g of Tris Base (USB), 1.142 mL of glacial acetic acid (Merck), 2 mL of EDTA solution (0.5 M, pH 8.0; EDTA was obtained as Titriplex III from Merck) up to 1000 mL of Millipore water. After separation, signals of DNA were detected by UV light (254 nm) and excised with a clean, sharp scalpel. DNA was extracted from the agarose gel with the Qia quick Gel extraction Kit (Qiagen) according to the manufacturer's instructions. Extracted DNA was stored at -20 °C or directly used for digestion by restriction enzymes.

4.2.2.1.2 Digestion of DNA by restriction enzymes and dephosphorylation of the plasmid

DNA extracted from PCR samples was concentrated to a final volume of approx. 15 µL by the Savant Speed Vac® Plus SC 110A (Global Medical Instrumentation, Ramsey, USA) at low speed. Samples were prepared according to a final volume of 50 µL by addition of 5 µL of 10x Tango® buffer (MBI Fermentas) or 10x buffer R (MBI Fermentas), 40-80 U of the respective restriction enzymes (*Hind*III and *Xho*I were from MBI Fermentas whereas *Apa*I was obtained from GE Healthcare, Freiburg, Germany) and Millipore water as required.
Digestions were performed for 1 h at 37 °C. Samples were stored at -20 °C or directly used for ligation. 2.0 µL of plasmid DNA (1 µg / µL) were mixed with 1.5 µL of 10x Tango® buffer or buffer R, respectively. 20-40 U of restriction enzymes and Millipore water as required were added. Digestions were performed over a time period of 2 h at 37 °C. In order to avoid a possible self-ligation of the digested plasmid, 1.1 µL of a calf intestinal phosphorylase (0.1 U / µL; Boehringer Mannheim, Mannheim, Germany) were added, resulting in a concentration of 0.05 U of phosphorylase per pmol DNA-end.
After an additional incubation period of 1 h at 37 °C, the sample was heated at 80 °C for 20 min in order to inactivate the phosphorylase. Samples were stored at -20 °C or directly used for ligation experiments.

4.2.2.1.3 Ligation of DNA fragments

Separation of the DNA fragments was performed by agarose gel electrophoresis (see section 4.2.1.1.5). Recovery and purification of the respective DNA fragments were performed according to section 4.2.2.1.1.
For ligation, the amount of DNA was assessed in the scope of an agarose gel analysis by comparing the signals of the samples with the intensity of the DNA fragments of the marker. Approx. 25 ng of the digested, dephosphorylated vector and 24.5 ng of the digested insert were used for the preparation of the ligation sample according to a 5-fold excess of the insert over the vector with regard to molar amounts.
Millipore water required to achieve a final volume of 17 µL was added. The sample was heated for 5 min at 45 °C in order to dissolve dimers.
2 µL of T4-DNA-ligase buffer (10x, including 10 mM of ATP; New England Biolabs, Ipswich Massachusetts, USA) and 1 µL of T4-DNA-ligase (1 Weiss-U / µL; New England Biolabs) were added. Incubation was performed at room temperature overnight. After the incubation, the sample was heated at 65 °C for 10 min in order to inactivate the ligase. Samples were stored at -20 °C or directly used for transformation of competent bacteria.

4.2.2.1.4 Preparation of media and agar plates

For the preparation of LB medium, 10 g of bacto tryptone (Difco, Detroit, USA), 5 g of yeast-extract (Roth) and 10 g of NaCl (Merck) were dissolved to 1000 mL of Millipore water, pH 7.5. The solution was autoclaved at 121 °C and stored at 4 °C.
Selective LB medium was prepared by addition of ampicillin (Sigma) to LB medium under sterile conditions according to a final concentration of 100 µg / mL.
For the preparation of selective agar plates, 15 g of agar-agar (Roth) were added to 1 L of LB medium without antibiotic. The suspension was continuously stirred and heated for approx. 2 h in order to dissolve the agar-agar. The solution was autoclaved and cooled to 55 °C.
Ampicillin was added to a final concentration of 100 µg / mL under sterile conditions.
The solution was immediately poured into the bottom-parts of culture plates (diameter: 9 cm) under sterile conditions. After solidification, the plates were stored at 4 °C.
SOC medium was prepared by dissolving 2 g of bacto tryptone, 0,5 g of yeast-extract, 50 mg of NaCl, 1 mL of KCl (0,25 M), 0,5 mL of $MgCl_2$ (2 M) in 100 mL of Millipore water. The solution was autoclaved and cooled on room temperature. Finally, 2 mL of glucose (1 M) were added under sterile conditions (KCl, $MgCl_2$ and glucose were from Merck).
SOC medium was stored at 4 °C.

4.2.2.1.5 Preparation of competent bacteria

Competent bacteria were prepared by analogy with a previously described procedure (Hofinger, 2007): 10 µL of *E. coli* TOP10 bacteria suspension (Invitrogen) were added to 10 mL of LB medium under sterile conditions and cultured overnight at 37 °C and 200 rpm.
Next day, 200 mL of LB medium were inoculated with 2 mL of the overnight culture and incubated at 37 °C and 200 rpm until an OD_{600} of approx. 0.2 was achieved (4 h).
Then, the suspension was aliquoted into 4 polypropylene tubes (50 mL) and stored on ice for 10 min. Subsequently, bacteria were centrifuged for 7 min at 1500 g and 4 °C. The supernatant was discarded under sterile conditions and 8 mL of an ice-cold $CaCl_2$-solution (pH 7.0) containing 60 mM of $CaCl_2$, 15 % of glycerol and 10 mM of PIPES (Gerbu, Gaiberg, Germany) were added to each tube. The bacterial pellets were resuspended and then stored on ice for 30 min. The samples were centrifuged for 5 min at 1000 g. The supernatant was discarded and each pellet was resuspended in 1.6 mL of ice-cold $CaCl_2$-solution.
The samples were aliquoted under sterile conditions to autoclaved 1.5 mL microfuge tubes corresponding to 100 µL per tube. The samples were stored for another 2 h on ice. Finally, bacteria were frozen in liquid nitrogen and stored at -80 °C.

4.2.2.1.6 Transformation of bacteria

Competent bacteria were thawed on ice and approx. 10 ng of plasmid-DNA were added to 100 µL of suspension after 10 min. The mixture was incubated for 30 min on ice. The suspension was heated at 42 °C for 60 s and afterwards cooled on ice for 3 min. 900 µL of SOC medium were added and the mixture was incubated at 37 °C and continuous shaking (200 rpm) for 1 h. 100 µL of the suspension were plated on an ampicillin containing agar plate. The rest of the suspension (900 µL) was centrifuged at 3000 rpm for 5 min. 800 µL of the supernatant were discarded. The pellet was resuspended in the residual volume of 100 µL and plated on another selective agar-plate. The agar-plates were incubated overnight at 37 °C. The plates with grown bacteria were stored at 4 °C for up to 4 weeks.

4.2.2.1.7 Investigation of clones by colony-PCR

Colonies were investigated according to a previously described protocol (Hofinger, 2007) with minor modifications: Briefly, colonies were picked with a sterile pipet tip. 1 mL of ampicillin containing LB medium were inoculated with the colony in a sterile reaction vessel and incubated for 5 h at 37 °C under continuous shaking (200 rpm). An ampicillin containing agar-plate was inoculated with the pipet tip that was used for the picking of the colony, incubated overnight at 37 °C and finally stored at 4 °C.
After incubation for 3 min, the bacterial suspension was centrifuged at 6000 rpm. The supernatant was discarded and the pellet was resuspended in 50 µL of Millipore water. The sample was incubated at 100 °C for 5 min. Then, 10 µL of the sample were mixed with each 0.5 µL of the primers (10 µM in each case) used for the cloning of the respective cDNA, 2 µL of dNTP-mix (2 mM), 2 µL of Taq-reaction-buffer including 15 mM of $MgCl_2$ (10x, Qiagen), 4.8 µL of Millipore water and 0.2 µL of Taq-polymerase (5 U / µL, Qiagen). For reference, the template of the PCR (pcDNA3.0-Neo-FLAG-hH_2R-His_6 or pcDNA3.1(+)-Hygro-qi5-HA, respectively; see also sections 4.2.2.2 and 4.2.2.3) was used: 2 µL of a solution that contained 10 ng of the DNA-construct / µL were diluted with 8 µL of Millipore water and further processed as described for the sample of the colony. Samples were amplified according to HOFINGER (Hofinger, 2007) and subsequently separated by agarose gel electrophoresis. Data analysis was performed as described in section 4.2.1.1.5. Colonies which were identified to incorporate the DNA of interest were chosen for further amplification and processed in the Maxi-Prep.

4.2.2.1.8 Colony amplification, glycerol culture and preparation of plasmid DNA (Maxi-Prep)

The colony of interest was picked with a sterile pipet tip. Approx. 200 mL of LB medium containing ampicillin (100 µg / mL) were inoculated with the bacteria. The suspension was grown overnight at 37 °C and 200 rpm in a 500 mL Erlenmeyer flask. 700 µL of the overnight culture were mixed with 300 µL of a 50 % (v/v) glycerol solution in a 1.5 mL microfuge tube and stored at -80 °C. The preparation of plasmid DNA from the rest of the overnight culture was performed with the Plasmid Purification Kit (Qiagen) according to the manufacturer's instructions.

4.2.2.1.9 Determination of DNA concentration and sequencing

Maxi-Prep DNA was diluted 1:50 with Millipore water. The DNA concentration was determined by UV spectroscopy according to the following equation:
$c\ [\mu g / mL] = 50 \cdot (70 \cdot A_{260} - 40 \cdot A_{280})$.
Sequencing of Maxi-Prep DNA was performed by Entelechon (Regensburg, Germany).

4.2.2.2 Subcloning of the hH_2R

The previously described vector pcDNA3.0-Neo-FLAG-hH_2R-His_6 (Schneider, 2005) was used as template for the PCR.
In order to increase the protein expression in mammalian cells, a Kozak consensus-sequence (Kozak, 2002) was integrated in the sense-primer: for suited annealing properties of the primers, the letters ATT were incorporated before the start codon ATG. As the first triplet after the ATG begins with a G, the common sequence of such a consensus-sequence (bold letters) is realized: G/A NN ATG G (Kozak, 1987), where N represents variable bases. Furthermore, a recognition site for *Hind*III (AAGCTT) and an overhang (lower case letters) in order to ensure appropriate cleavage by the restriction enzyme were included in the sense primer. In addition, the primer incorporated the 18 bases encoding the first 6 amino acids of the receptor (counted from ATG). The antisense primer consists of an overhang (lower case letters), a recognition site for the restriction enzyme *Xho*I (CTCGAG) and the last 21 bases of the receptor cDNA:

sense:	5'-gcgcgAAGCTT**ATT**ATG**G**CACCCAATGGCACA-3'
antisense:	5'-atataCTCGAGTTACCTGTCTGTGGCTCCCTG-3'

Both primers were created in the way that bases encoding the FLAG epitope and the hexahistidine tag were not amplified by PCR (Fig. 4.2).

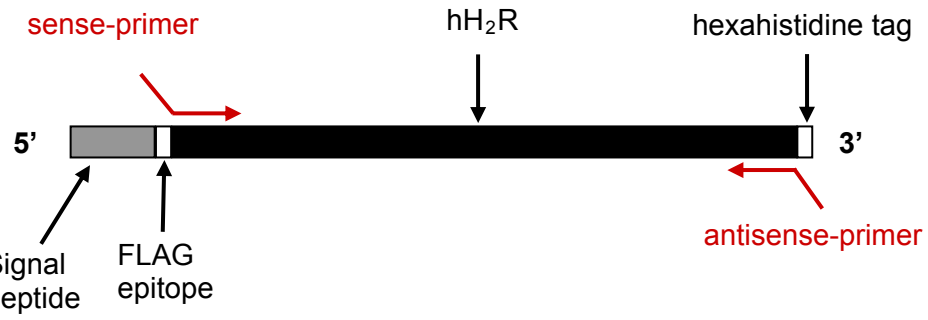

Fig. 4.2: *Structure of the hH_2R gene construct, inserted into the pcDNA3.0-Neo-FLAG-hH_2R-His_6 plasmid, and annealing points of the primers (red arrows; according to (Schneider, 2005)).*

The PCR was performed according to 4.2.2.1.1 and led to the signal with the expected size of 1095 bp (Fig. 4.3).

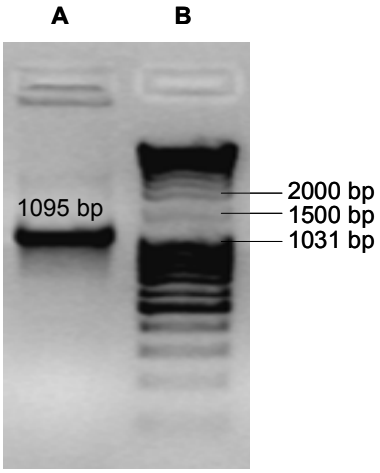

Fig. 4.3: *Agarose gel analysis of the PCR-product.* **A***: HindIII-hH_2R-XhoI* **B***: Marker*

The PCR product was purified as described in 4.2.2.1.1. The purified DNA was digested with the enzymes *Hind*III and *Xho*I (40 U in 50 µL in each case) in presence of buffer R and purified according to 4.2.2.1.2. As vector for the incorporation of the digested and purified insert, the vector pcDNA3.1(+)-Neo (Invitrogen) was chosen: it was digested with the same restriction enzymes (20 U in 20 µL in each case) and the same buffer as the insert. The digested vector was purified and dephosphorylated as explained in 4.2.2.1.2.

Ligation of insert and vector was performed according to 4.2.2.1.3. Transformation, colony-PCR, colony-propagation, isolation and characterisation of plasmid DNA was performed according to the sections 4.2.2.1.6 to 4.2.2.1.9.

One conservative mutation was detected by sequencing at position 1041 (counted from the start-codon ATG): G1041T.

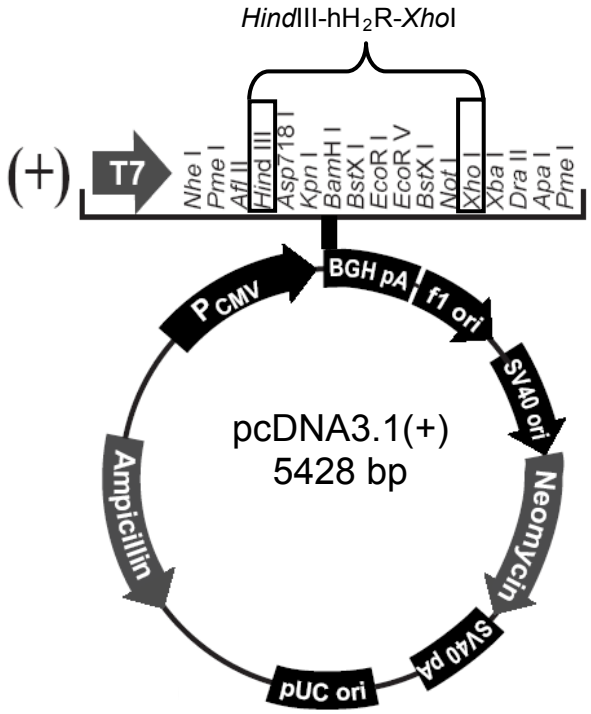

Fig. 4.4: *Insertion of the gene for the hH$_2$R in pcDNA3.1(+)-Neo via the HindIII (5') and XhoI (3') restriction sites.*

4.2.2.3 Subcloning of qs5-HA

The pcDNA1-qi5-HA vector was a generous gift from Prof. Dr. Bruce R. Conklin, Gladstone Institute of Cardiovascular Disease, University of California, San Francisco, USA. It was previously subcloned in the pcDNA3.1(+)-Hygro vector in our workgroup (Ziemek et al., 2006). In order to redirect the stimulation of the hH$_2$R by an agonist to an increase in the intracellular calcium level, the cDNA encoding qi5-HA had to be converted into the respective cDNA encoding the chimeric G-protein appropriate for a G$_s$-coupled GPCR, i.e. qs5-HA (Conklin et al., 1996; Conklin et al., 1993; Wood et al., 2000).

Therefore, the bases encoding the five C-terminal amino acids of qi5-HA were replaced with those of qs5-HA by site-directed mutagenesis. A sense primer was created for the introduction of an overhang (lower case letters) and the recognition site of the restriction enzyme *Hind*III (AAGCTT). Furthermore, the 18 bases encoding the first 6 amino acids of the chimera qi5-HA (these are in agreement with those of qs5-HA) were incorporated into the primer. The antisense primer incorporates an overhang (lower case letters), the recognition site of the restriction enzyme *Apa*I (GGGCCC), the stop codon (TTA), the 15 bases encoding the 5 amino acids to be replaced (italics) and the 15 bases of the cDNA encoding the amino acids -6 to -11 of qi5-HA.

sense: 5'- gcgcgAAGCTTATGACTCTGGAGTCCATC-3'

antisense: 5'- atataGGGCCCTTA*GAGTAGTTCGTATTG*CTTAAGGTTCAGCTGCAG-3'

Hence, the bases encoding the C-terminal pentapeptide of qi5-HA (DCGLF) are not amplified whereas those encoding the 5 C-terminal amino acids of qs5-HA (QYELL) are incorporated by PCR (Fig. 4.5, (Conklin et al., 1993))

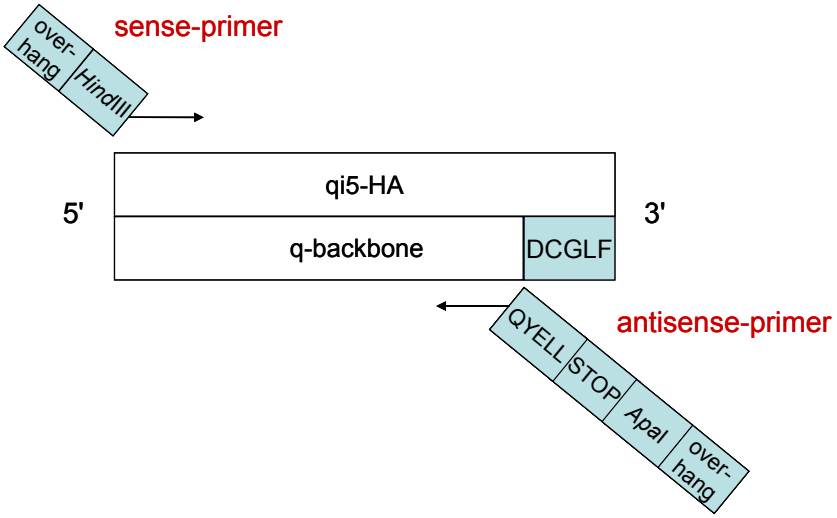

Fig. 4.5: *Principle of the site-directed mutagenesis of qi5-HA to qs5-HA.*

The PCR was performed according to 4.2.2.1.1 and led to a single signal with the expected size of 1102 bp (Fig. 4.6).

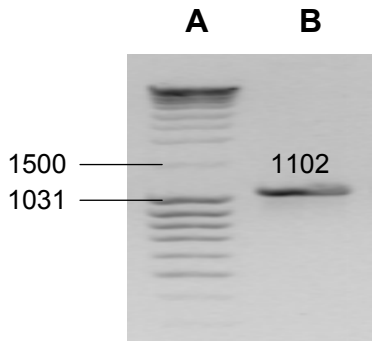

Fig. 4.6: *Agarose gel analysis of the PCR-product.* **A***: Marker* **B***: HindIII-qs5-HA-ApaI*

The PCR product was purified as described in 4.2.2.1.1. The purified DNA was digested with the enzymes *Hind*III and *Apa*I (40 U or 80 U in 50 µL, respectively) in presence of Tango® buffer and purified according to 4.2.2.1.2. As vector for the incorporation of the digested and purified insert, the vector pcDNA3.1(+)-Hygro (Invitrogen) was chosen: it was digested with the same restriction enzymes (20 U of *Hind*III and 40 U of *Apa*I in 20 µL) and the same buffer as the insert. The digested vector was purified and dephosphorylated as explained in 4.2.2.1.2. Ligation of insert and vector was performed according to 4.2.2.1.3. Transformation, colony-PCR, colony-propagation, isolation and characterisation of plasmid DNA was performed according to the sections 4.2.2.1.6 to 4.2.2.1.9.

Eight conservative mutations were detected by comparison of the sequencing result with the theoretical sequence: G144A, A157T, G158C, C159G, G288A, G1059T, G1071A, G1074A (counted from the start codon ATG). The five conservative mutations mentioned first were already reported by ZIEMEK (Ziemek, 2006). The conservative mutations in position 1071 and 1074 were introduced into the antisense-primer in order to improve its annealing properties. The conservative mutation in position 1059 is due to the difference between the template of the PCR, the cDNA of qi5-HA, and the cDNA of qs5-HA in that position.

4.2.2.4 Transfection experiments and cell propagation

HEK293 cells (DSMZ) were cultured in DMEM + 10 % FBS in a water-saturated atmosphere at 37 °C and 5 % CO_2. Cells were passaged twice a week (1:10). On the day before transfection, approx. $2.5 \cdot 10^5$ cells were seeded in a cavity of a 24-well-plate (Becton Dickinson, Heidelberg, Germany). On the day of transfection, cells had reached approx. 90 % confluence. Cells were transfected with the plasmid pcDNA3.1(+)-Neo-hH_2R using Lipofectamine™ 2000 (Invitrogen) and cultured in the presence of G418 (Sigma, 400 µg / mL) for 4 weeks. These cells were then cotransfected with the plasmid pcDNA3.1(+)-Hygro-qs5-HA in the same way and cultured in the presence of hygromycin B (Mobitec, Göttingen, Germany; 100 µg / mL) and G418 as mentioned before for at least another two months prior to the performance of the binding assays.
Stably transfected HEK293-hH_2R-qs5-HA cells were frozen in medium (DMEM + 10 % FBS, 400 µg / mL G418 and 100 µg / mL hygromycin B) including 10 % DMSO according to the procedure described in section 3.2.1.

4.2.3 Determination of ligand affinity in binding assays for the hH_2R

4.2.3.1 Radioligand binding assays for the hH_2R

4.2.3.1.1 Radioligand binding to whole cells

HEK293-hH_2R-qs5-HA cells were cultured in DMEM supplemented with 10 % FBS and selection antibiotics (400 µg / mL of G418 and 100 µg / mL of hygromycin B) in a water-saturated atmosphere containing 5 % CO_2 at 37 °C. Cells were passaged (1:10) twice a week. For the assays, approx. $5 \cdot 10^5$ cells were seeded into 175-cm^2 culture flasks (Nunc) and grown to approx. 70 % confluency (6 days) before the radioligand binding assays. Cells were detached with DMEM + 10 % FBS and centrifuged for 5 min at 300 g. Cells were once washed in Leibovitz' L-15 medium without phenol red + 1 %, counted in a hemocytometer

and finally suspended in Leibovitz' L-15 medium without phenol red + 1 % FBS according to a density of 1-2·10^6 cells / mL.

In addition to HEK293-hH_2R-qs5-HA cells, HEK293-FLAG-hH_2R-His_6 cells, which were kindly provided by Dr. Dietmar Gross (Institute of Pharmacy, Department of Pharmacology and Toxicology, University of Regensburg) were investigated for reference. Those cells were cultured in selective medium (DMEM + 10 % FBS + 400 µg / mL G418) and passaged 1:10 twice a week without Trypsin / EDTA treatment.

For saturation binding experiments, 20 µL of a ranitidine solution (10 mM in PBS) or 20 µL of a PBS-solution were pipetted per cavity of a 96-well plate (Greiner) either for the determination of unspecific or total binding, respectively. 160 µL of the cell suspension were added per well. Samples were completed by addition of 20 µL of the respective [^{3}H]-tiotidine solution (10-fold concentrated feed-solutions compared to final concentration; for further information about the tracer see section 3.2.6). Samples were shaken at 100 rpm for 65 min under light protection prior to harvesting. Cell-bound radioactivity was transferred to a glass fibre filter GF / C (Skatron) pretreated with PEI (0.3 % (v/v); PEI was from Sigma) by the Combi Cell Harvester 11025. The filter was washed with PBS (4 °C) for approx. 10 s. Filter discs with the cell-bound radioactivity were further handled according to section 3.2.6. Decays per minute (dpm) were transferred to Microsoft® Office Excel 2003. In case of saturation binding experiments, specific binding was determined by subtraction of unspecific binding from the respective values for total binding. Data were transferred to SigmaPlot® 9.0 and analyzed with the multiple scatter - error bars option. Curve fitting for total and specific binding was determined according to the ligand binding, one site saturation option whereas unspecific binding was analyzed by the standard curves, linear curve option. As data were obtained in 2 independent experiments (in each case n = 3), values for total, unspecific and specific binding were plotted in % of the B_{max}-value of specific binding against the concentration of [^{3}H]-tiotidine (Fig. 4.13). For competition binding experiments, cells were incubated with the ligands of interest in presence of either 5 nM (HEK293-hH_2R-qs5-HA cells) or 10 nM (HEK293-FLAG-hH_2R-His_6 cells) of [^{3}H]-tiotidine according to the conditions for the saturation binding experiments. The dpm values of the samples for unspecific binding were subtracted from the investigated concentrations of the respective competitor and the samples representing the total binding. Residuals were converted into percentage values. The data were analyzed with the multiple scatter - error bars option. Sigmoidal curves were calculated with the standard curves, four parameter logistic function. IC_{50}-values were converted into K_i-values according to the Cheng-Prusoff equation (Cheng and Prusoff, 1973): $K_i = IC_{50} \cdot K_d / (K_d + [L])$, where [L] represents the concentration of [^{3}H]-tiotidine used in competition binding experiments.

4.2.3.1.2 Assays on membranes

Membranes of HEK293-hH_2R-qs5-HA cells were obtained by analogy with a procedure described by MAYER (Mayer, 2002), but cells were not rinsed with homogenizing buffer due to the weak adherence of the cells.
Membranes of Sf9 cells expressing a hH_2R-$G_{s\alpha S}$ fusion protein were obtained from the Department of Pharmacology and Toxicology (Institute of Pharmacy, University of Regensburg).
For competition binding experiments, membranes were thawed, centrifuged (15,000 g, 15 min, 4 °C) and resuspended in binding buffer (12.5 mM $MgCl_2$, 1 mM EDTA, 75 mM Tris / HCl, pH 7.4). Competition binding experiments were essentially performed as described for whole cells. Membrane preparations containing 10 µg (HEK293-hH_2R-qs5-HA cells) or 13 µg (Sf9 cells expressing hH_2R-$G_{s\alpha S}$ fusion proteins) of protein were used per sample. For assays performed with membranes, 10 nM of [^{3}H]-tiotidine were used.

4.2.3.2 Squaramide derivatives

Compounds **6**-**8** were synthesized in our workgroup by Daniela Erdmann. Compounds **6** and **7** incorporate fluorescent moieties in order to perform fluorescence-based binding assays at the flow cytometer or the confocal microscope, respectively. Compound **8** is non-fluorescent and represents the cold form of a potential radioligand for the hH_2R which can be obtained by replacement of the propionyl moiety by a [^{3}H]-propionyl residue.

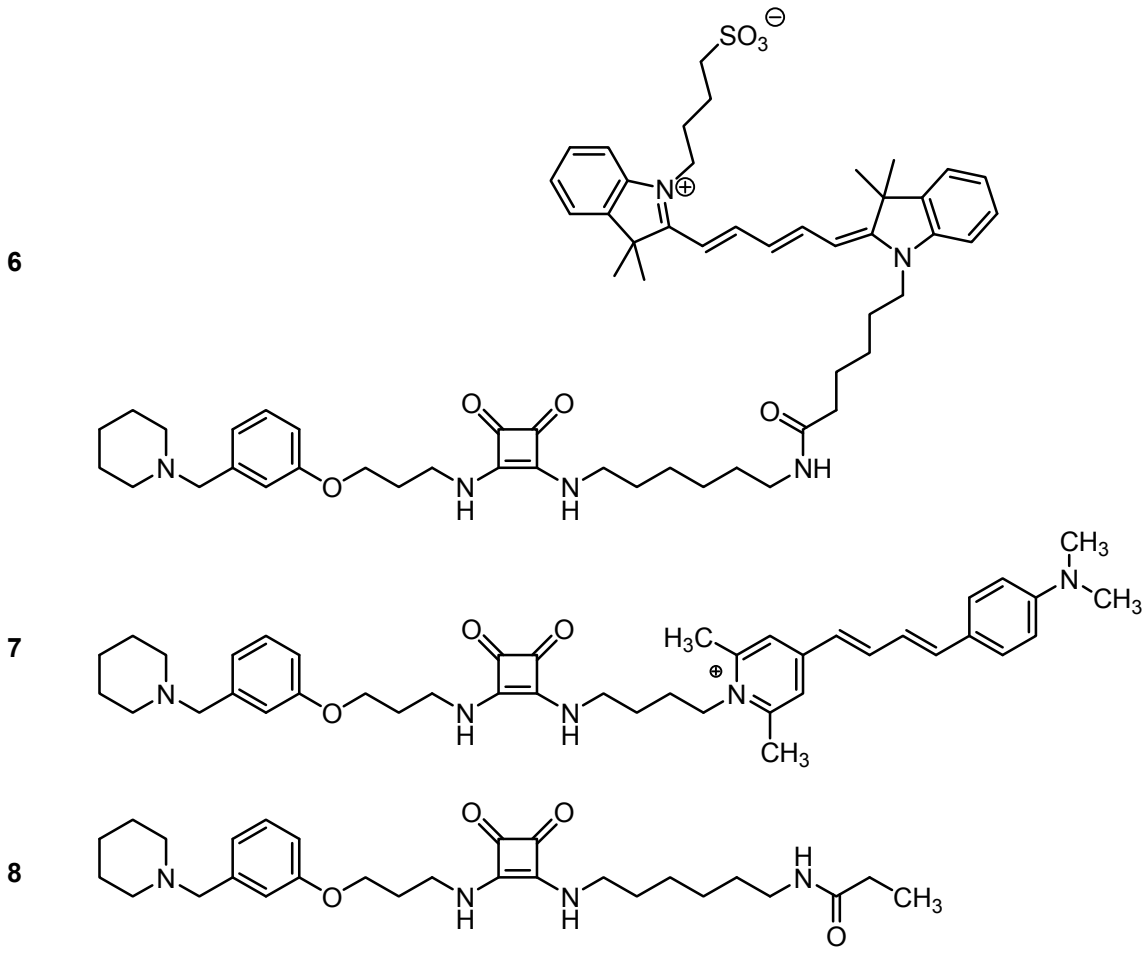

Fig. 4.7: *Chemical structures of the compounds* **6**-**8.**

4.2.3.3 Confocal microscopy

HEK293-hH_2R-qs5-HA cells were cultured according to section 4.2.3.1.1.

2 days prior to microscopy, approx. 4 · 10^4 HEK293-hH_2R-qs5-HA cells were seeded per cavity of a Lab-Tek® II 8 Chamber # 1.5 German Coverglass System (Nalge Nunc, Naperville, USA) in 200 µL of selective culture medium (DMEM + 10 % FBS + 400 µg / mL G418 + 100 µg / mL hygromycin B).

On the day of the investigation, the selection medium was replaced by 200 µL of Leibovitz' L-15 medium without phenol red (Invitrogen) containing 1 % FBS. By exchanging the culture medium, most cells of the weakly adhering population were removed from the polystyrene substrate. Thus, cells were post-incubated at 37 °C for 1.5 h in order to allow reattachment prior to microscopy. Subsequently, the sample for the total binding was prepared by addition of 200 µL of Leibovitz' L-15 + 1 % FBS including 160 nM of **6** per cavity. Hence, the final concentration of **6** was 80 nM. The sample of the unspecific binding was prepared in a different cavity in the same way, but famotidine was added according to a final concentration of 10 µM. Cells were incubated for 45 min at 37 °C in a water saturated atmosphere without

addition of CO_2. Subsequently, the samples were analyzed with a Carl Zeiss Axiovert 200 M microscope: the laser scanner LSM 510 was used in combination with the C-Apochromat 40 x / 1.2 W corr.-objective (Immersol™ W was used for water immersion mediating the refraction index of water). Laser excitation was performed with a power of 7 % at 633 nm; detection of emitted fluorescence was recorded with the 650 nm long pass filter. The scanning mode was plane, multi track, 12 bit. The pinhole was adjusted to 90 µm.

4.2.3.4 Determination of ligand affinity by flow cytometric binding assays

HEK293-hH_2R-qs5-HA cells were essentially cultured and prepared for flow cytometric measurements as described in section 4.2.3.1.1, but cells were not washed prior to the adjustment of their density. For saturation binding or competition binding experiments, 196 µL of cell suspension were mixed with 2 µL of **6** or **7** (100-fold concentrated feed solutions relative to final assay concentration in 30 % DMSO / PBS (v/v)), respectively, and 2 µL of 100-fold concentrated feed solutions compared to final concentration of the respective ligands (famotidine, ranitidine (Sigma), cimetidine, tiotidine (Tocris Cookson) or compound **8**, respectively) in DMSO. Incubations were peformed for 37 min at room temperature under light protection prior to the flow cytometric measurements. In saturation binding experiments, unspecific binding was determined in the presence of 30 µM of famotidine. In competition binding experiments, samples for total binding (fluorescent tracer) and unspecific binding (fluorescent tracer plus 100 µM of famotidine) were included and taken into account for data analysis. For the investigation of agonists (histamine, dimaprit and arpromidine), these conditions were maintained with the exception that the incubation period was reduced to 15 min in order to prevent internalization of agonist-occupied receptors. 100-fold concentrated feed solutions compared to the final assay concentration of arpromidine and histamine were prepared in 30 % DMSO / PBS (v/v) whereas DMSO was used for the respective solutions of dimaprit. For the optimisation of assay parameters, 10-fold concentrated feed solutions relative to the final concentration of dimaprit were prepared in PBS. Furthermore, the stock solution of **7** (20 µM) was prepared in only 2 % DMSO / PBS (v/v). Consequently, samples were prepared by addition of 2 µL of **7** (20 µM) and 20 µL of 10-fold concentrated feed solutions of dimaprit to 178 µL of cell suspension leading to a final DMSO concentration of 0.02 % (v/v) in the assay. Samples were incubated for 15 or 65 min, respectively. Flow cytometric measurements were performed with the FACSCalibur™ flow cytometer (Becton Dickinson, Heidelberg, Germany) according to the subsequent instrument settings: excitation: 488 nm (argon laser, compound **7**) or 635 nm (red diode laser, compound **6**), respectively; threshold forward scatter light (FSC) and sideward scatter light (SSC): 52;

secondary parameters: none; FSC: E-1; SSC: 320; Fl-3: 650 (compound **7**) or Fl-4: 800 (compound **6**), respectively; gated events: 10000.

Data were analyzed with WinMDI 2.8: the SSC signals of the investigated cells were plotted on the y-axis against their FSC signals on the x-axis. A small subpopulation amounting to approx. 3000 cells was identified by gating and taken into account for data analysis. Cells in this gate (gated events) were plotted on the y-axis against their fluorescence intensities determined in Fl-3 or Fl-4, respectively, resulting in histograms (for an example see section 4.3.2.3, Fig. 4.18). Geometric means were calculated and transferred to Microsoft® Office Excel 2003. In case of saturation binding experiments, specific binding was determined by subtraction of unspecific binding from the respective values for total binding.

Data were transferred to SigmaPlot® 9.0 and analyzed with the multiple scatter - error bars option. Curve fitting for total and specific binding was determined according to the ligand binding, one site saturation option whereas unspecific binding was analyzed by the standard curves, linear curve option. In case of competition binding experiments, the geometric means of the samples for unspecific binding were subtracted from the investigated concentrations of the respective competitor and the samples representing the total binding. Further data analysis was performed by analogy with radioligand binding competition experiments in section 4.2.3.1.1.

4.3 Results and discussion

4.3.1 Investigation of HEK293 cells for the expression of human histamine receptors

4.3.1.1 Expression analysis of human histamine receptors in HEK293 cells at the mRNA level

The control mRNA encoding β-actin corresponds to the expected size (304 bp), indicating successful mRNA isolation (Fig. 4.8). The mRNA encoding the hH_2R was also detected with the expected size of 370 bp (Fig. 4.8). By contrast, mRNAs of the hH_1R, hH_3R or the hH_4R were not detectable.

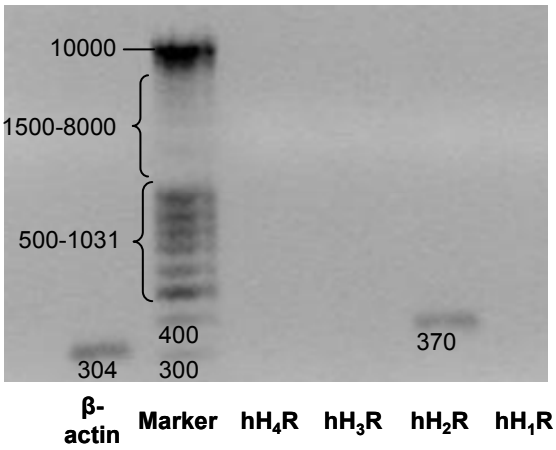

Fig. 4.8: *Determination of histamine receptor subtype mRNA in HEK293 cells.*

The amplification of plasmids incorporating the hH_3R (pVL1392-SF-hH_3R) or the hH_4R (pGEM-3Z-SF-hH_4R), respectively, worked accurately under the chosen PCR conditions (Fig. 4.9) which underlines the validity of the used method.

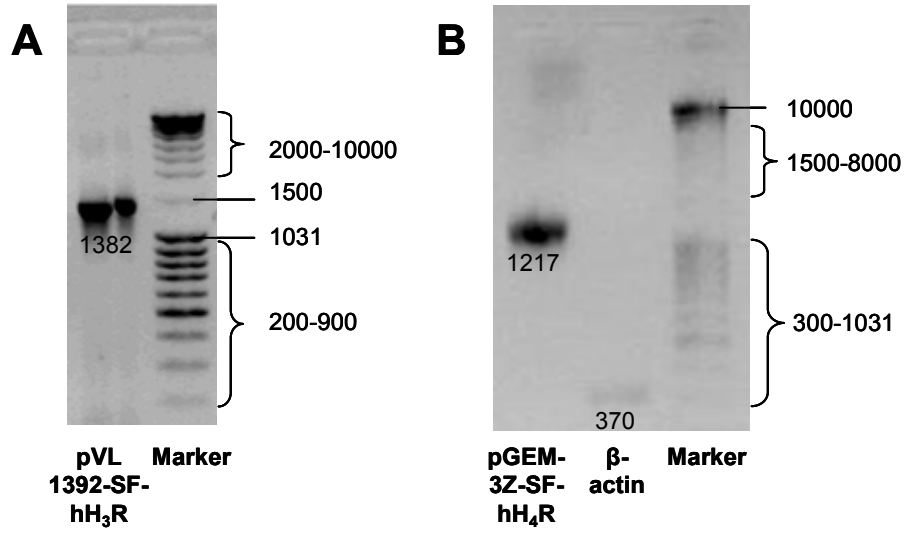

Fig. 4.9: *Confirmation of the suitability of the PCR conditions for the amplification of DNA encoding* **A***: the hH_3R and* **B***: the hH_4R.*

As the detection of mRNA does not mandatorily correlate with the expression of a protein (Schneider, 2005), western blot experiments were performed in order to investigate the expression of the hH_2R in HEK293 cells.

4.3.1.2 Western blot analysis of the hH_2R expression

4.3.1.2.1 Development of a method for the characterisation of the hH_2R expression

A first experiment, using the mouse anti-FLAG primary antibody and the biotinylated anti-mouse / rabbit secondary antibody, revealed only a weak band for the positive control in the presence of a high background (data not shown). When the primary antibody was omitted, an immunopositive reaction was obtained in any investigated sample (Fig. 4.10, A). Thus, the biotinylated secondary antibody appeared to be unspecific and was replaced by the secondary antibody which is linked to a peroxidase (Fig. 4.10, B).

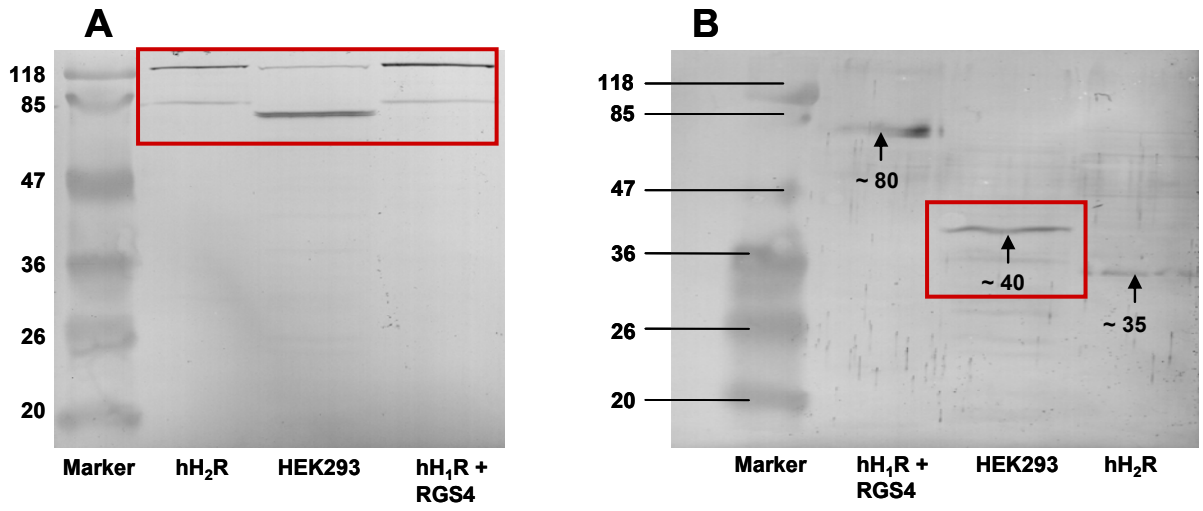

Fig. 4.10: *Approaches with the semi-dry western blot technique on membranes.* **A**: *Unspecific binding of the biotinylated secondary antibody in absence of a primary antibody (red box);* **B**: *unspecific binding of the anti-FLAG primary antibody and the secondary antibody linked to horseradish peroxidase on membranes of HEK293 cells (red box). The indicated numbers represent the molecular mass of the respective bands in kDa.*

The use of the secondary antibody linked to peroxidase with the anti-FLAG primary antibody revealed signals for the hH_2R and the sample with the hH_1R and RGS4, respectively (Fig. 4.10, B). This apparently corresponded to the expected results (Preuss et al., 2007; Seifert et al., 2003). However, the HEK293 sample gave a positive reaction, too (Fig. 4.10, B), although membranes of HEK293 cells should not contain a FLAG-epitope. Thus, the false-positive reaction reflects unspecific binding. Therefore, the method of the wet western blot was used for further investigations instead of the semi-dry variant.

The investigation of histamine receptor expression using the anti-FLAG primary antibody and the secondary antibody linked to peroxidase led to the expected signals (Fig. 4.11, A). This is valid for the sample with the hH_1R (Seifert et al., 2003) and that with the hH_2R (Preuss et al., 2007) as well for the membranes of HEK293 and HEK293 T cells, which did not give a positive reaction.

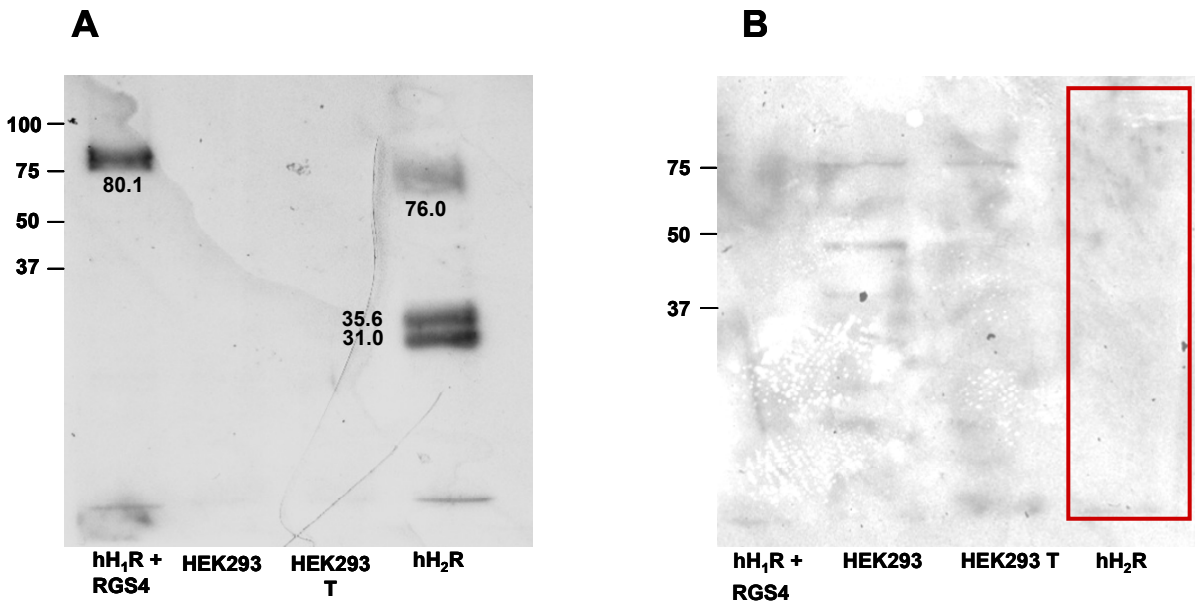

Fig. 4.11: *Approaches with the wet western blot on membranes.* **A***: Specific binding of the anti-FLAG primary antibody,* **B***: lack of specific binding of the rabbit anti-human histamine H_2 receptor primary antibody on membranes from Sf9 insect cells expressing the hH_2R (red box). The indicated numbers represent the molecular mass of the respective bands in kDa.*

When the rabbit anti-human histamine H_2 receptor primary antibody was used instead of the anti-FLAG primary antibody, the detection of the expected protein failed for membranes from Sf9 insect cells which expressed the hH_2R including two artificial amino acid attachments (FLAG-epitope and hexa-His-tag; Fig. 4.11, B). In order to investigate, if the detection failed due to those artificial attachments, membranes from HL-60 HD cells expressing a native hH_2R which neither incorporates a FLAG epitope nor a hexahistidine tag were prepared according to section 4.2.1.2.1 and used as positive control for the determination of the hH_2R expression (section 4.3.1.2.2).

4.3.1.2.2 Detection of the hH_2R protein

The use of membranes from HL-60 HD cells instead of membranes from Sf9 insect cells expressing an hH_2R with artificial attachments revealed the expected band of 40.1 kDa (Fig. 4.12; the theoretical molecular mass of the hH_2R is 40,098 Da according to http://www.uniprot.org/uniprot/P25021, February 2009). Neither in the trace of the negative control nor in the traces of membranes from HEK293 or HEK293 T cells, a signal was detected (Fig. 4.12).

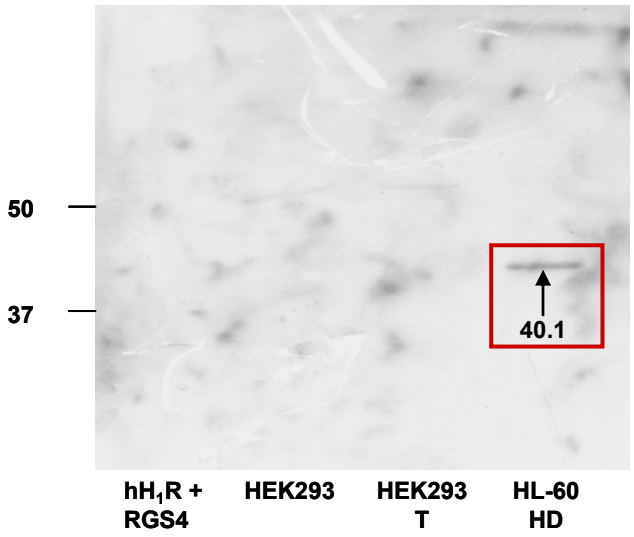

Fig. 4.12: *Specific binding of the rabbit anti-human histamine H_2 receptor primary antibody on membranes from HL-60 HD cells (red box). The indicated numbers represent the molecular mass of the respective bands in kDa.*

Thus, western blot experiments neither revealed a hH_2R protein in HEK293 nor in HEK293 T cells. Probably, the FLAG epitope or the hexahistidine tag impeded the binding of the rabbit anti-human histamine H_2 receptor primary antibody on membranes which expressed such an artificial variant of the hH_2R. Since an alteration of the hH_2R pharmacology by those artificial attachments can not be ruled out, those residues were excluded in the scope of the cloning of the hH_2R. Furthermore, the results suggest HEK293 cells to be appropriate for the expression of human histamine receptors due to the lack of endogenous histamine receptor proteins. As HEK293 T cells are not as widely used in expression studies as HEK293 cells (Thomas and Smart, 2005), further experiments were performed with the latter cell line.

4.3.2 Determination of binding data for the hH_2R

4.3.2.1 Radioligand binding assays for the hH_2R

Saturation binding experiments gave comparable K_d-values for [^{3}H]-tiotidine with both investigated cell lines (Fig. 4.13, Table 4.2). Data are in agreement with values reported in the literature (Kelley et al., 2001).

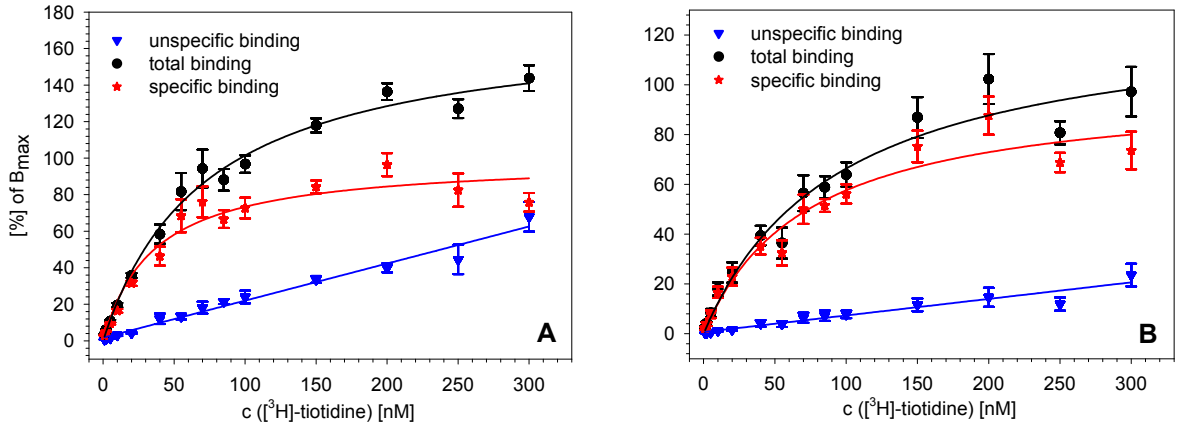

Fig. 4.13: *Saturation binding of [^{3}H]-tiotidine.* **A***: HEK293-FLAG-hH_2R-His$_6$ cells.* **B***: HEK293-hH_2R-qs5-HA-cells. Unspecific binding was determined in the presence of 1 mM of ranitidine (mean values ± SEM; n = 6).*

The hH_2R affinities of ranitidine and standard agonists (arpromidine, dimaprit and histamine) determined in competition binding experiments with [^{3}H]-tiotidine were comparable at both cell types (Fig. 4.14, A and B; Table 4.2). The K_i-values were calculated according to the Cheng-Prusoff equation (Cheng and Prusoff, 1973).

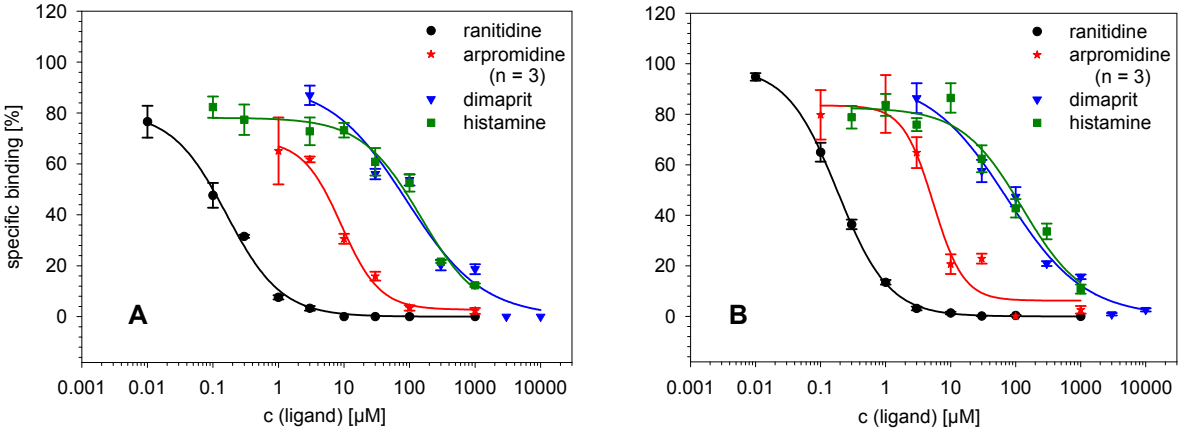

Fig. 4.14: *Competition binding experiments with various H_2R ligands.* **A***: HEK293-FLAG-hH_2R-His$_6$ cells.* **B***: HEK293-hH_2R-qs5-HA-cells. Unspecific binding was determined in the presence of 1 mM of ranitidine (mean values ± SEM; n = 6, unless otherwise indicated).*

Furthermore, results for the agonists were consistent with regard to data from studies using membrane preparations of HEK293-hH_2R-qs5-HA cells and whole cells (Fig. 4.15, Table 4.2). The affinity of arpromidine was lower compared to data reported in literature that were determined with membrane preparations of Sf9 cells expressing a hH_2R-$G_{s\alpha S}$ fusion protein (Fig. 4.15, Table 4.2, (Xie et al., 2006)). This observation might be due to this artificial fusion protein because the low affinity binding site of arpromidine was confirmed with the

established assay on those membranes expressing the fusion protein whereas a high affinity binding site was not detected (Fig. 4.15; Table 4.2; (Xie et al., 2006)).

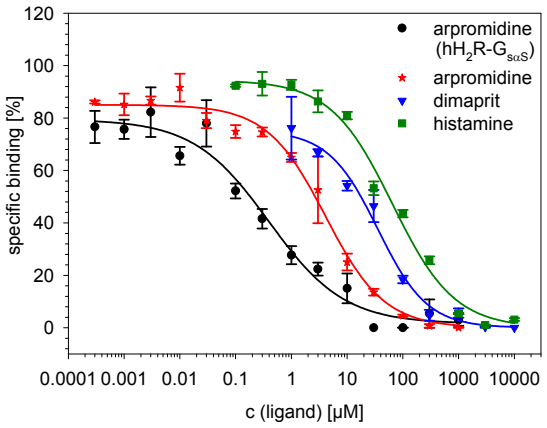

Fig. 4.15: *Competition binding experiments with various H_2R ligands. Membranes of Sf9 cells expressing hH_2R-$G_{s\alpha S}$ (black curve) and of HEK293-hH_2R-qs5-HA cells (red, blue and green curve). Mean values ± SEM; n = 3.*

Table 4.2: *Comparison of binding data obtained in radioligand binding assays with reference values from literature. Indicated are mean values ± SEM: (K_d) or K_i [µM].*

Ligand	HEK293-hH_2R-qs5-HA cells	HEK293-hH_2R-qs5-HA membranes	HEK293-FLAG-hH_2R-His_6 cells	hH_2R-$G_{s\alpha S}$ Sf9 membranes	reference data from literature
[^{3}H]-tiotidine	(0.073 ± 0.013)	(n.d.)	(0.036 ± 0.006)	(n.d.)	(0.032 ± 0.005)[1]
ranitidine	0.172 ± 0.011	n.d.	0.127 ± 0.020	n.d.	0.085 ± 0.004[2]
arpromidine	5.4 ± 1.3	3.6 ± 0.7	7.1 ± 2.1	0.301 ± 0.100	0.010 (0.007-0.017); 0.450 (0.230-1.200)[3]
dimaprit	67.4 ± 20.2	31.4 ± 8.4	69.7 ± 18.0	n.d.	25 ± 5[2]
histamine	118.2 ± 53.8	57.3 ± 8.6	116.6 ± 52.1	n.d.	81 ± 15; 2.0 ± 1.2[2]

[1]Kelley et al., 2001; [2]Leurs et al., 1994; [3]Xie et al., 2006

The K_i-values of the H_2R ligands ranitidine, dimaprit and histamine were in the same order of magnitude as data reported in literature, but there was no hint to a high affinity binding site for histamine (Table 4.2; (Leurs et al., 1994)).

Taken together, the hH_2R binding is not significantly affected by the coexpression of the receptor and the chimeric G-protein qs5-HA (Table 4.2).

4.3.2.2 Specific binding of the fluorescent compound 6 to HEK293-hH_2R-qs5-HA cells in confocal microscopy

As shown in Fig. 4.16, specific binding of compound **6** was detected in the cell membranes of HEK293-hH_2R-qs5-HA cells.

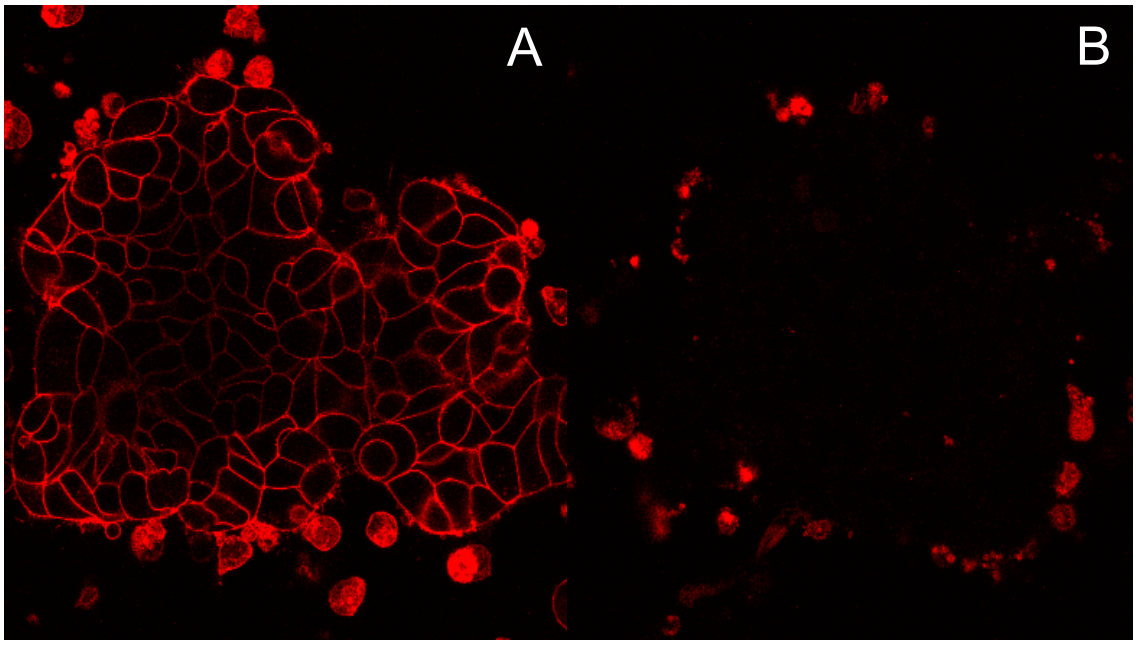

Fig. 4.16: *Confocal microscopy of HEK293-hH_2R-qs5-HA cells incubated with 80 nM of* **6**. **A***: total binding and* **B***: unspecific binding (determined in the presence of 10 µM famotidine).*

4.3.2.3 Flow cytometric binding assays for the hH_2R

Gating of the data revealed cells which do not correctly express the hH_2R (Fig. 4.17): in the control sample for the detection of unspecific binding, the fluorescence intensity detected in Fl-3 was only in part decreased compared to the total binding (Fig. 4.17, right). Hence, compound **7** was not completely displaced by the H_2R antagonist famotidine. Therefore, the gate was readjusted as shown in Fig. 4.18.

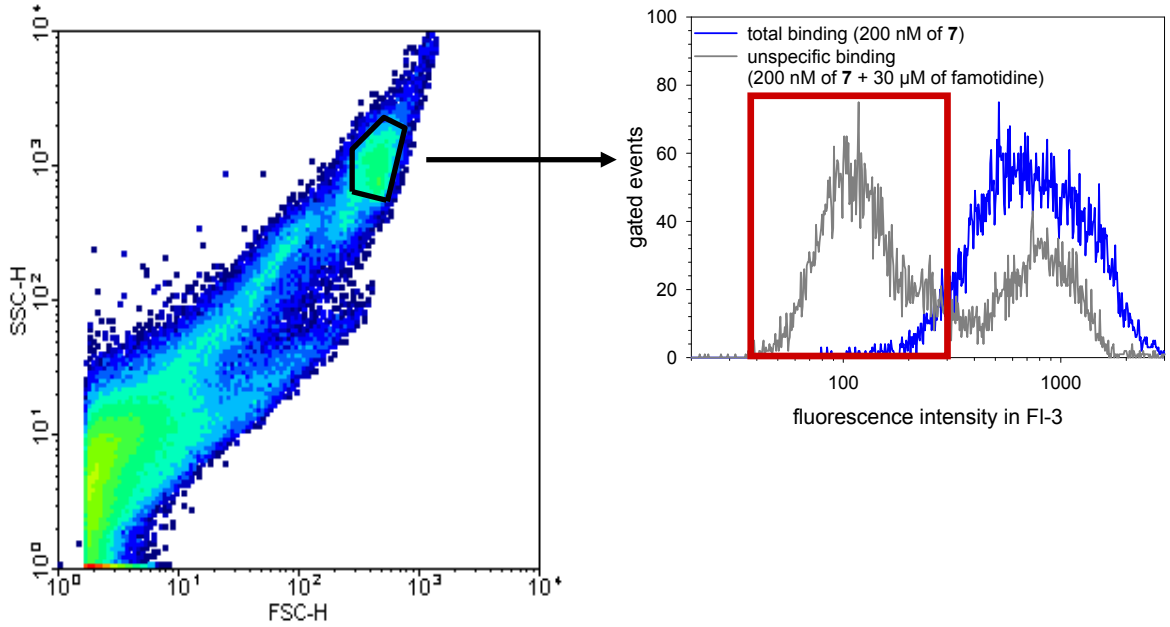

Fig. 4.17: *Binding of compound* **7** *to HEK293-hH$_2$R-qs5-HA cells. Cells in the red rectangle (right) correctly express the hH$_2$R (Further details are described in the text).*

In contrast to the result of the first approach (Fig. 4.17) the small subpopulation of cells enclosed by this adjusted gate showed a pronounced difference in total and unspecific binding of **7** (Fig. 4.18). Thus, this gate was considered for further data analysis.

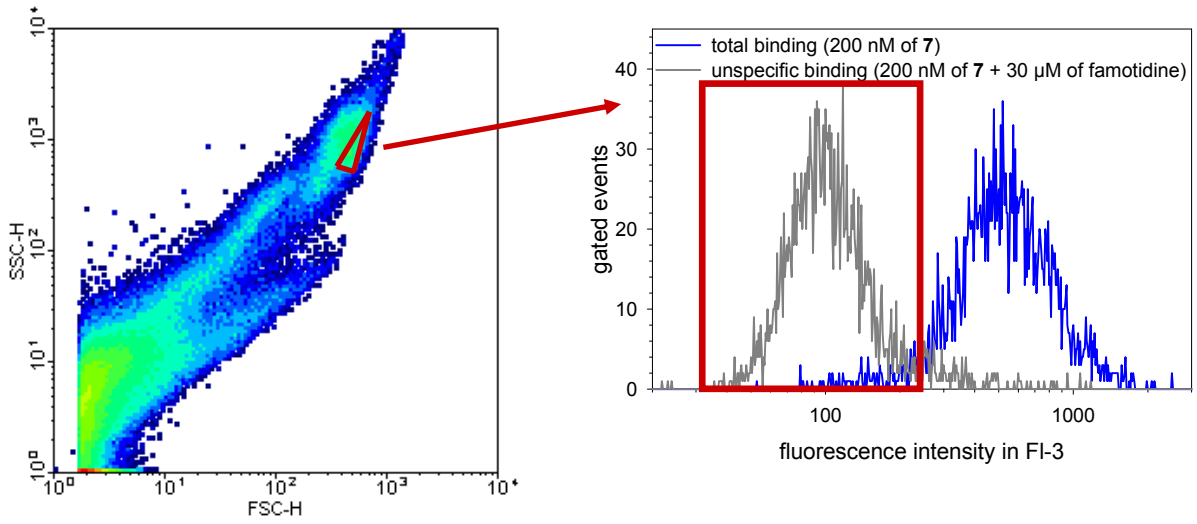

Fig. 4.18: *Specific binding of* **7** *to HEK293-hH$_2$R-qs5-HA cells. Cells in the red triangle of the density plot (left) were considered for the calculation of histograms (right).*

With K_d-values of 166 ± 39 nM (compound **6**) and 181 ± 38 nM (compound **7**), the investigated fluorescent ligands showed remarkably low extents of unspecific binding at HEK293-hH$_2$R-qs5-HA cells (Fig. 4.19).

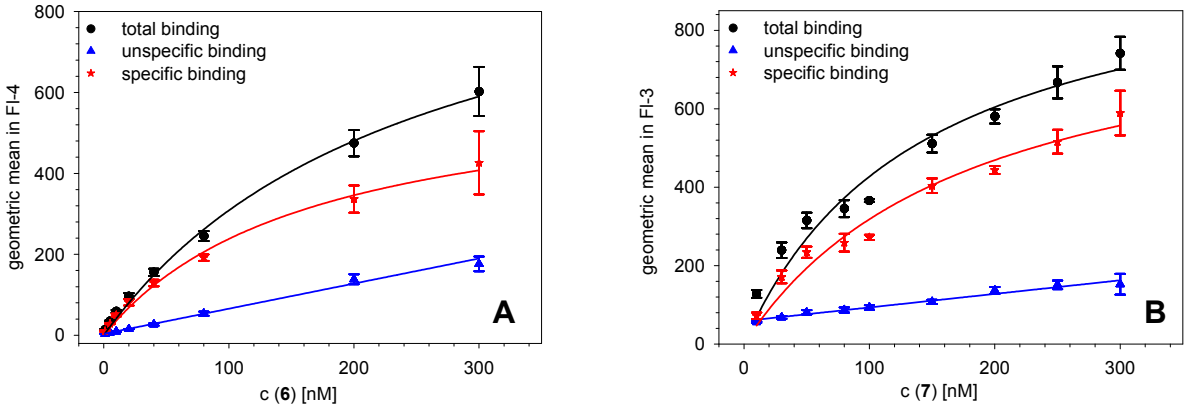

Fig. 4.19: *Saturation binding experiments with* **A***: compound* **6** *and* **B***: compound* **7** *on HEK293-hH_2R-qs5-HA-cells (mean values ± SEM; n = 3). Unspecific binding was determined in the presence of 30 µM of famotidine.*

For the purpose of validation, flow cytometric competition binding experiments using various H_2R ligands were performed. The fluorescence-labelled compound **7** was used at a concentration of 200 nM which is in the range of the K_d-value. All 8 investigated ligands decreased the specific binding of the fluorescent probe in a concentration-dependent manner (Fig. 4.20).

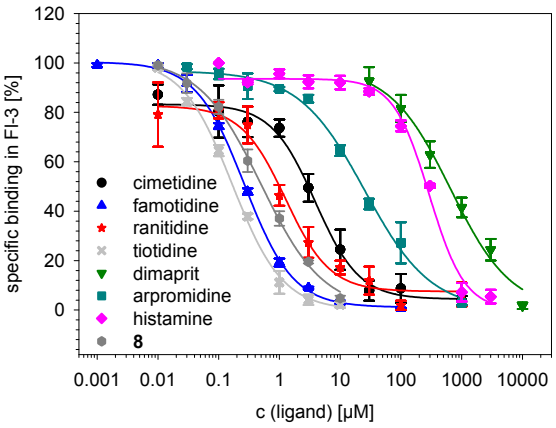

Fig. 4.20: *Concentration-dependent displacement of* **7** *(200 nM) by various H_2R ligands. Unspecific binding was determined in the presence of 100 µM of famotidine (mean values ± SEM; n = 3).*

The K_i-values calculated for standard antagonists (cimetidine, famotidine, ranitidine and tiotidine) were in agreement with K_b-values obtained in GTPase activity assays (Table 4.3, (Kelley et al., 2001; Preuss et al., 2007)). Except for cimetidine, the affinities determined for those antagonists in the flow cytometric assay were significantly lower compared to radioligand binding data reported by LEURS (Table 4.3, (Leurs et al., 1994)). Nevertheless, the rank order of the K_i-values (famotidine ≈ tiotidine < ranitidine < cimetidine) were confirmed in competition binding experiments performed with flow cytometry. Compound **8** showed an affinity in the same order of magnitude as famotidine and tiotidine. The low affinity binding site reported for histamine was determined with 138 ± 15 µM which is in agreement with data reported in literature (Leurs et al., 1994). However, a high affinity binding site reported by LEURS (2.0 ± 1.2 µM; (Leurs et al., 1994)) was not detected.

Table 4.3: *Comparison of the affinities [µM] calculated from the flow cytometric measurements with data from literature (mean values ± SEM, unless otherwise indicated).*

Ligand	Flow cytometry K_i [µM]	GTPase assay K_b [µM]	Radioligand binding assays K_i [µM]
cimetidine	1.847 ± 0.443	1.700 ± 0.430[1]	0.660 ± 0.220[3]
famotidine	0.126 ± 0.006	0.048 ± 0.010[1]	0.016 ± 0.003[3]
ranitidine	0.597 ± 0.164	0.840 ± 0.094[1]	0.085 ± 0.004[3]
tiotidine	0.080 ± 0.009	0.060 (0.030-0.130)[2]	0.017 ± 0.006[3]
dimaprit	311 ± 107	-	25 ± 5[3]
arpromidine	12 ± 2	-	0.010 (0.007-0.017); 0.450 (0.230-1.200)[4]
histamine	138 ± 15	-	2.0 ± 1.2; 81 ± 15[3]
8	0.237 ± 0.041	n.d.	n.d.

[1]Preuss et. al, 2007; [2]Kelley et al., 2001 (numbers in parentheses represent the 95 % confidence interval); [3]Leurs et al., 1994; [4]Xie et al., 2006 (numbers in parentheses represent the 95 % confidence interval)

Further differences with regard to binding data were found for the agonists dimaprit and arpromidine (Table 4.3, (Leurs et al., 1994; Xie et al., 2006). As the affinity of dimaprit was first determined in presence of 1.30 % (v/v) DMSO, the influence of reduced DMSO concentrations on the affinity of dimaprit was investigated (Fig. 4.21). Furthermore, the influence of a higher incubation period on the binding data of dimaprit was investigated (Fig. 4.21). The reduction of the DMSO concentration from 1.30 % (v/v) to 0.02 % (v/v) slightly increased the affinity of dimaprit whereas an increase in the incubation period from 15 to 65 min did not significantly alter the binding data of dimaprit (Fig. 4.21, Table 4.4).

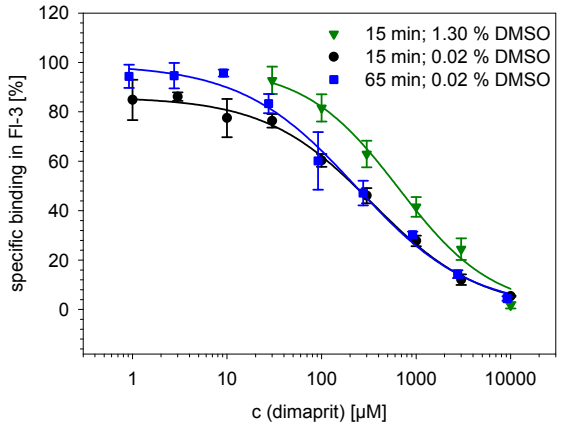

Fig. 4.21: *Effect of DMSO concentration and the incubation period on the affinity of dimaprit. Indicated are mean values ± SEM; n = 3.*

Table 4.4: *Comparison of K_i-values [µM] determined for dimaprit in the presence of various concentrations of DMSO at different incubation periods (mean values ± SEM).*

Incubation period [min]	DMSO concentration, % (v/v)	K_i-value [µM]
15	1.30	311 ± 107
15	0.02	163 ± 50
65	0.02	116 ± 39

Hence, a possible reason for the reduced affinities determined for famotidine, ranitidine, tiotidine and dimaprit compared to data reported by LEURS (Leurs et al., 1994) is the use of 1.30 % (v/v) DMSO. The results obtained for histamine and arpromidine in the presence of only 0.6 % (v/v) DMSO suggest this assumption, too: the calculation of a low affinity binding site for histamine revealed a value which is in the same order of magnitude as described in literature (Leurs et al., 1994) and the affinity for arpromidine was comparable to data obtained in radioligand binding experiments (compare data from table 4.2 and table 4.3)

4.4 Summary and conclusions

HEK293-hH_2R-qs5-HA cells are appropriate for the performance of both radioligand and flow cytometric binding assays for the hH_2R. The coexpression of the chimera in HEK293-hH_2R-qs5-HA cells did not significantly influence the hH_2R binding properties of the investigated ligands.

In order to avoid the use of the red diode laser which is quite sensitive with regard to vibration, flow cytometric competition binding experiments with standard ligands for validation were performed with **7**, which could be excited with the less susceptible argon laser, indispensible in flow cytometry. Those measurements revealed in part lower affinities for standard ligands in comparison to radioligand binding data determined within the scope of this work or reported in literature, respectively (Table 4.5). Since the use of DMSO was identified as a possible reason for these discrepancies, investigations at reduced concentrations of DMSO are recommended if possible. In case of famotidine and of tiotidine, the omission of DMSO could lead to insufficient solubility. As flow cytometric competition binding experiments revealed an affinity of compound **8** comparable to tiotidine, its radioactive form incorporating a [^{3}H]-propionyl moiety represents a promising radioligand for the hH_2R.

Table 4.5: *Comparison of binding data determined in flow cytometric and radioligand binding experiments on HEK293-hH_2R-qs5-HA cells with radioligand binding data reported in literature (K_i [µM]; mean values ± SEM).*

Ligand	Flow cytometry K_i [µM]	Radioligand binding assay K_i [µM]	Reported data (Leurs et al., 1994) K_i [µM]
arpromidine	12 ± 2	5.4 ± 1.2	n.d.
dimaprit	311 ± 107[1] 163 ± 50[2] 116 ± 39[3]	67 ± 20	25 ± 5
histamine	138 ± 15	118 ± 54	81 ± 15; 2.0 ± 1.2
ranitidine	0.597 ± 0.164	0.172 ± 0.011	0.085 ± 0.004
famotidine	0.126 ± 0.006	n.d.	0.016 ± 0.003
cimetidine	1.847 ± 0.443	n.d.	0.660 ± 0.220
tiotidine	0.080 ± 0.009	n.d.	0.017 ± 0.006

[1] 1.30 % (v/v) DMSO, incubation: 15 min
[2] 0.02 % (v/v) DMSO, incubation: 15 min
[3] 0.02 % (v/v) DMSO, incubation: 65 min

4.5 References

Arima, N., Yamashita, Y., Nakata, H., Nakamura, A., Kinoshita, Y., Chiba, T., 1991. Presence of histamine H_2-receptors on human gastric carcinoma cell line MKN-45 and their increase by retinoic acid treatment. *Biochem. Biophys. Res. Commun.* **176**, 1027-1032.

Bohn, B., 1980. Flow cytometry: A novel approach for the quantitative analysis of receptor-ligand interactions on surfaces of living cells. *Mol. Cell. Endocrinol.* **20**, 1-15.

Buckland, K.F., Williams, T.J., Conroy, D.M., 2003. Histamine induces cytoskeletal changes in human eosinophils via the H_4 receptor. *Br. J. Pharmacol.* **140**, 1117-1127.

Burde, R., Seifert, R., 1996. Stimulation of histamine H_2- (and H_1)-receptors activates Ca^{2+} influx in all-*trans*-retinoic acid-differentiated HL-60 cells independently of phospholipase C or adenylyl cyclase. *Naunyn-Schmiedeberg's Arch. Pharmacol.* **353**, 123-129.

Cheng, Y.-C., Prusoff, W.H., 1973. Relationship between the inhibition constant (K_i) and the concentration of inhibitor which causes 50 per cent inhibition (IC_{50}) of an enzymatic reaction. *Biochem. Pharmacol.* **22**, 3099-3108.

Conklin, B., Herzmark, P., Ishida, S., Voyno-Yasenetskaya, T., Sun, Y., Farfel, Z., Bourne, H., 1996. Carboxyl-terminal mutations of Gq alpha and Gs alpha that alter the fidelity of receptor activation. *Mol. Pharmacol.* **50**, 885-890.

Conklin, B.R., Farfel, Z., Lustig, K.D., Julius, D., Bourne, H.R., 1993. Substitution of three amino acids switches receptor specificity of Gq alpha to that of Gi alpha. *Nature* **363**, 274-276.

Edwards, B.S., Oprea, T., Prossnitz, E.R., Sklar, L.A., 2004. Flow cytometry for high-throughput, high-content screening. *Curr. Opin. Chem. Biol.* **8**, 392-398.

Hofinger, E., 2007. Recombinant Expression, Purification and Characterization of Human Hyaluronidases. In: *Doctoral Thesis, University of Regensburg*. http://www.opus-bayern.de/uni-regensburg/volltexte/2007/788/.

Hulme, E.C., Birdsall, N.J.M., 1992. Strategy and tactics in receptor-binding studies. In: *Receptor-Ligand Interactions: A Practical Approach (Practical Approach Series)*, Hulme, E.C. (Ed.). Oxford University Press, New York, pp. 63-176.

Hulme, E.C., Buckley, N.J., 1992. Receptor preparations for binding studies. In: *Receptor-Ligand Interactions: A Practical Approach (Practical Approach Series)*, Hulme, E.C. (Ed.). Oxford University Press, New York, pp. 177-212.

Keen, M., 1995. The problems and pitfalls of radioligand binding. In: *Methods in Molecular Biology, Vol. 41: Signal Transduction Protocols*, Kendall, D.A., Hill, S.J. (Eds.). Humana Press, Totowa, pp. 1-16.

Kelley, M.T., Bürckstümmer, T., Wenzel-Seifert, K., Dove, S., Buschauer, A., Seifert, R., 2001. Distinct Interaction of Human and Guinea Pig Histamine H_2-Receptor with Guanidine-Type Agonists. *Mol. Pharmacol.* **60**, 1210-1225.

Kozak, M., 1987. An analysis of 5'-noncoding sequences from 699 vertebrate messenger RNAs. *Nucleic Acids Res.* **15**, 8125-8148.

Kozak, M., 2002. Pushing the limits of the scanning mechanism for initiation of translation. *Gene* **299**, 1-34.

Kracht, J., 2001. Bestimmung der Affinität und Aktivität subtypselektiver Histamin- und Neuropeptid Y-Rezeptorliganden an konventionellen und neuen pharmakologischen In-vitro-Modellen. In: *Doctoral Thesis, University of Regensburg*.

Kuckuck, F.W., Edwards, B.S., Sklar, L.A., 2001. High throughput flow cytometry. *Cytometry* **44**, 83-90.

Lazareno, S., 2001. Quantification of receptor interactions using binding methods. *J. Recept. Signal Transduct.* **21**, 139 - 165.

Leurs, R., Smit, M.J., Wiro, M.B.P., Timmerman, H., 1994. Pharmacological characterization of the human histamine H_2 receptor stably expressed in Chinese hamster ovary cells. *Br. J. Pharmacol.* **112**, 847-854.

Mayer, M., 2002. Entwicklung fluorimetrischer Methoden zur Bestimmung der Affinität und Aktivität von Liganden G-Protein-gekoppelter Rezeptoren an intakten Zellen. In: *Doctoral Thesis, University of Regensburg*. http://www.opus-bayern.de/uni-regensburg/volltexte/2002/71/.

McFarthing, K.G., 1992. Selection and synthesis of receptor-specific radioligands. In: *Receptor-Ligand Interactions: A Practical Approach (Practical Approach Series)*, Hulme, E.C. (Ed.). Oxford University Press, New York, pp. 1-18.

Preuss, H., Ghorai, P., Kraus, A., Dove, S., Buschauer, A., Seifert, R., 2007. Constitutive Activity and Ligand Selectivity of Human, Guinea Pig, Rat, and Canine Histamine H_2 Receptors. *J. Pharmacol. Exp. Ther.* **321**, 983-995.

Ramirez, S., Aiken, C.T., Andrzejewski, B., Sklar, L.A., Edwards, B.S., 2003. High-throughput flow cytometry: Validation in microvolume bioassays. *Cytometry A* **53A**, 55-65.

Schneider, E., 2005. Development of Fluorescence-Based Methods for the Determination of Ligand Affinity, Selectivity and Activity at G-Protein Coupled Receptors. In: *Doctoral Thesis, University of Regensburg*.

Schneider, E., Mayer, M., Ziemek, R., Li, L., Hutzler, C., Bernhardt, G., Buschauer, A., 2006. A Simple and Powerful Flow Cytometric Method for the Simultaneous Determination of Multiple Parameters at G Protein-Coupled Receptor Subtypes. *ChemBioChem* **7**, 1400-1409.

Seifert, R., Wenzel-Seifert, K., Bürckstümmer, T., Pertz, H.H., Schunack, W., Dove, S., Buschauer, A., Elz, S., 2003. Multiple Differences in Agonist and Antagonist Pharmacology between Human and Guinea Pig Histamine H_1-Receptor. *J. Pharmacol. Exp. Ther.* **305**, 1104-1115.

Thomas, P., Smart, T.G., 2005. HEK293 cell line: A vehicle for the expression of recombinant proteins. *J. Pharmacol. Toxicol. Methods* **51**, 187-200.

Wang, J.-X., Yamamura, H.I., Wang, W., Roeske, W.R., 1992. The use of the filtration technique in in vitro radioligand binding assays for membrane-bound and solubilized receptors. In: *Receptor-Ligand Interactions: A Practical Approach (Practical Approach Series)*, Hulme, E.C. (Ed.). Oxford University Press, New York, pp. 213-234.

Wood, M., Chaubey, M., Atkinson, P., Thomas, D.R., 2000. Antagonist activity of meta-chlorophenylpiperazine and partial agonist activity of 8-OH-DPAT at the 5-HT_7 receptor. *Eur. J. Pharmacol.* **396**, 1-8.

Wurm, F., Bernard, A., 1999. Large-scale transient expression in mammalian cells for recombinant protein production. *Curr. Opin. Biotechnol.* **10**, 156-159.

Xie, S.-X., Ghorai, P., Ye, Q.-Z., Buschauer, A., Seifert, R., 2006. Probing Ligand-Specific Histamine H_1- and H_2-Receptor Conformations with N^G-Acylated Imidazolylpropylguanidines. *J. Pharmacol. Exp. Ther.* **317**, 139-146.

Young, S.M., Bologa, C.M., Fara, D., Bryant, B.K., Strouse, J.J., Arterburn, J.B., Ye, R.D., Oprea, T.I., Prossnitz, E.R., Sklar, L.A., et al., 2009. Duplex high-throughput flow cytometry screen identifies two novel formylpeptide receptor family probes. *Cytometry A* **75A**, 253-263.

Ziemek, R., 2006. Development of binding and functional assays for the neuropeptide Y Y_2 and Y_4 receptors. In: *Doctoral Thesis, University of Regensburg*. http://www.opus-bayern.de/uni-regensburg/volltexte/2006/679/.

Ziemek, R., Brennauer, A., Schneider, E., Cabrele, C., Beck-Sickinger, A.G., Bernhardt, G., Buschauer, A., 2006. Fluorescence- and luminescence-based methods for the determination of affinity and activity of neuropeptide Y_2 receptor ligands. *Eur. J. Pharmacol.* **551**, 10-18.

Chapter 5

Development of luminescence-based functional assays for the human histamine H_2 receptor

5.1 Introduction

Activation of the H_2R preferentially leads to recruitment of G_s-proteins which mediate an increase in the intracellular cAMP level. Available assay systems for the determination of cAMP suffer from several drawbacks. For instance, radiometric proximity assays (Williams, 2004) use [^{125}I]-cAMP and are consequently accompanied with the general disadvantages of radioactivity like high costs due to special handling (Schneider et al., 2006). The determination of cAMP in the scope of assays for drug development by FRET-techniques (Nikolaev et al., 2004) might be hampered by the relative low signal-to-noise ratio of that kind of measurement. Reporter-gene assays for the determination of the intracellular cAMP-level offer the advantage of relative high signal-to-noise ratios, but exhibit other drawbacks like the need of long incubation periods or the overestimation of low-efficacy agonists (Baker, 2008; Hill et al., 2001). In contrast, the determination of receptor-mediated changes in intracellular calcium levels is a preferred assay technique in drug discovery ((Siehler, 2008), compare also section 3.1). The spectrofluorimetric fura-2 assay was successfully used for the determination of ligand activity at several GPCRs in our workgroup, i.e. the neuropeptide Y receptors hY_1R, hY_2R and hY_4R (Gessele, 1998; Ziemek et al., 2006; Ziemek et al., 2007), respectively, and the hH_1R (Kracht, 2001). However, with regard to the hH_2R, the stimulation of the receptor by an agonist has to be redirected to an increase in the intracellular calcium level. In previous studies, CHO K1 cells were cotransfected with the cDNAs encoding the hH_2R and the $G\alpha_{16}$ protein in order to establish a calcium assay for the hH_2R (Schneider, 2005). Unfortunately, among other difficulties with the transfected cells, an inexplicable upregulation of the hH_1R was discovered whereas hH_2R-mediated calcium transients were not detectable (Schneider, 2005). Therefore, in the present work a different approach was tried. Choice of cell line, transfection method and selection of cells were performed by analogy with a protocol for the cloning of the hH_4R (Morse et al., 2001), because an upregulation of the hH_1R due to the transfection process was not reported in this study ((Morse et al., 2001); section 4.2.2.4).

Furthermore, the previously described strategy to redirect the activation of the G_i-coupled receptors hY_2R and hY_4R by coexpression of qi5-HA to an increase in the intracellular calcium level (Ziemek et al., 2006; Ziemek et al., 2007) was adapted to the hH_2R instead of using $G\alpha_{16}$. Therefore, in place of qi5-HA, the respective chimeric Gα-protein suited for the $G\alpha_s$-coupled hH_2R was used for the establishment of HEK293-hH_2R-qs5-HA cells, i.e. qs5-HA. (see chapter 4). This assay principle was successfully applied to other GPCRs which preferentially couple to G_s-proteins like the 5-hydroxytryptamine 5-HT_7 receptor (Wood et al., 2000) or the vasopressin V_2 receptor (Conklin et al., 1996).

The stable coexpression of mitochondrially targeted apoaequorin (mtAEQ) besides the receptor of interest (hY_2R, hY_4R) and a chimeric Gα-protein enabled the measurement of intracellular transients with a bioluminescence assay in the 96-well format (Ziemek et al., 2006; Ziemek et al., 2007).

As the bioluminescence signal is a consequence of an enzymatic reaction that is accompanied with emission of visible light (λ_{max} = 470 nm), no excitation is needed for the creation of the readout signal. Therefore, no autofluorescence is provoked in this assay. In addition, luminescent proteins that could impair the measurements are usually absent in mammalian cells. Thus, the main advantage of this bioluminescence readout over the fluorescence-based assays using calcium-chelating dyes like fura-2 for the determination of calcium transients is the considerably elevated signal-to-noise ratio (cf. Ziemek, 2006). Thus, this assay was established for the determination of hH_2R-ligand activity in addition to the fura-2 assay.

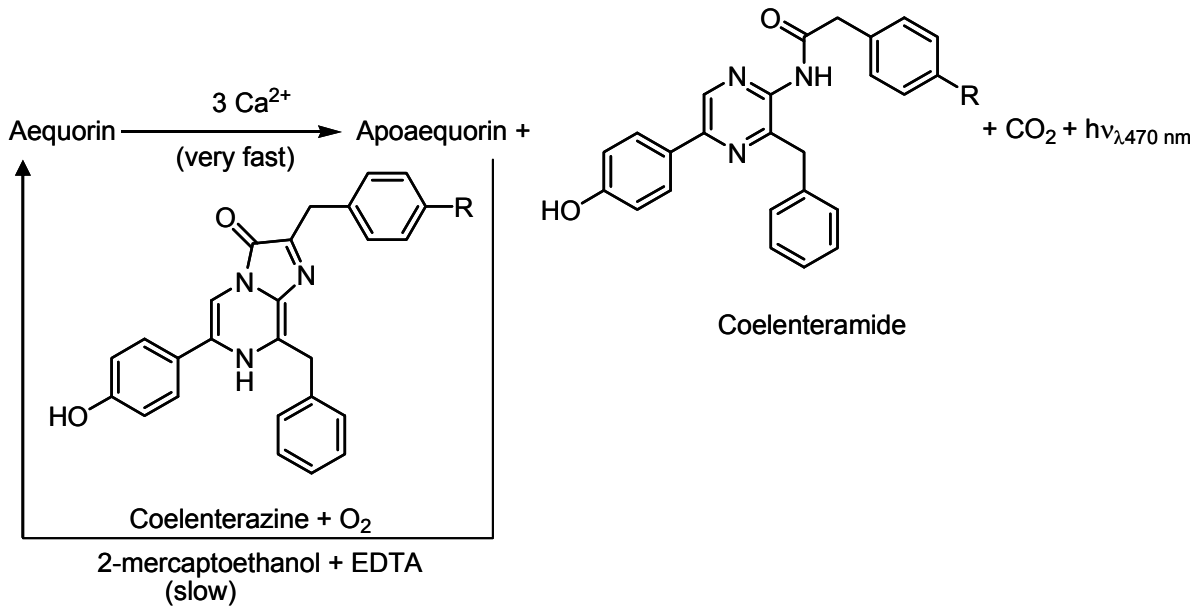

Fig. 5.1: *Bioluminescence reaction and regeneration of aequorin in vitro. Native coelenterazine (R = OH) or coelenterazine h (R = H) is converted to the respective coelenteramide accompanied by emission of light (adapted from Ziemek, 2006).*

5.2 Materials and methods

5.2.1 Fura-2 assays for the determination of ligand activity at the hH_2R

5.2.1.1 Spectrofluorimetric fura-2 assays

Histamine and famotidine were from Sigma whereas dimaprit was synthesized in our laboratories. Histamine and dimaprit were dissolved in PBS, whereas famotidine was dissolved in 30 % (v/v) DMSO / PBS as 200-fold concentrated feed solutions with respect to the final concentration.

Furthermore, the acylguanidine **9**, a compound which was selected as a representative of a new class of bivalent histamine H_2R agonists developed in our workgroup (Kraus, 2007), was investigated for its agonistic potency and efficacy in the fura-2 assay. The substance addresses the hH_2R and incorporates two sets of pharmacophoric groups linked by a spacer (Fig. 5.2). The investigation of this twin compound in steady-state GTPase assays revealed a highly potent (EC_{50} = 12.4 ± 6.4 nM) partial agonism (53 ± 4 % relative to histamine) on Sf9 cell membranes expressing a hH_2R-$G_{s\alpha S}$ fusion protein (Kraus, 2007). Furthermore, the compound proved to be highly selective for the hH_2R over other histamine receptors due to the introduction of the 2-amino-4-methylthiazol-5-yl moieties instead of imidazol-4-yl residues (Kraus, 2007; Kraus et al., 2009). The N^G-acylation of the guanidine moieties reduces the basicity and accounts for improved pharmacokinetic properties (Ghorai et al., 2008; Kraus et al., 2009).

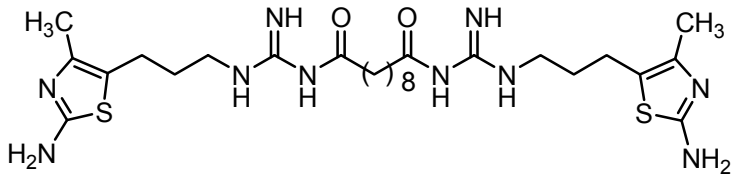

Fig. 5.2: *Chemical structure of the bivalent acylguanidine-type H_2R agonist* **9**.

HEK293-hH_2R-qs5-HA-cells were cultured in DMEM supplemented with 10 % FBS and selection antibiotics (400 µg / mL of G418 and 100 µg / mL of hygromycin B) in a water-saturated atmosphere containing 5 % CO_2 at 37 °C. Cells were passaged (1:10) twice a week. For the calcium assays, approx. $5 \cdot 10^5$ cells were seeded into 175-cm^2 culture-flasks and grown to 25-75 % confluency (3-4 days) in the presence of the respective selection antibiotics before the assays.

Cells were loaded with fura-2 / AM according to section 3.2.2. However, due to the relatively weak adherence of the cells, the treatment with trypsin / EDTA was omitted. The assay was

performed as described for HEL cells by GESSELE (Gessele, 1998). 1 mL of the cell suspension ($1 \cdot 10^6$ cells / mL) was diluted in a cuvette with 1 mL of loading buffer (for composition see section 3.2.2) and continuously stirred in the LS 50 B spectrofluorimeter (PerkinElmer, Überlingen, Germany) at 25 °C and low speed. The baseline was recorded for approx. 20 s prior to the challenge of the loaded cells by agonists. Antagonists were pipetted to the cuvette 15 min prior to the addition of a fixed concentration of agonist. Every fourth measurement was a reference signal (investigation of agonists: 1 mM of histamine; investigation of antagonists: 10 µM of histamine in the absence of antagonist). Instrument settings were: excitation wavelengths: 340 and 380 nm (alternating), slit: 10 nm (in each case); emission wavelengths: 510 nm (in each case), slits: 10 nm (in each case); resolution: 0.1; measurement time: 300 s (maximal).

For preliminary experiments in section 5.3.1 (Fig. 5.3), raw data were transferred to Microsoft® Office Excel 2003 in order to determine ratios. The minimal ratio due to the addition of histamine to cotransfected cells challenged in the absence of antagonists (Fig. 5.3, A; red curve, approx. 24 s) was set as 0 % for the relative calcium increase. The maximal relative calcium increase was determined in the absence of antagonist for co-transfected cells and was set as 100 % (Fig. 5.3, A; red curve, approx. 44 s). All other values were related to this 100 % signal. Values were transferred to SigmaPlot® 9.0 for the construction of kinetic curves (Fig. 5.3). Calcium concentrations were calculated according to the Grynkiewicz equation (Grynkiewicz et al., 1985):

$$[Ca^{2+}] = K_d * \frac{(R - R_{min})}{(R_{max} - R)} * SFB$$

The K_d-value represents the dissociation constant of the fura-2-Ca^{2+} complex. R is the ratio of emission at 510 nm after excitation at 340 and 380 nm, respectively. R_{max} is the fluorescence ratio in presence of saturating Ca^{2+} concentration, determined after cell lysis and subsequent saturation of fura-2 with the calcium ions of the surrounding loading buffer by addition of digitonin (10 µL of an aqueous solution; 2 % (v/v); digitonin was from Sigma, Deisenhofen, Germany). R_{min} represents the ratio in the absence of free Ca^{2+}, determined after addition of EGTA (50 µL of a 600 mM solution in Tris, 1 M, pH 8.7) to cells that were lysed with digitonin. SFB is a correction factor representing the emission at 510 nm after excitation at 380 nm of the Ca^{2+} free and the Ca^{2+} saturated dye, respectively.

Calculated calcium concentrations were transferred to SigmaPlot® 9.0 for the depiction of kinetic measurements (Fig. 5.4). For the construction of concentration response curves, calculated calcium concentrations were converted into percentage values and analyzed with SigmaPlot® 9.0 according to the multiple scatter, error bars option. Curve fitting was performed with the standard curves, four parameter logistic function.

5.2.1.2 The fura-2 assay in the 384-well format

Arpromidine and cimetidine were synthesized in our laboratories whereas tiotidine was from Tocris Cookson (Ballwin, USA). HEK293-hH_2R-qs5-HA cells were cultured and prepared for the fura-2 assays according to section 5.2.1.1.

In general, samples were in part randomized in order to exclude misinterpretations due to different time periods between the loading procedure with fura-2 / AM and the registration of the fluorescence (i.e. time period of post-incubation).

Agonists were characterised by analogy with the procedure described in section 3.2.4.1, investigations in 384 well-plates. However, a blank value (pure PBS without agonist) was included for every investigated concentration of dimaprit and arpromidine.

Feed solutions of **9** were prepared 5-fold concentrated with respect to the final concentration in DMSO / PBS 1.5 % (v/v). Accordingly, the determination of blank values, arpromidine controls and histamine references (1 mM) in assays with **9** were performed in presence of 0.3 % (v/v) of DMSO, too.

Investigations of reference antagonists and H_2R ligands **6**-**8** (consider section 4.2.3.2) were performed as explained in 3.2.4.2.2 with minor modifications: 100-fold concentrated feed solutions compared to final assay concentration were prepared in DMSO. 1 µL of the respective solution was pipetted in the cavities of the 384-well plate. 89 µL of the fura-2 loaded cells ($1 \cdot 10^6$ cells / mL) were added per well. Incubations were performed for 15 min under light protection at room temperature without shaking. Calcium transients were elicited with 10 µL of histamine in PBS (100 µM). Thus, the final concentration of DMSO in antagonist assays was 1 % (v/v). Investigations of antagonists were performed with 120 measurement cycles except for tiotidine (46 cycles).

Data analysis was performed by subtraction of the blank value from the samples of the respective concentration and from the histamine reference. Further data analysis was performed according to section 3.2.7.

5.2.2 The aequorin assay for the functional characterisation of hH_2R ligands in the 96-well format

5.2.2.1 Transfection of HEK293-hH_2R-qs5-HA cells and selection

The pMTAEQ vector incorporating the gene encoding mitochondrially targeted apoaequorin (mtAEQ) was a generous gift from Prof. Dr. Stan Thayer, Department of Pharmacology, University of Minnesota, USA. The cDNA of mtAEQ was subcloned in the pcDNA3.1(+)-Zeo vector (Invitrogen, Karlsruhe, Germany) by ZIEMEK (Ziemek et al., 2006).

HEK293-hH_2R-qs5-HA cells were cultured and passaged as explained in 5.2.1.1. Cells were seeded in a 24-well plate according to 4.2.2.4. 4 d after seeding, cells had reached approx. 95 % confluence. Cells were transfected with the plasmid pcDNA3.1(+)-Zeo-mtAEQ using Lipofectamine™ 2000 (Invitrogen) and cultured according to 5.2.1.1 including Zeocin™ (100 µg / mL; InvivoGen, San Diego, USA) for 4 weeks prior to the performance of bioluminescence assays.
Stably transfected HEK293-hH_2R-qs5-HA-mtAEQ cells were frozen in medium (DMEM + 10 % FBS, 400 µg / mL G418, 100 µg / mL hygromycin B and 100 µg / mL Zeocin™) including 10 % DMSO as described in section 3.2.1.

5.2.2.2 Preparation of the cells, assay performance and data analysis

Approx. $5 \cdot 10^5$ HEK293-hH_2R-qs5-HA-mtAEQ cells were seeded into 175-cm^2 culture-flasks and incubated in a water saturated atmosphere at 37 °C and 5 % CO_2 in the presence of all selection antibiotics (G418, hygromycin B and Zeocin™). Due to the slow growth, cells were just propagated to approx. 25 % confluency (10-14 d) before the assays.
Cells were prepared for the assay as described previously (Ziemek et al., 2006) with minor modifications: cells were detached by DMEM + 10 % FBS without trypsin / EDTA treatment and centrifuged at 300 g for 5 min. Cells were resuspended in DMEM without phenol red (Invitrogen) including 1 % of FBS, counted and adjusted to a density of $1 \cdot 10^7$ cells / mL. Coelenterazine h (500 µM stock solution in methanol; Biotrend, Köln, Germany) was added to a final concentration of 2 µM to the cells. Cells were incubated under light protection at room temperature without movement for 2 h. The cells were diluted with loading buffer (for composition see section 3.2.2) to a density of $5 \cdot 10^5$ cells / mL and incubated for another 3 h under light protection at room temperature and gentle stirring.
The cavities of a white 96-well plate (Greiner, Frickenhausen, Germany) were provided with 18 µL of the 10-fold concentrated feed solutions compared to the final concentration of the ligands (arpromidine: PBS; **9**: DMSO / PBS 3 % (v/v)). In general, samples were in part randomized in order to exclude misinterpretations due to different time periods between the incubation with Coelenterazine h and the registration of the luminescence (i.e. time period of post-incubation).
162 µL of the gently stirred cell suspension ($5 \cdot 10^5$ cells / mL) were injected after cycle 4 (approx. 0.9 s) with a speed of 25, 100 or 200 µL / s, respectively. For the consumption of residual coelenterazine h, 20 µL of a triton-X-100 solution (Roth, Karlsruhe, Germany; 1 % (v/v) in loading buffer) were injected before cycle 200 (200 µL / s) per sample. Luminescence was recorded for another 100 cycles. Thus, the whole measurement lasted 300 cycles according to approx. 66 s.

Instrument settings were: measurement mode: luminescence; integration time (manual): 200 ms; attenuation: none; time between move and integration: 50 ms; well kinetic number: 300; well kinetic interval (minimal): 220 ms; injector A delay: 880 ms; injector B delay: 45400 ms; injection mode: standard.

For every investigated concentration, a blank value (PBS in case of the validation with arpromidine or DMSO / PBS 3 % (v/v) for the characterisation of **9**, respectively) was determined. A maximal calcium response was determined with histamine (1 mM) in the same way.

Luminescence [RLU] was plotted against time [s] and the area under the peak was calculated with SigmaPlot® 9.0. For the total luminescence, cycle 1-300 was taken into account, whereas the agonist-mediated response was calculated from cycle 1-199. Fractional luminescence was determined as ratio of the agonist-mediated area under the peak and that of the total luminescence. The blank value was subtracted from the investigated samples of the respective concentration and from the histamine signal. Residual values were related on the histamine reference. Sigmoidal curves were established with the multiple scatter – error bars option. Curve fitting was realized with the standard curves - four parameter logistics function.

5.3 Results and discussion

5.3.1 Determination of ligand activity at the hH_2R with the fura-2 assay

HEK293-hH_2R-qs5-HA cells responded with a strong increase in the intracellular calcium level upon stimulation with histamine (30 µM), whereas the untransfected cells showed no significant calcium transient upon agonist challenge (Fig. 5.3, A). The signal was completely suppressed by the hH_2R antagonist famotidine but remained unaffected by the hH_1R antagonist mepyramine (Fig. 5.3, B).

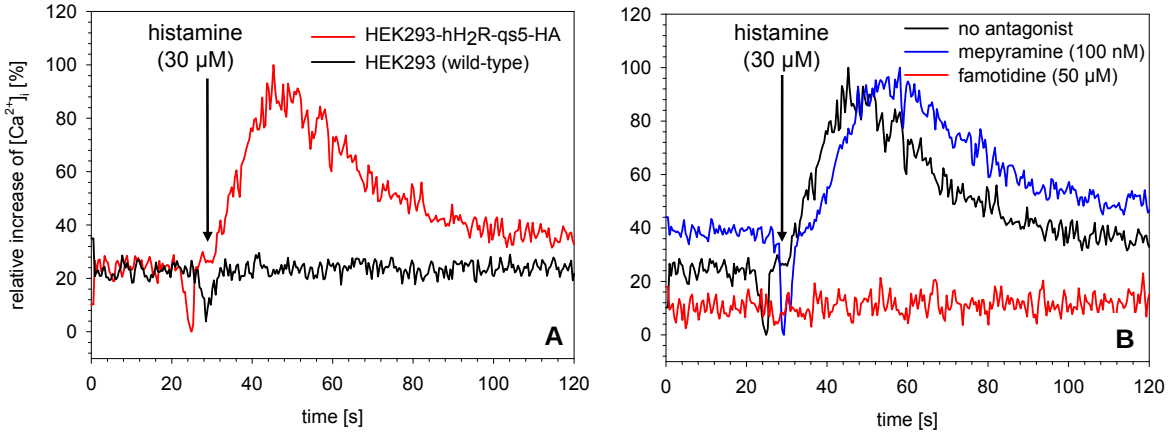

Fig. 5.3: *Investigation of HEK293-hH_2R-qs5-HA cells in the spectrofluorimetric fura-2 assay.*
A*: Histamine-induced calcium response in cotransfected cells compared to wild-type cells*
B*: Effect of mepyramine and famotidine on the histamine-induced calcium signal in HEK293-hH_2R-qs5-HA-cells.*

HEK293-hH_2R-qs5-HA-cells responded in a concentration-dependent manner to histamine (Fig. 5.4).

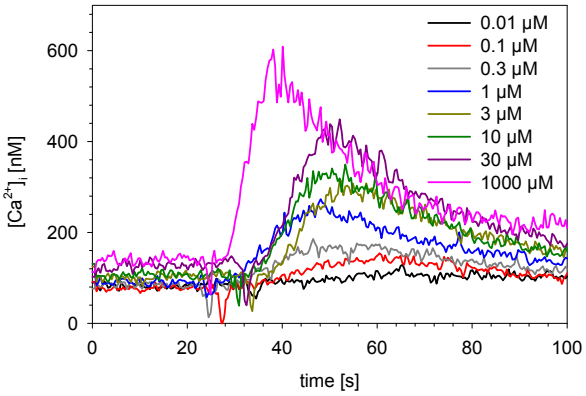

Fig. 5.4: *Concentration-dependent increase in the intracellular calcium-level by histamine in HEK293-hH_2R-qs5-HA cells.*

Data analysis enabled the construction of sigmoidal concentration-response curves. Dimaprit behaved as a partial agonist using histamine (1 mM) as reference (Fig. 5.5, A). The hH_2R antagonist famotidine decreased the histamine-induced calcium signal in a concentration-dependent manner (Fig. 5.5, B).

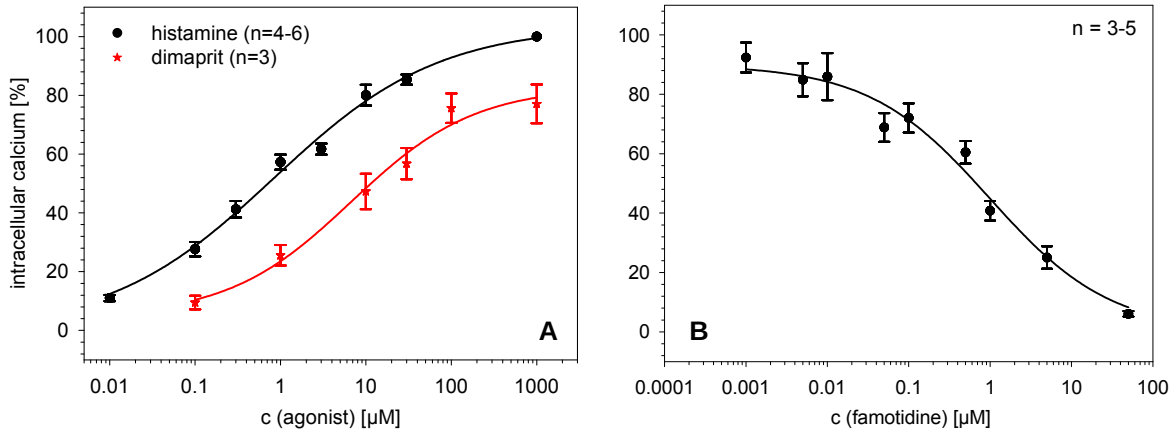

Fig. 5.5: *Influence of agonists and the antagonist famotidine on the calcium transients in HEK293-hH_2R-qs5-HA cells (mean values ± SEM; n as indicated).* **A***: Concentration-dependent increase in the intracellular Ca^{2+} level induced by histamine and dimaprit. The maximal calcium signal was elicited with 1 mM of histamine.* **B***: Concentration-dependent decrease in the histamine (10 µM)-stimulated Ca^{2+} response by famotidine.*

In order to economize the characterisation of putative hH_2R ligands with the fura-2 assay, measurements were performed in the 384-well format. Injection of the fura-2 loaded cells to various concentrations of histamine led to a concentration-dependent increase in the intracellular calcium level (Fig. 5.6, A). Increasing amounts of famotidine almost completely suppressed the histamine-induced calcium transient in HEK293-hH_2R-qs5-HA cells (Fig. 5.6, B). The injection of PBS, which was used as the solvent for histamine, in the presence of 50 µM famotidine led to a comparable increase in the calcium signal as monitored after the addition of histamine (10 µM), indicating the injection process to account for that alteration of the calcium level (Fig. 5.6, B). This effect corresponding to 21.6 % of the maximal histamine signal (n=5) was taken into account by subtraction from raw data (compare also section 3.3.2.2.1) when H_2R antagonists were investigated.

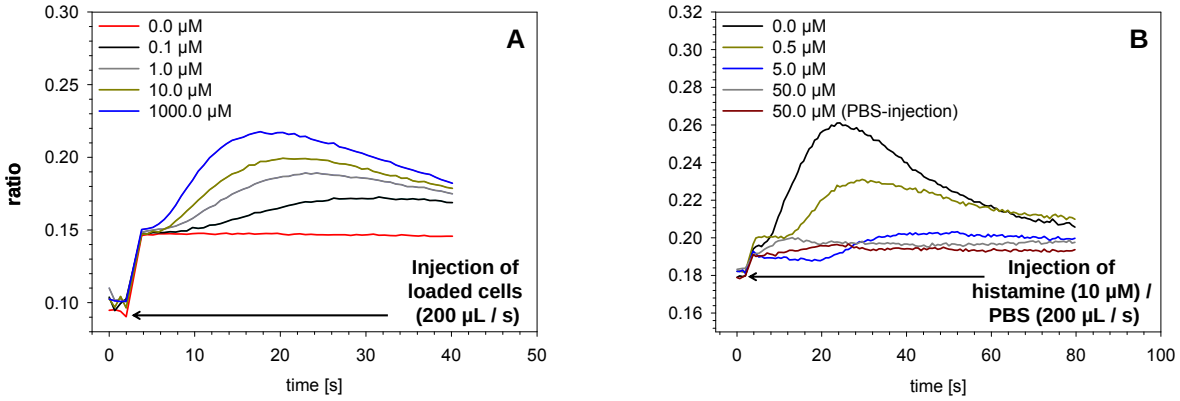

Fig. 5.6: *Investigation of fura-2 loaded HEK293-hH_2R-qs5-HA cells in 384-well microtitre plates.* **A***: Effect of increasing amounts of histamine on the intracellular Ca^{2+} level* **B***: Effect of increasing amounts of famotidine on the histamine-induced calcium signal and influence of the PBS-injection. Calcium signals were registered as the ratio of emission at 535 nm after excitation at 340 nm and 380 nm, respectively.*

HEK-293-hH_2R-qs5-HA-cells responded in a concentration-dependent manner to histamine. Data analysis enabled the calculation of sigmoidal curves. Dimaprit and arpromidine were characterised as partial agonists compared to histamine (1 mM) as reference (Fig. 5.7, A). The H_2R antagonists cimetidine, famotidine and tiotidine decreased the histamine-induced calcium signal in a concentration-dependent manner (Fig. 5.7, B). The K_b-values of the antagonists were calculated according to CHENG and PRUSOFF (Cheng and Prusoff, 1973).

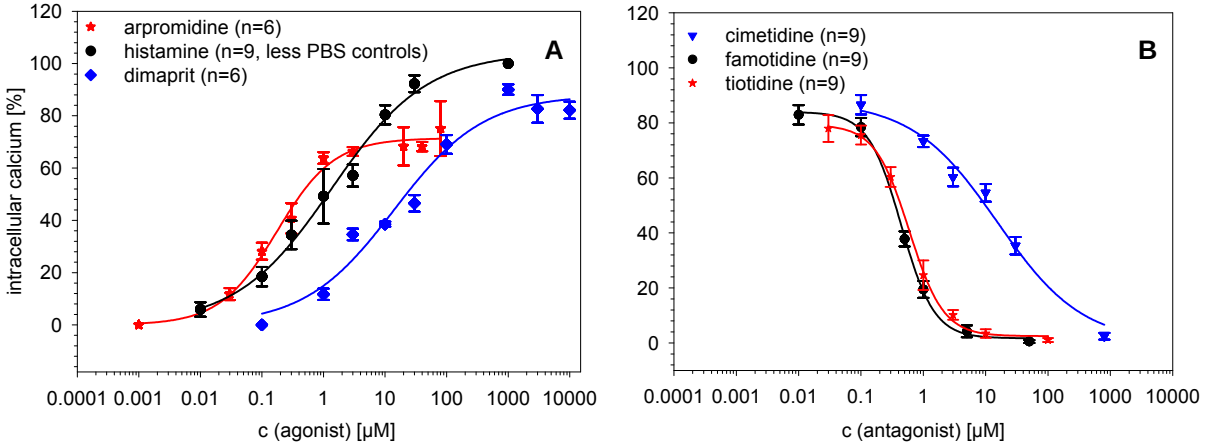

Fig. 5.7: *Sigmoidal curves for agonists and antagonists.* **A***: Concentration-dependent increase in the intracellular Ca^{2+} level by histamine, dimaprit and arpromidine.* **B***: Concentration-dependent decrease in the histamine (10 µM)-stimulated Ca^{2+} response by cimetidine, famotidine and tiotidine. Mean values ± SEM, n as indicated.*

The results obtained in spectrofluorimetric measurements were in agreement with those obtained in 384-well plates. As exemplarily confirmed for tiotidine, the reduction of the measurement time from 120 cycles to 46 cycles did not impair the determination of the antagonistic activity (Fig. 5.7, B).

A summary of data determined in fura-2 assays compared to data reported in literature is shown in Table 5.3: results obtained in fura-2 assays mainly agree with data determined in GTPase activity assays (Kelley et al., 2001; Preuss et al., 2007). However, a higher potency was found in the GTPase assay for dimaprit (Preuss et al., 2007). Similar observations were previously made for histamine on the hH_1R: in the GTPase assay on membranes of hH_1R expressing Sf9 cells, an EC_{50}-value of 184 ± 94 nM was determined (Seifert et al., 2003), whereas in the fura-2 assay on U-373 MG cells, the EC_{50}-value was in the low micromolar range (see chapter 3 and (Kracht, 2001)). Discrepancies may result from differences of both assay systems. On the one hand, human cells co-express an unmodified hH_2R and the chimera qs5-HA, whereas hH_2R-$G_{s\alpha S}$ fusion proteins in membranes from Sf9 insect cells are used in the scope of GTPase assays. In addition, the hH_2R used in GTPase assays incorporates a FLAG epitope and a hexahistidine tag. Finally, in the GTPase assay, an event close to receptor activation is measured whereas the calcium response is an effect more downstream in the signalling cascade, and the readout systems are remarkably different (liquid scintillation counting versus fluorescence emission).

Furthermore, the results from the fura-2 assay correspond to data which were determined in a fluo-3 assay (Esbenshade et al., 2003). However, dimaprit showed a decreased potency and efficacy relative to histamine on clone B1 of the investigations performed by ESBENSHADE (Esbenshade et al., 2003) compared to the results of the fura-2 assay (this thesis) and data obtained for clone A5 by ESBENSHADE (Esbenshade et al., 2003). A possible reason for this observation is a difference in constitutive activity of those cell types. In general, a decrease in constitutive activity is accompanied with a decrease of potency observed for agonists. Furthermore, the effect mediated by partial agonists compared to full agonists is decreased in such systems, too (Preuss et al., 2007). Thus, clone B1 (Esbenshade et al., 2003) might be less constitutively active than clone A5 (Esbenshade et al., 2003) and HEK293-hH_2R-qs5-HA cells.

Recently, H_2R ligands were investigated in cAMP assays (Baker, 2008). The order of potency and efficacy obtained in fura-2 assays for histamine and dimaprit was in agreement with data from those cAMP measurements. The antagonistic activities determined in the paper of BAKER (Baker, 2008) were in the same order of magnitude as data obtained in fura-2 assays. However, the potencies of both agonists were higher in cAMP measurements than in fluo-3 assays (Esbenshade et al., 2003) and fura-2 assays, presumably, due to preferential coupling of the hH_2R to $G\alpha_s$ rather than $G\alpha_q$ (Esbenshade et al., 2003).

Table 5.1: *Comparison of pharmacological data determined in fura-2 assays (spectro-fluorimeter and 384-well plate) with results published in literature. Mean values ± SEM, unless otherwise indicated.*

Ligand	Fura-2 assay (384-well format)		Fura-2 assay (spectro-fluorimeter)		Fluo-3 assay[1]		GTPase assay	
	intrinsic activity	EC_{50} or K_b [µM]	intrinsic activity	EC_{50} or K_b [µM]	intrinsic activity	EC_{50} or K_b [µM]	intrinsic activity	EC_{50} or K_b [µM]
histamine	1.00	1.40 ± 0.55	1.00	0.83 ± 0.29	1.00[2] 1.00[3]	0.71-0.78[2] 1.66-1.82[3]	1.00[4]	0.99 ± 0.09[4]
dimaprit	0.88 ± 0.03	14.00 ± 4.14	0.83 ± 0.09	6.74 ± 4.38	≈ 0.80[2] ≈ 0.50[3]	11.48-13.18[2] 41.69-63.10[3]	0.85 ± 0.02[4]	0.91 ± 0.43[4]
arpromidine	0.72 ± 0.03	0.18 ± 0.05	n.d.	n.d.	n.d.	n.d.	0.84 ± 0.03[4]	0.07 ± 0.01[4]
cimetidine	-	*1.89 ± 0.56*	-	*n.d.*	*n.d.*	*n.d.*	-	*1.70 ± 0.43*[4]
famotidine	-	*0.05 ± 0.01*	-	*0.08 ± 0.04*	*n.d.*	*n.d.*	-	*0.05 ± 0.01*[4]
tiotidine	-	*0.07 ± 0.01*	-	*n.d.*	*n.d.*	*n.d.*	-	*0.06 (0.03-0.13)*[5]

[1]Esbenshade et al., 2003: [2]clone A5, [3]clone B1; EC_{50} values were determined from pEC_{50} values ± SEM; [4]Preuss et al., 2007; [5]Kelley et al., 2001 (Numbers in parentheses represent the 95 % confidence interval)

H_2R ligands synthesized in our workgroup were investigated in the fura-2 assay. For assays with compound **9** in 384-well plates, arpromidine was used as a reference compound at two concentrations (0.2 and 20 µM). Whereas arpromidine showed agonistic activity as expected, under the same conditions **9** did not show a concentration-dependent response. In contrast, the intracellular calcium-level was only slightly altered up to a concentration of 1000 nM whereas 3000 nM of **9** evoked a steep increase in $[Ca^{2+}]_i$. Similar observations were made for 10000 and 30000 nM of **9** (Fig. 5.8). In contrast, in spectrofluorimetric measurements, compound **9** behaved as highly potent partial agonist on HEK293-hH_2R-qs5-HA cells (the

final assay concentration of DMSO was 0.25 % (v/v) in spectrofluorimetric measurements (Fig. 5.8, Table 5.2).

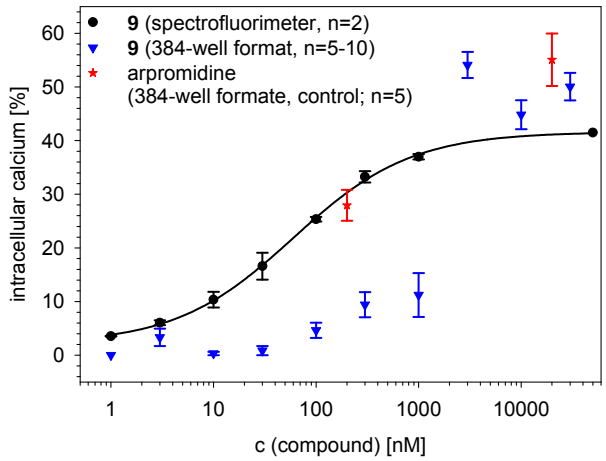

Fig. 5.8: *Influence of various concentrations of* **9** *on the intracellular calcium level in HEK293-hH_2R-qs5-HA cells determined with the 384-well format and the spectrofluorimeter. Mean values ± SEM; n as indicated.*

Compared to the results from the GTPase assay on membrane preparations from Sf9 cells expressing a hH_2R-$G_{s\alpha S}$ fusion protein (Kraus, 2007), slightly lower potency and intrinsic activity was found for **9** in the spectrofluorimetric calcium assay on HEK293-hH_2R-qs5-HA cells (Table 5.2). Thus, HEK293-hH_2R-qs5-HA cells proved to be in principle suited for the characterisation of **9**, but the application of the fura-2 assay in the 384-well format failed in this case. A possible explanation for this unexpected result might be the relative low dynamic range in fura-2 assays performed in the 384-well format (Fig. 5.6, A). In addition, even in the spectrofluorimetric fura-2 assay with its higher dynamic range (Fig. 5.4), a partial agonism of only approx. 40 % intrinsic activity relative to histamine was detected for **9** (Fig. 5.8). Thus, the relatively low efficacy of **9** and the instrument settings of the fura-2 assay in the 384-well format might hamper the appropriate characterisation of **9**.

Therefore, the aequorin assay with its increased signal-to-noise ratio compared to the fura-2 assay (Ziemek, 2006) was established (section 5.3.2) in order to overcome that problem.

Table 5.2: *Comparison of pharmacological data determined for compounds* **6**-**9** *in the fura-2 assay and the GTPase assay. Indicated are mean values ± SEM.*

Ligand	Fura-2 assay (384-well format)		Fura-2 assay (spectrofluorimeter)		GTPase assay	
	intrinsic activity	EC_{50} or K_b [µM]	intrinsic activity	EC_{50} or K_b [µM]	intrinsic activity	EC_{50} or K_b [µM]
6	-	*120 ± 30*	-	*n.d.*	-	*98 ± 26*[2]
7	-	*130 ± 34*	-	*n.d.*	-	*22 ± 2*[2]
8	-	*150 ± 20*	-	*n.d.*	-	*43 ± 8*[2]
9	failed	failed	0.42 ± 0.01	60 ± 10	0.53 ± 0.04[1]	12 ± 6[1]

[1]Kraus, 2007; [2]Erdmann, D., 2009, personal communication

Compounds **6**-**8** suppressed the histamine-induced calcium signal in a concentration-dependent manner with comparable antagonistic activities (Table 5.2, Fig. 5.9).

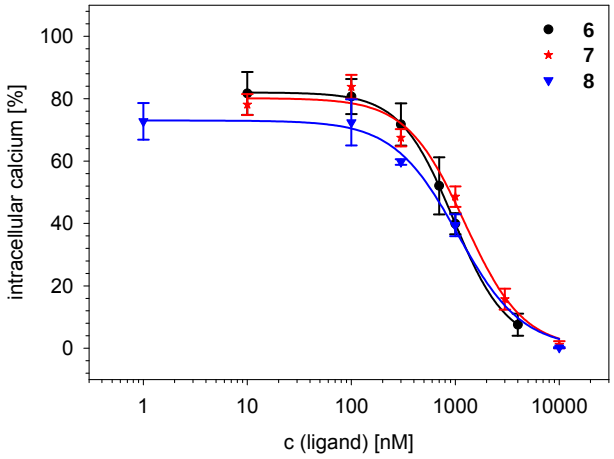

Fig. 5.9: *Influence of various concentrations of compounds* **6**-**8** *on the intracellular calcium level evoked with histamine (10 µM) in HEK293-hH_2R-qs5-HA cells (384-well format). Mean values ± SEM; n = 6.*

In the GTPase assays, compounds **6** and **8** showed antagonistic activities comparable to results in fura-2 assays whereas **7** showed a higher antagonistic activitiy (Table 5.2).

In order to investigate the reliability of calcium signals with respect to the time period between the loading procedure with fura-2 / AM and the registration of the fluorescence (i.e. time period of post-incubation), the potency and efficacy of arpromidine as well as of the antagonistic activity of famotidine were determined in the 384-well format.

With respect to arpromidine, only the samples measured immediately after termination of the loading procedure provided reliable results (1-64 min, 72 samples). Concentration-response curves constructed from data collected after prolongued post-incubation exhibited an increase in the signal obtained at the lowest concentration of arpromidine. Accordingly, the concentration-response curves seemed to be shifted to the left and the respective EC_{50} values dropped compared to data obtained directly after termination of the loading procedure (Fig. 5.10, Table 5.3).

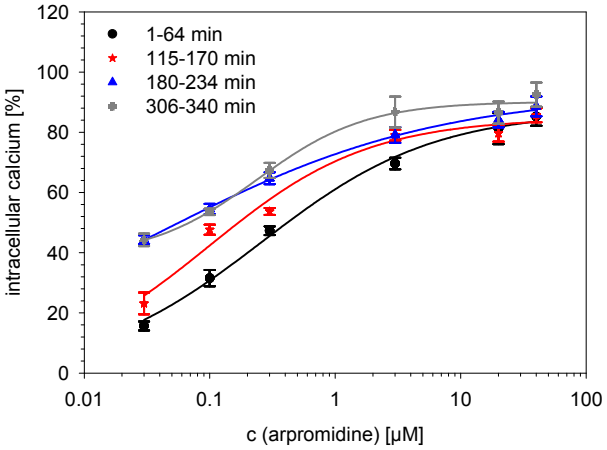

Fig. 5.10: *Concentration-dependent increase of the intracellular calcium level by arpromidine determined at various time periods of post-incubation in HEK293-hH_2R-qs5-HA cells (fura-2 assay, 384-well format). Further details are described in the text. Mean values ± SEM; n = 5.*

Table 5.3: *Comparison of pharmacological data calculated from sigmoidal curves shown in Fig. 5.10. Indicated are mean values ± SEM (n =5). Further details are described in the text.*

Time period of post-incubation [min]	EC_{50} [µM]	Intrinsic activity, relative to histamine = 100 [%]
1- 64	0.259 ± 0.159	87 ± 5
115-170	0.100 ± 0.103	85 ± 4
180-234	0.039 ± 0.188	93 ± 11
306-340	0.239 ± 0.108	90 ± 3

In view of famotidine, measurements performed within the time period from 165 to 357 min after termination of loading with fura-2 / AM still led to a concentration-dependent decrease of the histamine-induced calcium-signals by the antagonist (Fig. 5.11).

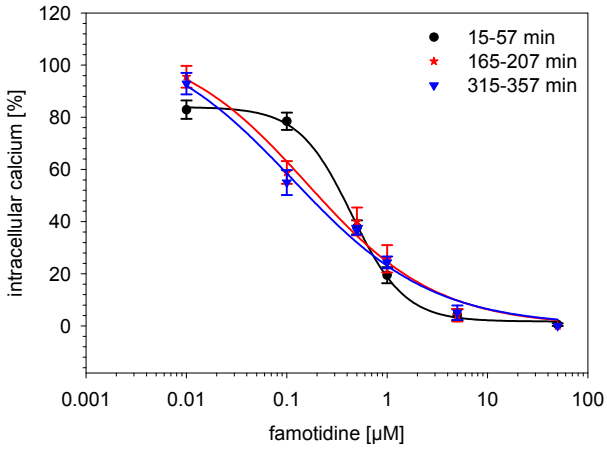

Fig. 5.11: *Concentration-dependent decrease in the intracellular calcium level elicited with histamine (10 µM) by famotidine in HEK293-hH_2R-qs5-HA cells at various time periods of post-incubation (fura-2 assay, 384-well format). Further details are desbribed in the text. Mean values ± SEM; n as indicated in Table 5.4.*

Table 5.4: *Comparison of pharmacological data determined for famotidine at various times periods of post-incubation (mean values ± SEM, n as indicated). Further details are described in the text.*

Time period of post-incubation [min]	n	IC_{50} [µM]	K_b [µM]
15- 57	9	0.442 ± 0.043	0.054 ± 0.005
165-207	3	0.159 ± 0.080	0.020 ± 0.010
315-357	3	0.115 ± 0.064	0.014 ± 0.008

The calculated IC_{50}-values and the respective K_b-values were in the same order of magnitude at every investigated time frame (Table 5.4). Thus, experiments should be feasible up to a measurement time of approx. 6 h.

5.3.2 The aequorin assay in the 96-well format for the determination of hH_2R ligand activity

Arpromidine and the reference compound, histamine, led to concentration-dependent increases in the luminescence signal upon injection of the cells (Fig. 5.12, A). In contrast, the injection of triton-X-100 provoked lower luminescence signals for agonist-pre-stimulated samples than for the sample of the blank value due to the consumption of a diminished amount of residual coelenterazine h (Fig. 5.12, B).

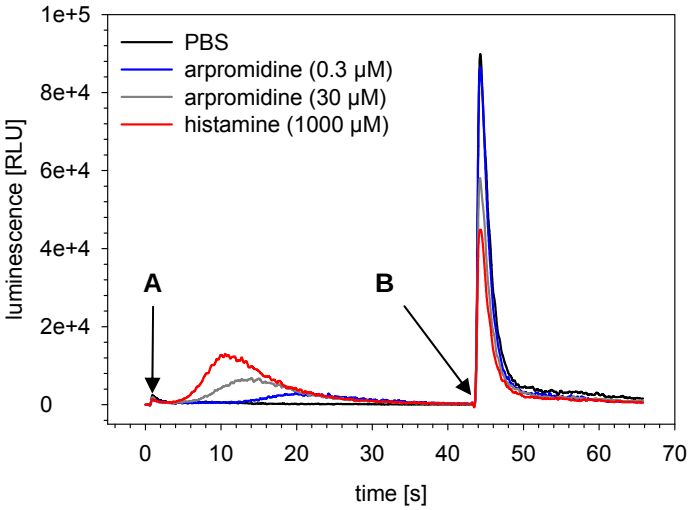

Fig. 5.12: *Aequorin assay for arpromidine with histamine as reference in HEK293-hH_2R-qs5-HA-mtAEQ cells.* **A***: injection of cell-suspension (100 µL / s)* **B***: injection of triton-X-100 (200 µL / s).*

Arpromidine was recognized as a partial agonist relative to histamine irrespective of the chosen injection speed (Fig. 5.13, A). The assay performed with an injection speed of 25 µL / s revealed - despite a good signal-to-noise ratio - a lower potency and efficacy relative to histamine, respectively, compared to data obtained with fura-2 assays in the 384-well format (Table 5.1 and 5.5; Fig. 5.13 A, B). By contrast, the potency obtained at an injection speed of 200 µL / s was in agreement with the result of the fura-2 assay, but the intrinsic activity relative to histamine was still slightly decreased. In addition, the signal-to-noise ratio was considerably decreased compared to the results obtained at lower speed of injection (Table 5.1 and 5.5; Fig. 5.13 A, B).

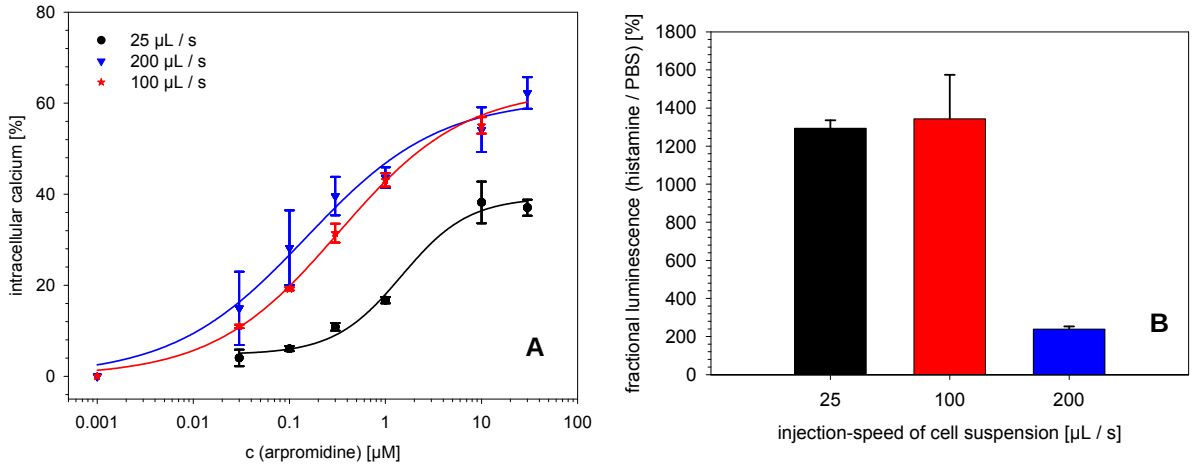

Fig. 5.13: *Influence of the speed of injection of suspended HEK293-hH_2R-qs5-HA-mtAEQ on* **A***: the calculation of sigmoidal curves (mean values ± SEM; n = 4);* **B***: the signal-to-noise ratio in the aequorin assay (mean values ± SEM; n = 6).*

An injection speed of 100 µL / s led to the most reliable data: the potency of arpromidine was comparable to data from the fura-2 assay. The efficacy relative to histamine was slightly decreased at this injection speed, too (Table 5.1 and 5.5; Fig. 5.13 A). The signal-to-noise ratio was comparable to that obtained at an injection speed of 25 µL / s but in each case higher than for 200 µL / s (Fig. 5.13, B).

Table 5.5: *Comparison of pharmacological data obtained for arpromidine at various injection speeds in the aequorin assay.*

Injection speed [µL / s]	*EC_{50} [µM]*	*intrinsic acitivity, relative to histamine = 100 [%]*
25	1.47 ± 0.50	39 ± 9
100	0.33 ± 0.05	63 ± 2
200	0.15 ± 0.09	61 ± 7

Thus, the injection speed of 100 µL / s enabled the correct estimation of the pharmacological properties of arpromidine accompanied with an appropriate signal-to-noise ratio (Table 5.1, Table 5.5; Fig. 5.13, B).

For assays with compound **9**, arpromidine was used as reference at two concentrations (200 and 20000 nM, "arpromidine (control)" in Fig. 5.14). Those reference compounds showed agonistic activity as expected, however, under the same conditions, **9** did not exhibit a concentration-dependent response up to a concentration of 300 nM.

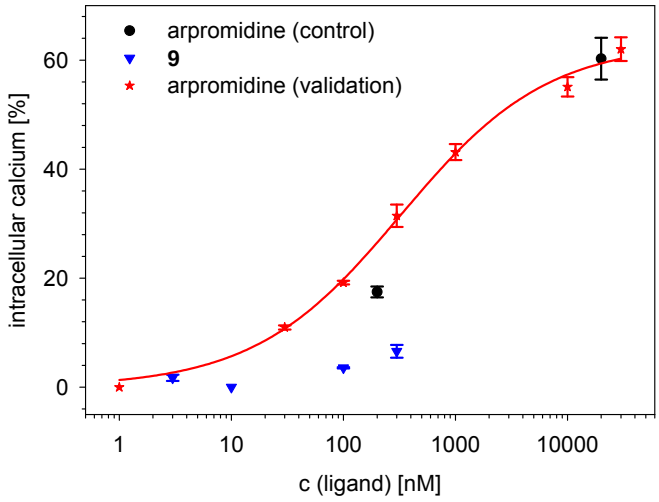

Fig. 5.14: *Influence of various concentrations of* **9** *on the intracellular calcium level in HEK293-hH_2R-qs5-HA-mtAEQ cells determined with the aequorin assay (speed of injection of the cell-suspension: 100 µL / s). The red curve shown in Fig. 5.13 is here depicted again for comparison (arpromidine (validation). Mean values ± SEM; n = 4.*

Higher concentrations of **9** were not investigated because the results for concentrations up to 300 nM were comparable to those determined in the 384-well format with the fura-2 assay. As the data for arpromidine determined in the aequorin assay and in 384-well plates using the fura-2 assays were comparable regarding potency and efficacy relative to histamine, it is unlikely that concentrations of **9** higher than 300 nM would lead to a concentration-dependent increase in the intracellular calcium level (see section 5.3.1). Hence, the determination of the pharmacological properties of the bivalent H_2R agonist **9** was not achieved by using the aequorin assay (Fig. 5.14).

5.4 Summary and conclusions

The stable coexpression of the hH_2R and the chimeric Gα-protein qs5-HA in HEK293 cells enabled the establishment of the fura-2 assay for the hH_2R. Standard H_2R agonists (histamine, arpromidine and dimaprit) and H_2R antagonists (famotidine, cimetidine and tiotidine) were characterised in the spectrofluorimetric and in the 384-well microtitre assay format. The results for histamine and dimaprit were consistent with data reported for a fluo-3 assay (Esbenshade et al., 2003) and were predominantly in agreement with results obtained in GTPase activity assays. However, dimaprit showed a decreased potency in fura-2 assays compared to results from GTPase assays (Preuss et al., 2007). Agonistic potencies were lower in fura-2 assays than in cAMP assays reported in literature (Baker, 2008) whereas antagonistic activities of cimetidine, famotidine and tiotidine were in agreement with data reported in literature (Kelley et al., 2001; Preuss et al., 2007), as well by reduction of the measurement time from 120 to 46 cycles. Investigations on the reliability of calcium signals with respect to the time period between the loading procedure with fura-2 / AM and the registration of the fluorescence (i.e. time period of post-incubation) revealed an appropriate characterisation of 72 samples (measurement time: 64 min) in the agonist-mode after loading of the cells. In case of antagonists, reliable measurements should be feasible up to approx. 6 h after termination of loading. The investigation of the compounds **6**-**8** with the fura-2 assay in the 384-well format revealed antagonistic activities in the same order of magnitude (K_b = 120 – 150 nM). Since the characterisation of the potent partial hH_2R agonist **9** succeeded at the spectrofluorimeter with the fura-2 assay but failed in the 384-well format, HEK293-hH_2R-qs5-HA cells were stably cotransfected with mtAEQ in order to establish a calcium assay with an improved signal-to-noise ratio. The characterisation of arpromidine led to data that were in agreement with those determined in fura-2 assays or reported in literature, respectively (Preuss et al., 2007). The characterisation of **9** in the microtitre format failed with this alternative readout, too. Therefore, the characterisation of bivalent H_2R agonists like compound **9** at whole cells in functional assays is to date most convenient with the spectrofluorimetric fura-2 assay.

5.5 References

Baker, J.G., 2008. A study of antagonist affinities for the human histamine H_2 receptor. *Br. J. Pharmacol.* **153**, 1011-1021.

Cheng, Y.-C., Prusoff, W.H., 1973. Relationship between the inhibition constant (K_i) and the concentration of inhibitor which causes 50 per cent inhibition (IC_{50}) of an enzymatic reaction. *Biochem. Pharmacol.* **22**, 3099-3108.

Conklin, B., Herzmark, P., Ishida, S., Voyno-Yasenetskaya, T., Sun, Y., Farfel, Z., Bourne, H., 1996. Carboxyl-terminal mutations of Gq alpha and Gs alpha that alter the fidelity of receptor activation. *Mol. Pharmacol.* **50**, 885-890.

Esbenshade, T.A., Kang, C.H., Krueger, K.M., Miller, T.R., Witte, D.G., Roch, J.M., Masters, J.N., Hancock, A.A., 2003. Differential Activation of Dual Signaling Responses by Human H_1 and H_2 Histamine Receptors. *J. Recept. Signal Transduct.* **23**, 17 - 31.

Gessele, K., 1998. Zelluläre Testsysteme zur pharmakologischen Charakterisierung neuer Neuropeptid Y-Rezeptorantagonisten. In: *Doctoral Thesis, University of Regensburg*.

Ghorai, P., Kraus, A., Keller, M., Götte, C., Igel, P., Schneider, E., Schnell, D., Bernhardt, G., Dove, S., Zabel, M., et al., 2008. Acylguanidines as Bioisosteres of Guanidines: N^G-Acylated Imidazolylpropylguanidines, a New Class of Histamine H_2 Receptor Agonists. *J. Med. Chem.* **51**, 7193-7204.

Grynkiewicz, G., Poenie, M., Tsien, R., 1985. A new generation of Ca^{2+} indicators with greatly improved fluorescence properties. *J. Biol. Chem.* **260**, 3440-3450.

Hill, S.J., Baker, J.G., Rees, S., 2001. Reporter-gene systems for the study of G-protein-coupled receptors. *Curr. Opin. Pharm.* **1**, 526-532.

Kelley, M.T., Bürckstümmer, T., Wenzel-Seifert, K., Dove, S., Buschauer, A., Seifert, R., 2001. Distinct Interaction of Human and Guinea Pig Histamine H_2-Receptor with Guanidine-Type Agonists. *Mol. Pharmacol.* **60**, 1210-1225.

Kracht, J., 2001. Bestimmung der Affinität und Aktivität subtypselektiver Histamin- und Neuropeptid Y-Rezeptorliganden an konventionellen und neuen pharmakologischen In-vitro-Modellen. In: *Doctoral Thesis, University of Regensburg*.

Kraus, A., 2007. Highly potent, Selective Acylguanidine-Type Histamine H_2 Receptor Agonists: Synthesis and Structure-Activity Relationships. In: *Doctoral Thesis, University of Regensburg*. http://www.opus-bayern.de/uni-regensburg/volltexte/2008/904/.

Kraus, A., Ghorai, P., Birnkammer, T., Schnell, D., Elz, S., Seifert, R., Dove, S., Bernhardt, G., Buschauer, A., 2009. N^G-Acylated Aminothiazolylpropylguanidines as Potent and Selective Histamine H_2 Receptor Agonists. *ChemMedChem* **4**, 232-240.

Morse, K.L., Behan, J., Laz, T.M., West, R.E., Jr., Greenfeder, S.A., Anthes, J.C., Umland, S., Wan, Y., Hipkin, R.W., Gonsiorek, W., et al., 2001. Cloning and Characterization of a Novel Human Histamine Receptor. *J. Pharmacol. Exp. Ther.* **296**, 1058-1066.

Nikolaev, V.O., Bunemann, M., Hein, L., Hannawacker, A., Lohse, M.J., 2004. Novel Single Chain cAMP Sensors for Receptor-induced Signal Propagation. *J. Biol. Chem.* **279**, 37215-37218.

Preuss, H., Ghorai, P., Kraus, A., Dove, S., Buschauer, A., Seifert, R., 2007. Constitutive Activity and Ligand Selectivity of Human, Guinea Pig, Rat, and Canine Histamine H_2 Receptors. *J. Pharmacol. Exp. Ther.* **321**, 983-995.

Schneider, E., 2005. Development of Fluorescence-Based Methods for the Determination of Ligand Affinity, Selectivity and Activity at G-Protein Coupled Receptors. In: *Doctoral Thesis, University of Regensburg*.

Schneider, E., Mayer, M., Ziemek, R., Li, L., Hutzler, C., Bernhardt, G., Buschauer, A., 2006. A Simple and Powerful Flow Cytometric Method for the Simultaneous Determination of Multiple Parameters at G Protein-Coupled Receptor Subtypes. *ChemBioChem* **7**, 1400-1409.

Seifert, R., Wenzel-Seifert, K., Bürckstümmer, T., Pertz, H.H., Schunack, W., Dove, S., Buschauer, A., Elz, S., 2003. Multiple Differences in Agonist and Antagonist Pharmacology between Human and Guinea Pig Histamine H_1-Receptor. *J. Pharmacol. Exp. Ther.* **305**, 1104-1115.

Siehler, S., 2008. Cell-based assays in GPCR drug discovery. *Biotechnol. J.* **3**, 722-727.

Williams, C., 2004. cAMP detection methods in HTS: selecting the best from the rest. *Nat. Rev. Drug Discov.* **3**, 125-135.

Wood, M., Chaubey, M., Atkinson, P., Thomas, D.R., 2000. Antagonist activity of meta-chlorophenylpiperazine and partial agonist activity of 8-OH-DPAT at the 5-HT_7 receptor. *Eur. J. Pharmacol.* **396**, 1-8.

Ziemek, R., 2006. Development of binding and functional assays for the neuropeptide Y Y_2 and Y_4 receptors. In: *Doctoral Thesis, University of Regensburg*. http://www.opus-bayern.de/uni-regensburg/volltexte/2006/679/.

Ziemek, R., Brennauer, A., Schneider, E., Cabrele, C., Beck-Sickinger, A.G., Bernhardt, G., Buschauer, A., 2006. Fluorescence- and luminescence-based methods for the determination of affinity and activity of neuropeptide Y_2 receptor ligands. *Eur. J. Pharmacol.* **551**, 10-18.

Ziemek, R., Schneider, E., Kraus, A., Cabrele, C., Beck-Sickinger, A.G., Bernhardt, G., Buschauer, A., 2007. Determination of Affinity and Activity of Ligands at the Human Neuropeptide Y Y_4 Receptor by Flow Cytometry and Aequorin Luminescence. *J. Recept. Signal Transduct.* **27**, 217 - 233.

Chapter 6

Summary

G-protein coupled receptors (GPCRs) are one of the largest superfamilies in the druggable human genome, targeted by a significant portion of the currently available pharmaco-therapeutics and are considered promising biological targets for drug discovery programmes. With respect to the pecularities of this class of drug targets, the research projects of the Graduiertenkolleg (Research Training Group) Medicinal Chemistry (GRK 760) address histamine receptors as prototypes of aminergic GPCRs, their ligands (agonists, antagonists, modulators) and signal transduction (second messenger, signal proteins, gene regulation) at the molecular level. As a part of this Graduate Training Programme, this thesis aimed at the development of binding and functional in vitro assays for the human histamine H_1, H_2 and H_4 receptor, respectively. Such methods are required for both the screening of compound libraries and the detailed pharmacological characterisation of compounds in terms of affinity, quality of action (agonism or antagonism) and receptor subtype selectivity.

Whereas the ratiometric fura-2 based calcium assay in cuvettes has been state of the art for the determination of intracellular calcium for decades, this method has not become a standard procedure in the microtitre plate format. Instead, non-ratiometric dyes such as fluo-4 are preferred in high throughput screening. In order to combine the advantages of ratiometric calcium measurements with increased throughput in the microplate format, human H_1R (hH_1R) expressing U-373 MG cells were used as a model. Compared to the conventional protocol, the sequence of the test procedure had to be changed, e.g. for agonists fura-2 loaded cells were injected into the wells containing the test compounds. The characterisation of the agonist histamine yielded reliable data both in 96-well and 384-well plates. The determination of antagonistic activity was most effective in the 384-well format. The procedure was validated and optimized using standard H_1R antagonists. Sequential reduction of the measurement time enabled the characterisation of 480 samples in one assay per day in the 384-well format. As a proof-of-concept, the applicability of this approach was confirmed by the identification of potent hH_1R antagonists as lead compounds from a library of more than thousand new chemical entities provided by a pharmaceutical company.

Due to the lack of appropriate wild-type cells expressing the hH_2R or the hH_4R, transfection experiments using the well characterised HEK293 cells were performed to establish cellular binding and functional assays. Since little information has been available on the expression pattern of human histamine receptor subtypes, those cells were investigated both on the mRNA level and by Western blot. Although a band corresponding to the hH_2R was identified by mRNA analysis, the respective receptor protein was not detected in Western blots. Therefore, HEK293 cells were considered appropriate for the expression of human histamine receptor subtypes.

To establish a functional assay, HEK293 cells were stably co-transfected with the hH_2R and the chimeric Gα-protein qs5-HA, thereby redirecting the agonist-mediated receptor stimulation to a robust calcium signal. For validation, radioligand binding experiments were performed comparing the co-transfected cells (HEK293-hH_2R-qs5-HA cells) with HEK293-FLAG-hH_2R-His_6 cells as reference. The affinities determined for the investigated standard ligands were on both cell types and on membranes from HEK293-hH_2R-qs5-HA cells in the same order of magnitude and mainly in agreement with data reported in literature, except for the H_2R agonist arpromidine, which showed lower affinity than reported for binding experiments performed in a different model (hH_2R-$G_{s\alpha S}$ fusion proteins). Generally, the binding properties of the investigated ligands were not significantly influenced by the co-expression of qs5-HA in HEK293-hH_2R-qs5-HA cells.

As an alternative to the use of hazardous and expensive radioligands, fluorescence-based binding assays were developed. The specific binding of a cyanine-dye-labelled H_2R ant-agonist to HEK293-hH_2R-qs5-HA cells was visualized by confocal microscopy. In addition, flow cytometric saturation binding experiments were performed on HEK293-hH_2R-qs5-HA cells with this cyanine-labelled compound and with a pyrylium-dye (Py)-labelled H_2R ligand. The fluorescent ligands showed moderate submicromolar affinities, but remarkably low extents of unspecific binding. Affinities determined in binding experiments by displacing the Py-labelled ligand with H_2R standard ligands were slightly lower for some compounds than reference data from literature, possibly due to the presence of DMSO in the assay (supported by investigations using varying DMSO concentrations).

For the determination of the functional activity of hH_2R ligands, fura-2 assays were established in cuvettes and in the microtitre format. Data obtained in the fura-2 assays were in agreement with results reported for calcium measurements performed with fluo-3 and were essentially in the same order of magnitude as reported for GTPase activity.

Preliminary experiments aiming at the development of binding and functional assays for the hH_4R were performed as described in the appendix.

Taken together, the established flow cytometric binding assay using fluorescence-labelled ligands and stably co-transfected cells represents an innovative alternative to radioligand binding assays for the determination of ligand affinity on the hH_2R. The principle of stable co-expression of receptor and chimeric G_{qs5}-protein allowed the development of fluorescence-based calcium measurements, which can be performed in the microtitre format, thereby enabling reasonable throughput. The developed methods will contribute to the characterisation of compounds on histamine receptor subtypes with regard to affinity, receptor subtype selectivity, quality of action and potency.

Appendix

Towards binding and functional assays for the human histamine H_4 receptor

1 Introduction

In order to develop assays for the determination of ligand affinity and activity at the human histamine H_4 receptor, HEK293 cells should be stably co-transfected with the cDNA encoding the receptor and proteins enabling an appropriate readout to perform functional assays. In principle, the latter can be achieved by coupling the receptor to the chimeric Gα-protein qi5-HA (Conklin et al., 1996; Conklin et al., 1993; Morse et al., 2001) in order to redirect the hH_4R signalling to an intracellular calcium response. A cAMP-response element (CRE)-driven reporter gene assay represents an attractive alternative, since the H_4R is coupling to G_i-proteins resulting in a decrease in intracellular cAMP levels (de Esch et al., 2005). In this case, stimulation of the adenylyl cyclase activity is required to enable the quantification of the cAMP-decreasing effect induced by H_4R stimulation. Therefore, the diterpene forskolin (Fig. 1), a direct activator of the adenylyl cyclase (AC; (Tang and Hurley, 1998)), is added.

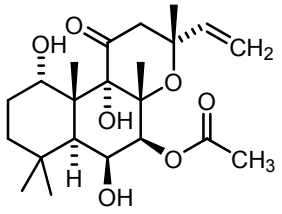

Fig. 1: *Chemical structure of the diterpene forskolin.*

Elevated cAMP levels switch on protein kinase A (PKA), which phosphorylates various proteins including CRE-binding protein, which in turn binds to the CRE. In genetically engineered cells, the CRE signalling cascade can be coupled to reporter gene expression, for instance luciferase (Fig. 2).

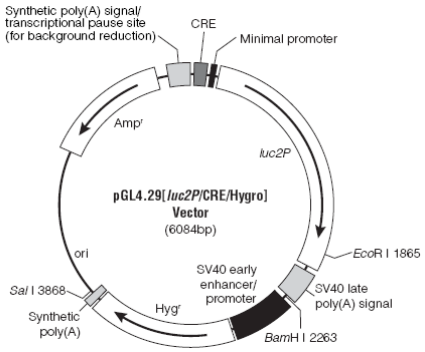

Fig. 2: *Map of the pGL4.29[luc2/CRE/Hygro] vector (Promega, Mannheim, Germany). The luc2P gene which encodes the luciferase is under control of CRE. The hygromycin resistance (Hyg) enables the stable expression in mammalian cells whereas the ampicillin resistance (Amp) accounts for the amplification of the vector in competent bacteria.*

The enzyme luciferase is capable of converting the substrate D-luciferin into oxyluciferin accompanied by an emission of visible light detectable in luminometers (Fig. 3; (Bronstein et

al., 1994)). Hence, the luminescence signals increase with the expression of the luciferase in a cAMP-dependent manner and decrease with hH_4R receptor activation, respectively.

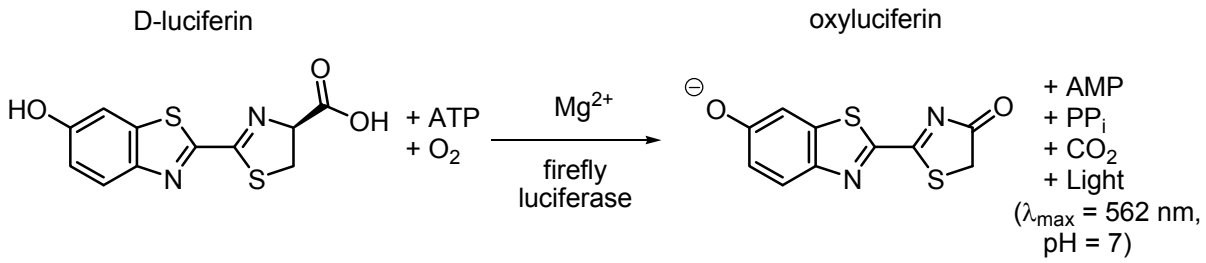

Fig. 3: *Conversion of D-luciferin by firefly luciferase to oxyluciferin (according to (Shinde et al., 2006)).*

HEK293 cells transfected with the hH_4R were characterised in radioligand binding experiments using the radioligand [^{3}H]UR-PI294 (Igel et al., 2009), which displays high affinity for both the hH_3R (K_d = 1.1 nM) and the hH_4R (K_d = 5.1 nM). The non-labelled ("cold") ligand UR-PI294 behaved as an almost full agonist at the hH_4R in GTPase assays (E_{max} = 0.90; (Igel et al., 2009).

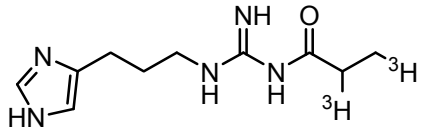

Fig. 4: *Chemical structure of [^{3}H]UR-PI294, the radioligand used for the binding experiments with hH_4R-transfected cells.*

In order to avoid misleading interpretations due to agonist-mediated receptor internalization, the influence of various incubation periods on the binding behaviour of the radioligand to hH_4R-tansfected cells was investigated.

2 Materials and methods

2.1 Propagation of DNA, cell culture and transfection experiments

The vector pcDNA3.1(+)-Neo-hH_4R was from the Guthrie cDNA resource center (Sayre, USA). Transformation of competent *E. coli* TOP10 bacteria, isolation and characterisation of DNA were performed according to section 4.2.2.1. Sequencing revealed no mutation in the cDNA encoding the hH_4R. HEK293 cells (Deutsche Sammlung für Mikroorganismen und Zellkulturen (DSMZ), Braunschweig, Germany) were cultured and transfected with the vector incorporating the cDNA encoding the hH_4R as described in section 4.2.2.4. Cells were then cultured in presence of G418 (400 µg / mL) for 4 weeks. Cells were either cotransfected with pcDNA3.1(+)-Hygro-qi5-HA (Ziemek et al., 2006) or pGL4.29[luc2/CRE/Hygro] (Promega, Mannheim, Germany), respectively, in the same way and cultured in each case for at least another 4 weeks in the presence of hygromycin B (100 µg / mL in each case) prior to the performance of assays. The established cell types were named HEK293-hH_4R, HEK293-hH_4R-qi5-HA or HEK293-hH_4R-CRE-Luc, respectively. Cells were frozen in medium (DMEM + 10 % FBS + respective selective antibiotics) including 10 % DMSO as described in section 3.2.1. In addition, HEK293-FLAG-hH_4R-His_6 cells were established and provided by David Schnell (Institute of Pharmacy, Department of Pharmacology and Toxicology, University of Regensburg). He used HEK293 cells from the American Type Culture Collection (ATCC, Rockville, USA) and performed transfection experiments with FuGENE® HD (Roche Diagnostics, Mannheim, Germany) according to the manufacturer's instructions. Ratios of transfection reagent [µL] to DNA [µg] of 4 to 2 and 6 to 2 were chosen. Transfected cells were cultured in DMEM + 10 % of FBS including 800 µg / mL of G418 for selection and further handled in presence of 600 µg / mL of G418 (Schnell, D., 2009, personal communication).

2.2 Spectrofluorimetric fura-2 assay

HEK293-hH_4R-qi5-HA cells were cultured as mentioned for HEK293-hH_2R-qs5-HA cells in section 5.2.1.1 and prepared for fura-2 assays according to section 3.2.2 without trypsin / EDTA treatment. 200-fold concentrated feed solutions with respect to final assay concentrations of histamine were prepared in PBS. Fura-2 loaded cells were investigated in spectrofluorimetric measurements as described in section 5.2.1.1 (investigation of agonists).

2.3 Reporter gene assay

Approx. 3.3 · 10^4 HEK293-hH_4R-CRE-Luc cells were seeded per cavity of a 24-well plate (Becton Dickinson, Heidelberg, Germany) in DMEM without phenol red (Invitrogen, Karlsruhe, Germany) supplemented with 10 % FBS and selective antibiotics (400 µg / mL of G418 and 100 µg / mL of hygromycin B). Cells were grown to 50 % confluency within 4 days at 5 % CO_2 and 37 °C in a water saturated atmosphere. For the assays, cell culture medium was carefully replaced with fresh medium (composition as mentioned above) including histamine at concentrations ranging from 0.1 to 10.000 nM. The cells were incubated with the agonist for 10 min. Samples were either not challenged or induced by addition of forskolin according to final assay concentrations of 100 or 1000 nM, respectively. Cells were cultured for 5 h as mentioned before. The medium was removed and 60 µL of lysis buffer (Biotium, Hayward, USA) were added per well. The cells were incubated under occasional tapping for 20 min at room temperature. Samples were transferred to microfuge tubes and centrifuged for 10 min at 11,000 rpm in a table top centrifuge. 30 µL of the supernatant from each reaction vessel were transferred into luminometer tubes. For the luminescence readouts, the injector of the luminometer Lumat LB 9501 (Berthold, Bundoora, Australia) was primed with the solution of D-luciferin in luciferase assay buffer (0.2 mg / mL; Biotium). Light emission was induced by injection of 100 µL of the D-luciferin solution per sample. Luminescence signals were recorded as relative light units [RLU]. In order to diminish errors due to different cell numbers per well, the comparability of the conditions was controlled, i.e. the protein amount was determined for every investigated well: 5 µL of each supernatant were pipetted into a cuvette and diluted with 95 µL of Millipore water. 1 mL of the 1:5 diluted Protein Assay Dye Reagent Concentrate (Bio-Rad Laboratories) was added per cuvette. Samples were mixed and investigated at 595 nm after 10 min by VIS spectroscopy. Protein amounts were calculated by a calibration curve determined with HSA (Behringwerke, Marburg, Germany).

2.4 Radioligand binding experiments

The established cell types described in section 2.1 were cultured and prepared for the radioligand binding experiments according to section 4.2.3.1.1. Transparent 96-well plates (Greiner) were either provided with 20 µL of PBS for the determination of total binding or 20 µL of thioperamide (100 µM) as samples for unspecific binding, respectively. 160 µL of the cell suspension were added per well. Samples were completed by addition of 20 µL of the radioactive tracer [^{3}H]UR-PI294 (50 nM in PBS). Samples were incubated at 100 rpm and room temperature for 5, 15, 30, 60 or 90 min, respectively. Further processing of the samples was performed as described in section 4.2.3.1.1.

3 Results and discussion

3.1 Spectrofluorimetric fura-2 assay

Loaded cells were challenged with various concentrations of histamine: neither 0.1, nor 3, nor 30 µM of histamine evoked a calcium response in HEK293-hH_4R-qi5-HA cells (data not shown).

3.2 Reporter gene assay

The samples that were not challenged by forskolin showed comparable signals at every investigated concentration of histamine. The induction of the cells by either 100 or 1000 nM of forskolin led to a clear increase in the luminescent response, respectively. Unfortunately, histamine neither suppressed the cAMP-responses in samples challenged with 100 nM of forskolin nor in those induced by 1000 nM of forskolin (Fig. 5).

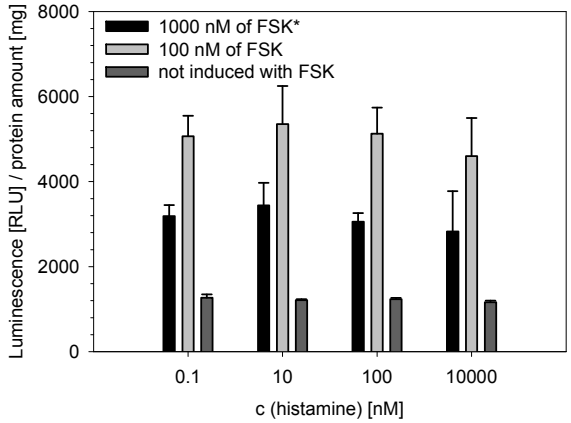

Fig. 5: *Influence of various concentrations of histamine on the readout. Samples were either not challenged or induced with 100 or 1000 nM of forskolin (FSK), respectively (mean values ± SEM; n = 3).*
**Samples for the luminescence readout were diluted 1:100 prior to the measurements.*

As neither calcium-transients (section 3.1) nor alterations of the intracellular cAMP-level were observed, the established cell types were investigated in radioligand binding assays in order to investigate ligand binding to the H_4R.

3.3 Radioligand binding experiments

Neither HEK293-hH_4R cells, nor HEK293-hH_4R-qi5-HA cells, nor HEK293-hH_4R-CRE-Luc cells showed a specific binding of the tracer (Fig. 6).

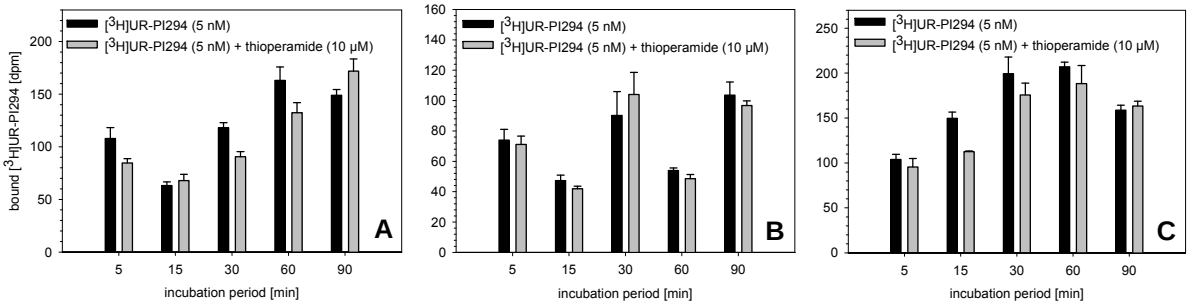

Fig. 6: *Investigation of hH_4R-transfected cells in radioligand binding experiments.* **A***: HEK293-hH_4R;* **B***: HEK293-hH_4R-qi5-HA;* **C***: HEK293-hH_4R-CRE-Luc cells (mean values ± SEM; n = 3).*

In contrast, 10 µM of thioperamide displaced the radioactive tracer on HEK293-FLAG-hH_4R-His_6 cells transfected with a ratio of 4 µL transfection reagent to 2 µg DNA after incubation periods of 60 or 90 min, respectively. With regard to HEK293-FLAG-hH_4R-His_6 cells transfected according to a ratio of 6 µL transfection reagent to 2 µg DNA, no significant differences in the presence or absence of thioperamide were observed, respectively (Fig. 7).

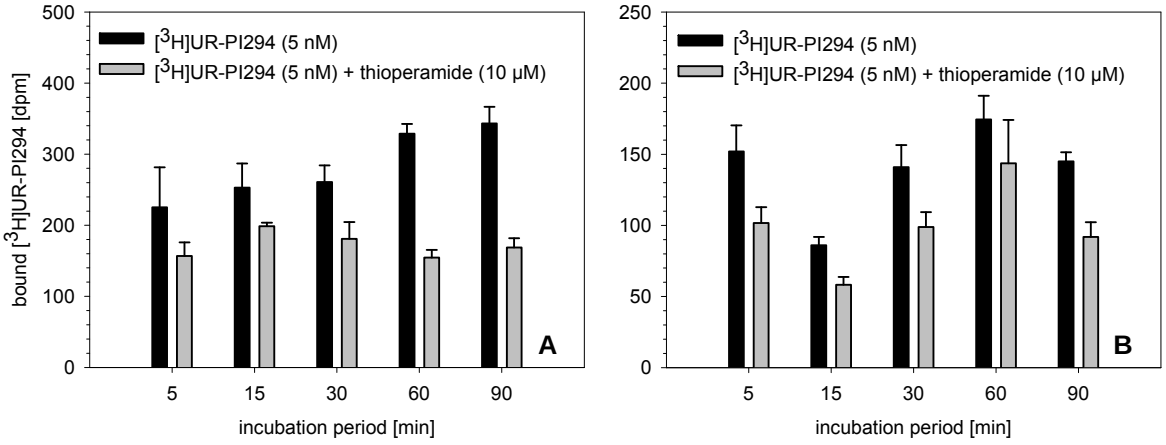

Fig. 7: *Investigation of HEK293-FLAG-hH_4R-His_6 cells in radioligand binding experiments. Cells transfected with a ratio of* **A***: 4 µL transfection reagent to 2 µg DNA;* **B***: 6 µL transfection reagent to 2 µg DNA. Indicated are mean values ± SEM; n = 3.*

4 Summary and outlook

Transfection of HEK293 cells (DSMZ) with the cDNA encoding the native hH_4R using Lipofectamine™ 2000 (Invitrogen) as the transfection reagent and subsequent selection did not result in a cell type appropriately incorporating the receptor of interest as revealed by radioligand binding experiments. In contrast, HEK293-FLAG-hH_4R-His_6 cells that were established by David Schnell (Institute of Pharmacy, Department of Pharmacology and Toxicology, University of Regensburg) by transfection of HEK293 cells (ATCC) with the cDNA encoding a modified hH_4R (FLAG-hH_4R-His_6) by FuGENE® HD (Roche Diagnostics) with a ratio of 4 µL transfection reagent to 2 µg DNA led to a specific binding of [^{3}H]UR-PI294 (approx. 50 % specific binding, compare Fig. 7, A). Given an incubation period of 90 min, recent radioligand binding experiments performed in our workgroup with HEK293-FLAG-hH_4R-His_6 cells according to both transfection approaches led to even more promising results: specific binding of [^{3}H]UR-PI294 was at least determined with 70 % (Nordemann, U., 2009, personal communication). Thus, those cell types seem to be suited for the development of radioligand binding assays, and with appropriate fluorescent ligands flow cytometric measurements could become feasible. With respect to a cellular functional assay for the hH_4R, the stable coexpression of a CRE-driven reporter gene (see above) seems promising, as similar successful approaches with transiently expressed reporter genes are described in literature (Lim et al., 2005; Liu et al., 2001). Given its commercial availability, a plasmid incorporating a serum-response-element (SRE)-driven luciferase and an appropriate eukaryotic marker would represent an alternative approach to establish a reporter gene assay. As the stimulation of the hH_4R leads to activation of the MAP-kinase pathway (de Esch et al., 2005; Morse et al., 2001), which accounts for an increased SRE-driven transcription (Hill and Treisman, 1995; Hill et al., 2001), readouts could become feasible that are directly and not inversely proportional to receptor activation as it would be the case in a forskolin-dependent CRE-driven reporter gene assay for the hH_4R.

As the stimulation of the hH_4R was successfully coupled to an increase in intracellular calcium levels by stable coexpression of $G\alpha_{16}$ (Crane and Shih, 2004), the corresponding genetic modification of HEK293-FLAG-hH_4R-His_6 cells should enable a fura-2 assay for the hH_4R (compare chapters 3 and 5). In addition, the disadvantage to overestimate low-efficacy agonists in reporter gene assays (Hill et al., 2001) could be overcome by this assay format.

5 References

Bronstein, I., Fortin, J., Stanley, P.E., Stewart, G.S.A.B., Kricka, L.J., 1994. Chemiluminescent and Bioluminescent Reporter Gene Assays. *Anal. Biochem.* **219**, 169-181.

Conklin, B., Herzmark, P., Ishida, S., Voyno-Yasenetskaya, T., Sun, Y., Farfel, Z., Bourne, H., 1996. Carboxyl-terminal mutations of Gq alpha and Gs alpha that alter the fidelity of receptor activation. *Mol. Pharmacol.* **50**, 885-890.

Conklin, B.R., Farfel, Z., Lustig, K.D., Julius, D., Bourne, H.R., 1993. Substitution of three amino acids switches receptor specificity of Gq alpha to that of Gi alpha. *Nature* **363**, 274-276.

Crane, K., Shih, D.-t., 2004. Development of a homogeneous binding assay for histamine receptors. *Anal. Biochem.* **335**, 42-49.

de Esch, I.J.P., Thurmond, R.L., Jongejan, A., Leurs, R., 2005. The histamine H_4 receptor as a new therapeutic target for inflammation. *Trends Pharmacol. Sci.* **26**, 462-469.

Hill, C.S., Treisman, R., 1995. Differential activation of c-fos promotor elements by serum, lysophosphatidic acid, G-proteins and polypeptide growth factors. *EMBO J.* **14**, 5037-5047.

Hill, S.J., Baker, J.G., Rees, S., 2001. Reporter-gene systems for the study of G-protein-coupled receptors. *Curr. Opin. Pharmacol.* **1**, 526-532.

Igel, P., Schnell, D., Bernhardt, G., Seifert, R., Buschauer, A., 2009. Tritium-Labeled N^1-[3-(1*H*-imidazol-4-yl)propyl]-N^2-propionylguanidine ([^{3}H]UR-PI294), a High-Affinity Histamine H_3 and H_4 Receptor Radiologand. *ChemMedChem* **4**, 225-231.

Lim, H.D., van Rijn, R.M., Ling, P., Bakker, R.A., Thurmond, R.L., Leurs, R., 2005. Evaluation of Histamine H_1-, H_2-, and H_3-Receptor Ligands at the Human Histamine H_4 Receptor: Identification of 4-Methylhistamine as the First Potent and Selective H_4 Receptor Agonist. *J. Pharmacol. Exp. Ther.* **314**, 1310-1321.

Liu, C., Ma, X.-J., Jiang, X., Wilson, S.J., Hofstra, C.L., Blevitt, J., Pyati, J., Li, X., Chai, W., Carruthers, N., et al., 2001. Cloning and Pharmacological Characterization of a Fourth Histamine Receptor (H_4) Expressed in Bone Marrow. *Mol. Pharmacol.* **59**, 420-426.

Morse, K.L., Behan, J., Laz, T.M., West, R.E., Jr., Greenfeder, S.A., Anthes, J.C., Umland, S., Wan, Y., Hipkin, R.W., Gonsiorek, W., et al., 2001. Cloning and Characterization of a Novel Human Histamine Receptor. *J. Pharmacol. Exp. Ther.* **296**, 1058-1066.

Shinde, R., Perkins, J., Contag, C.H., 2006. Luciferin Derivatives for Enhanced in Vitro and in Vivo Bioluminescence Assays *Biochemistry (Mosc).* **45**, 11103-11112.

Tang, W.-J., Hurley, J.H., 1998. Catalytic Mechanism and Regulation of Mammalian Adenylyl Cyclases. *Mol. Pharmacol.* **54**, 231-240.

Ziemek, R., Brennauer, A., Schneider, E., Cabrele, C., Beck-Sickinger, A.G., Bernhardt, G., Buschauer, A., 2006. Fluorescence- and luminescence-based methods for the determination of affinity and activity of neuropeptide Y_2 receptor ligands. *Eur. J. Pharmacol.* **551**, 10-18.

Ich erkläre hiermit an Eides statt, dass ich die vorliegende Arbeit ohne unzulässige Hilfe Dritter und ohne Benutzung anderer als der angegebenen Hilfsmittel angefertigt habe; die aus anderen Quellen direkt oder indirekt übernommenen Daten und Konzepte sind unter der Angabe des Literaturzitats gekennzeichnet.

Regensburg,

Johannes Mosandl